

การประยุกต์วิธีจำลองพลวัตเชิงโมเลกุลที่ผสมผสานกลศาสตร์ควอนตัมและ
กลศาสตร์โมเลกุล (QM/MM-MD) ในการศึกษาไอออนแอมโมเนียมและ
ไอออนไฮโดรเนียมในสารละลายน้ำ

นางสาวปทุมวดี อินทรเทพ

วิทยานิพนธ์นี้เป็นส่วนหนึ่งของการศึกษาตามหลักสูตรปริญญาวิทยาศาสตรดุษฎีบัณฑิต

สาขาวิชาเคมี

มหาวิทยาลัยเทคโนโลยีสุรนารี

ปีการศึกษา 2549

ISBN 974-533-573-8

**APPLICATIONS OF COMBINED QM/MM-MD
SIMULATIONS IN THE STUDY OF AMMONIUM AND
HYDRONIUM IONS IN AQUEOUS SOLUTION**

Pathumwadee Intharathep

A Thesis Submitted in Partial Fulfillment of the Requirements

for the Degree of Doctor of Philosophy in Chemistry

Suranaree University of Technology

Academic Year 2006

ISBN 974-533-573-8

**APPLICATIONS OF COMBINED QM/MM-MD SIMULATIONS
IN THE STUDY OF AMMONIUM AND HYDRONIUM IONS
IN AQUEOUS SOLUTION**

Suranaree University of Technology has approved this thesis submitted in partial fulfillment of the requirements for the Degree of Doctor of Philosophy.

Thesis Examining Committee

M. Tangsathitkulchai

(Assoc. Prof. Dr. Malee Tangsathitkulchai)

Chairperson

R. Sagarik

(Prof. Dr. Kritsana Sagarik)

Member (Thesis Advisor)

A. Tongraar

(Assoc. Prof. Dr. Anan Tongraar)

Member

S. Hannongbua

(Prof. Dr. Supot Hannongbua)

Member

Visit Vao-Soongnern

(Asst. Prof. Dr. Visit Vao-Soongnern)

Member

S. Thammathaworn

(Assoc. Prof. Dr. Sompong Thammathaworn)

S. Rattanaphani

(Assoc. Prof. Dr. Saowanee Rattanaphani)

Vice Rector for Academic Affairs

Dean of Institute of Science

ปทุมวดี อินทรเทพ : การประยุกต์วิธีจำลองพลวัตเชิงโมเลกุลที่ผสมผสานกลศาสตร์ควอนตัมและกลศาสตร์โมเลกุล (QM/MM-MD) ในการศึกษาไอออนแอมโมเนียมและไอออนไฮโดรเนียมในสารละลายน้ำ (APPLICATIONS OF COMBINED QM/MM-MD SIMULATIONS IN THE STUDY OF AMMONIUM AND HYDRONIUM IONS IN AQUEOUS SOLUTION)

อาจารย์ที่ปรึกษา : ศาสตราจารย์ ดร.กฤษณะ ศาคริก, 115 หน้า. ISBN 974-533-573-8

งานวิจัยเรื่องนี้ประยุกต์การจำลองพลวัตเชิงโมเลกุลที่ผสมผสานกลศาสตร์ควอนตัมและกลศาสตร์โมเลกุล (Quantum Mechanical/Molecular Mechanical-Molecular Dynamics, QM/MM-MD) เพื่อศึกษาสมบัติเชิงโครงสร้างและเชิงพลวัตของไอออนแอมโมเนียม (NH_4^+) และไอออนไฮโดรเนียม (H_3O^+) ในน้ำ โดยสนใจไอออนและชั้นซอลเวชันของไอออนซึ่งอธิบายโดยกลศาสตร์ควอนตัมในระดับฮาร์ตรี-ฟ็อก (Hartree-Fock, HF) ในขณะที่ส่วนที่เหลือของระบบอธิบายโดยฟังก์ชันศักย์คู่แบบฉบับ (classical pair potentials) ผลการจำลองพลวัตเชิงโมเลกุลที่ผสมผสานกลศาสตร์ควอนตัมและกลศาสตร์โมเลกุลแสดงให้เห็นชัดเจนว่า โครงสร้างซอลเวชันของไอออนแอมโมเนียมค่อนข้างยืดหยุ่น โดยมีน้ำจำนวนหนึ่งเข้ามามีส่วนร่วมในการเกิดชั้นซอลเวชันของไอออนที่น่าสนใจเป็นพิเศษคือ ผลการศึกษาแสดงว่า ไอออนแอมโมเนียมมีการเคลื่อนที่ (translation) และการหมุน (rotation) ที่รวดเร็ว ซึ่งสอดคล้องกับผลการทดลองเป็นอย่างดี ทั้งนี้ ลักษณะเชิงพลวัตดังกล่าว เป็นผลจากการที่ไอออนแอมโมเนียมมีเลขโคออร์ดิเนชันได้หลายค่า ซึ่งมีส่วนสนับสนุนให้ไอออนแอมโมเนียมมีการเคลื่อนที่และการหมุนที่ค่อนข้างอิสระภายใต้สภาวะที่มีน้ำล้อมรอบ นอกจากนี้ การคำนวณได้แสดงพฤติกรรมการสลายโครงสร้าง (“structure-breaking” behavior) ของไอออนแอมโมเนียมอย่างชัดเจนจากผลการวิเคราะห์กระบวนการแลกเปลี่ยนลิแกนด์และเวลาการอยู่เฉลี่ย (mean residence times, MRTs) ของน้ำในชั้นซอลเวชันของไอออนแอมโมเนียม ในกรณีระบบไอออนไฮโดรเนียมในน้ำ สารเชิงซ้อนไอเกน (Eigen complex, H_9O_4^+) พบบ่อยที่สุดในสารละลาย ทั้งนี้ การวิเคราะห์เชิงทฤษฎีชี้ให้เห็นว่า สารเชิงซ้อนไอเกนดังกล่าว จะเปลี่ยนรูปไปมากับโครงสร้างซุนเดล (Zundel structure, H_5O_2^+) และนอกเหนือจากน้ำจำนวนสามโมเลกุลที่ไฮเดรตโดยเกิดพันธะไฮโดรเจนกับไอออนไฮโดรเนียมแล้ว พบว่า ยังมีน้ำที่อยู่บริเวณใกล้เคียงกับไอออนไฮโดรเนียม (เช่น น้ำโมเลกุลที่สี่) ซึ่งมีปฏิสัมพันธ์บ่อยครั้งกับอะตอมออกซิเจนของไอออนไฮโดรเนียม ผลการวิเคราะห์กระบวนการแลกเปลี่ยนน้ำ และเวลาการอยู่เฉลี่ยของน้ำในชั้นซอลเวชันของไอออนไฮโดรเนียม แสดงว่า น้ำโมเลกุลอื่นๆ (ที่นอกเหนือจากสามโมเลกุลที่เกิดพันธะไฮโดรเจนกับไอออน) ที่อยู่รอบๆ ไอออนไฮโดรเนียมนั้น มีส่วนเกี่ยวข้องในการจัดเรียงตัวใหม่ของเครือข่าย

PATHUMWADEE INTHARATHEP : APPLICATIONS OF COMBINED
QM/MM-MD SIMULATIONS IN THE STUDY OF AMMONIUM AND
HYDRONIUM IONS IN AQUEOUS SOLUTION.

THESIS ADVISOR : PROF. KRITSANA SAGARIK, Ph.D. 115 PP.

ISBN 974-533-573-8

AMMONIUM/HYDRONIUM/WATER EXCHANGE/PROTON TRANSFER

Molecular dynamics (MD) simulations based on combined *ab initio* Quantum Mechanics/Molecular Mechanics (QM/MM) method have been performed to investigate the solvation structure and dynamics of NH_4^+ and H_3O^+ in water. The most interesting region, the sphere including a reference ion (NH_4^+ or H_3O^+) and its surrounding water molecules, was treated at the Hartree-Fock level of theory, while the rest of the system was described by means of classical pair potentials. According to the results obtained by QM/MM simulations, the solvation structure of NH_4^+ is rather flexible, in which many water molecules are cooperatively involved in the solvation shell of the ion. Of particular interest, the QM/MM results clearly show fast translation and rotation of NH_4^+ in water, which are in good agreement with the recent NMR measurements. This phenomenon has been attributed to the observed multiple coordination, which drives the NH_4^+ to translate and rotate quite freely within its surrounding water molecules. In addition, “structure-breaking” behavior of the NH_4^+ is well reflected by the detailed analysis on the water exchange process and the mean residence times (MRTs) of water molecules in the hydration shell of the ion. In the case of H_3O^+ in water, the Eigen complex (H_9O_4^+) is found to be the most prevalent

species in aqueous solution. The QM/MM results show that the Eigen complex frequently converts back and forth into the Zundel (H_5O_2^+) structure. Besides the three nearest-neighbor water molecules directly hydrogen-bonded to H_3O^+ , other neighbor waters, such as a fourth water molecule which interacts preferentially with oxygen atoms of H_3O^+ , are found occasionally near the ion. Analyses of the water exchange processes and the mean residence times of water molecules in the ion's hydration shell indicate that such next-nearest neighbour water molecules participate in the rearrangement of the hydrogen bond network during fluctuative formation of the Zundel complex, and thus contribute to the Grotthuss transport of the proton.

School of Chemistry

Academic Year 2006

Student's Signature P. Immanuel
Advisor's Signature R. Supriat
Co-advisor's Signature Tony A.

ACKNOWLEDGEMENTS

I would like to express my sincerest gratitude to my thesis advisor, Prof. Dr. Kritsana Sagarik, who has provided me with continuous support, encouragement and invaluable guidance throughout the period of my 5 years Ph.D. program. I owe a great debt to my thesis co-advisor, Assoc. Prof. Dr. Anan Tongraar, who has helped me through a lot of my research works and provided me with numerous powerful computational resources.

I would like to express my special appreciate to Asst. Prof. Dr. Sunan Rojchanakit, my respectful teacher at Ramkhamhaeng University, who has initiatively encouraged me to get involve in Ph.D. program. In addition, I would like to express my special thanks to Dr. Eckhard Spohr, researcher at Forschungszentrum Jülich, Germany, who provided me the valuable advices and suggestions with respect to some parts of my thesis work, as well as Prof. Dr. Christopher J Cramer, researcher and instructor at University of Minnesota, United State, who provided me a worthy of remembrance research experience in the future.

I also wish to express my sincere thanks to the thesis examining committee for their devoted times to read, suggest, and comment on my thesis book.

Thanks for all my friends in the computational chemistry research group, Suranaree University of Technology, and my colleagues in Cramer's group at University of Minnesota, United state, for their friendship and wonderful encouragement.

I would like to acknowledge the financial support by the Royal Golden Jubilee Ph.D. program from Thailand Research Fund (TRF, Grant No. PHD/0225/2543). Extended thanks to the School of Chemistry, Suranaree University of Technology, for computer facilities through my Ph.D. studies.

Finally, I would like to take this opportunity to express my deepest gratitude to my parents for their lot of love, understanding, and encouragement.

Pathumwadee Intharathep

CONTENTS

| | Page |
|--|-------------|
| ABSTRACT IN THAI..... | I |
| ABSTRACT IN ENGLISH..... | III |
| ACKNOWLEDGEMENTS..... | V |
| CONTENTS..... | VII |
| LIST OF TABLES..... | X |
| LIST OF FIGURES..... | XI |
| LIST OF ABBREVIATIONS..... | XV |
| CHAPTER | |
| I INTRODUCTION..... | 1 |
| 1.1 Development of computer simulations..... | 1 |
| 1.2 Subjects of interest: <i>Ab initio</i> QM/MM-MD Simulations of NH ₄ ⁺ and H ₃ O ⁺ in water..... | 4 |
| II RESEARCH METHODOLOGY..... | 11 |
| 2.1 QM/MM technique..... | 11 |
| 2.2 MD simulation method..... | 13 |
| 2.3 Effects of electron correlation..... | 15 |
| 2.4 MM interactions..... | 20 |
| 2.5 Simulation protocol..... | 24 |
| 2.6 Structural data..... | 25 |

CONTENTS (Continued)

| | Page |
|---|-------------|
| 2.7 Dynamical data..... | 26 |
| 2.7.1 Velocity autocorrelation functions (VACFs)..... | 26 |
| 2.7.2 Mean Residence Times (MRTs) and solvent exchange reactions. | 27 |
| 2.8 Computer softwares and facilities..... | 29 |
| III RESULTS AND DISCUSSION..... | 29 |
| 3.1 <i>Ab initio</i> QM/MM dynamics of NH_4^+ in water..... | 30 |
| 3.1.1 Structural properties..... | 30 |
| 3.1.2 Dynamical properties..... | 42 |
| 3.1.2.1 Translational motions..... | 42 |
| 3.1.2.2 Librational motions..... | 46 |
| 3.1.2.3 Water exchange in the hydration shell of NH_4^+ | 49 |
| 3.2 <i>Ab initio</i> QM/MM dynamics of H_3O^+ in water..... | 54 |
| 3.2.1 Structural properties..... | 54 |
| 3.2.2 Intramolecular geometry..... | 67 |
| 3.2.3 Dynamical properties..... | 69 |
| 3.2.3.1 Translational motions..... | 69 |
| 3.2.3.2 Water exchange in the hydration shell of H_3O^+ | 71 |
| 3.2.3.3 Proton transfer dynamics..... | 75 |
| IV CONCLUSION..... | 79 |
| REFERENCES..... | 82 |

CONTENTS (Continued)

| | Page |
|---|-------------|
| APPENDICES..... | 99 |
| Appendix A Lists of Presentations..... | 100 |
| Appendix B Lists of Publications..... | 102 |
| CIRRICULUM VITAE..... | 115 |

LIST OF TABLES

| Table | Page |
|--|-------------|
| 2.1 Average binding energies (in kcal mol ⁻¹) and average N _{am} -H _{am} ···O _w distances (in Å) of the optimized the NH ₄ ⁺ -(H ₂ O) ₄ complex, calculated at HF, DFT and higher correlated methods..... | 17 |
| 2.2 Structures and binding energies of the optimized H ₃ O ⁺ -(H ₂ O) ₃ complex, calculated at HF, B3LYP and higher correlated methods using DZP basis set..... | 19 |
| 2.3 Optimized parameters of the analytical pair potential for the interaction of water with NH ₄ ⁺ (interaction energies in kcal mol ⁻¹ and distances in Å).... | 21 |
| 2.4 Optimized parameters of the analytical pair potential for the interaction of water with H ₃ O ⁺ (interaction energies in kcal mol ⁻¹ and distances in Å).... | 24 |
| 3.1 Self-diffusion constants for NH ₄ ⁺ and water..... | 44 |
| 3.2 Mean residence times of water molecules in bulk and in the first solvation shell of each of hydrogen atoms of NH ₄ ⁺ , calculated within the H _{am} ···O _w distance of 2.5 Å..... | 53 |
| 3.3 Mean residence time of water molecules in the bulk and in the first hydration shell of the hydrogen atoms of H ₃ O ⁺ , calculated within the first minimum of H _{hy} ···O _w RDF..... | 74 |

LIST OF FIGURES

| Figure | Page |
|--|------|
| 2.1 The QM/MM scheme | 11 |
| 2.2 The MD scheme | 14 |
| 2.3 Comparison of the stabilization energies obtained from the SCF calculations and from the fitted analytical function of $\text{NH}_4^+ \text{-H}_2\text{O}$ | 22 |
| 2.4 Representation of the transition state for the spectrum of solvent of symmetrical ligand exchange process..... | 29 |
| 3.1 a) $\text{N}_{\text{am}}\text{-O}_{\text{w}}$, b) $\text{N}_{\text{am}}\text{-H}_{\text{w}}$, c) $\text{H}_{\text{am}}\text{-O}_{\text{w}}$ and d) $\text{H}_{\text{am}}\text{-H}_{\text{w}}$ RDFs and their corresponding integration numbers..... | 32 |
| 3.2 a) $\text{O}_{\text{w}}\text{-O}_{\text{w}}$, b) $\text{O}_{\text{w}}\text{-H}_{\text{w}}$, c) $\text{H}_{\text{w}}\text{-O}_{\text{w}}$ and d) $\text{H}_{\text{w}}\text{-H}_{\text{w}}$ RDFs and their corresponding integration numbers. The first atom of each pair refers to the atoms of the water molecule, whose oxygen position was defined as center of the QM region during the QM/MM simulation..... | 33 |
| 3.3 Simulated radial pair correlation function a) for nitrogen-oxygen obtained from CP MD simulation and b) for nitrogen-oxygen and nitrogen-hydrogen obtained from PCM MD simulation..... | 34 |
| 3.4 CN distributions, calculated up to the $\text{N}_{\text{am}} \cdots \text{O}_{\text{w}}$ distances of 3.0, 3.5 and 4.0 Å, respectively..... | 36 |

LIST OF FIGURES (Continued)

| Figure | Page |
|---|------|
| 3.5 $O_w \cdots N_{am} \cdots O_w$ angular distributions, calculated up to the $N_{am} \cdots O_w$ distances of 3.0, 3.5 and 5.0 Å, respectively..... | 40 |
| 3.6 $N_{am} - H_{am} \cdots O_w$ angular distributions, calculated up to the $H_{am} \cdots O_w$ distances of 1.8, 2.0 and 2.5 Å, respectively..... | 41 |
| 3.7 $H_{am} - N_{am} \cdots O_w$ angular distributions, calculated within the $N_{am} - O_w$ distance of 3.5 Å..... | 41 |
| 3.8 Distributions of θ , calculated within the $N_{am} \cdots O_w$ distance of 3.5 Å..... | 42 |
| 3.9 Power spectra of the translational motions of NH_4^+ and of water molecules in the bulk and in the hydration shell of the ion, calculated from the center-of-mass VACFs of the ion and water..... | 45 |
| 3.10 Power spectra of the librational motions of NH_4^+ and of water molecules in the bulk and in the hydration shell of the ion, as obtained by the QM/MM simulations..... | 48 |
| 3.11 Mean-square angular displacements of NH_4^+ in water as a function of time..... | 49 |
| 3.12 Water exchange in the first solvation shell of each of hydrogen atoms of NH_4^+ , emphasizing for only the first 8 ps of the QM/MM simulation..... | 50 |
| 3.13 a) $O_{hy} - O_w$ and b) $O_{hy} - H_w$ RDFs and their corresponding integration numbers..... | 56 |

LIST OF FIGURES (Continued)

| Figure | Page |
|--|------|
| 3.14 a) $O_{\text{hy}}-O_{\text{w}}$ radial distribution function and b) Left: the presence of three hydrogen-bonded water molecules; Right: the presence of a fourth neighboring water molecule obtained from the neutron diffraction experimental study..... | 57 |
| 3.15 O^*-O radial distribution functions of the $H_9O_4^+$ and $H_5O_2^+$ structures of H^+ in water obtained from CP-MD simulation..... | 58 |
| 3.16 a) The radial distribution function $gO^*O(r)$ centered around the oxygen O^* carrying the proton. b) The same but computed only for H_3O^+ structures. c) The same for $H_5O_2^+$ structures obtained from MS-EVB simulation. | 59 |
| 3.17 The water-hydronium RDF; gOO from CP-MD simulations using the BLYP (bright blue solid line) and HCTH (black solid line) XC functionals. | 60 |
| 3.18 Distributions of CN, calculated up to an $O_{\text{hy}}\cdots O_{\text{w}}$ distance of 3.2 Å..... | 61 |
| 3.19 Distribution of the angle β between the instantaneous “symmetry” axis of H_3O^+ and the $O_{\text{hy}}\cdots O_{\text{w}}$ distance vector, for $O_{\text{hy}}\cdots O_{\text{w}}$ distances ≤ 3.2 Å..... | 62 |
| 3.20 a) $H_{\text{hy}}-O_{\text{w}}$ and b) $H_{\text{hy}}-H_{\text{w}}$ RDFs and their corresponding integration numbers..... | 64 |
| 3.21 $O_{\text{hy}}-H_{\text{hy}}\cdots O_{\text{w}}$ angular distributions as indicated, calculated for $H_{\text{hy}}\cdots O_{\text{w}}$ distances ≤ 2.0 and ≤ 2.5 Å, respectively..... | 65 |

LIST OF FIGURES (Continued)

| Figure | Page |
|---|-------------|
| 3.22 Distributions of the angle θ , between the intramolecular OH vector and the water dipole vector, for $O_{\text{hy}} \cdots O_{\text{w}}$ distances $\leq 3.2 \text{ \AA}$ | 66 |
| 3.23 Distributions of a) bond lengths and b) bond angles between H_3O^+ and the nearest-neighbor water molecules..... | 68 |
| 3.24 Distributions of the longest intramolecular $O_{\text{hy}}\text{-H}_{\text{hy}}$ bond length (full line) and of the shortest intermolecular $\text{H}_{\text{hy}} \cdots O_{\text{w}}$ distance (dashed line)..... | 69 |
| 3.25 Fourier transformation of the translational VACF of the H_3O^+ ion in water | 71 |
| 3.26 Time dependence of $\text{H}_{\text{hy}} \cdots O_{\text{w}}$ distances..... | 72 |
| 3.27 Time dependence of $O_{\text{hy}}\text{-H}_{\text{hy}}$ bond lengths and $\text{H}_{\text{hy}} \cdots O_{\text{w}}$ distances, selecting only for a 4 ps period..... | 77 |

LIST OF ABBREVIATIONS

| | | |
|----------------|---|---|
| NMR | = | Nuclear Magnetic Resonance |
| QM | = | Quantum Mechanics |
| MM | = | Molecular Mechanics |
| MC | = | Monte Carlo |
| MD | = | Molecular Dynamics |
| CP | = | Car and Parrinello |
| PCM | = | Polarizable Continuum Model |
| MS-EVB | = | Multistate Empirical Valence Bond model |
| QM/MM | = | Combined Quantum Mechanical/Molecular Mechanical method |
| BLYP | = | Becke hybrid functional combined with Lee–Yang–Parr correlation function |
| B3LYP | = | Becke three-parameters hybrid functional combined with Lee–Yang–Parr correlation function |
| DFT | = | Density Functional Theory |
| HF | = | Hartree-Fock |
| $E_{xc}[\rho]$ | = | Exchange-correlation energy |
| MP2 | = | Second-order Møller-Plesset perturbation theory |
| MP4 | = | Møller-Plesset perturbation theory to fourth order |
| MP4(DQ) | = | Møller-Plesset perturbation theory to fourth order in the space of Double and Quadruple substitutions |

LIST OF ABBREVIATIONS (Continued)

| | | |
|--|---|---|
| CI-D | = | Configuration Interaction with all Double substitutions |
| CC-D | = | Coupled Cluster with Doubles excitations |
| CF2 | = | Central Force model version 2 |
| BJH | = | Flexible water model developed by Bopp, Jancsó, and Heinzinger |
| aug-cc-pvtz | = | Augmented, correlation consistent polarized valence triple zeta |
| DZV | = | Double Zeta Valence |
| DZP | = | Double-Zeta plus Polarization |
| BSSE | = | Basis Set Superposition Error |
| H ₂ O | = | Water |
| NH ₄ ⁺ | = | Ammonium ion |
| H ₃ O ⁺ | = | Hydronium ion |
| H ₅ O ₂ ⁺ | = | Zundel complex |
| H ₉ O ₄ ⁺ | = | Eigen complex |
| RNA | = | Ribonucleic Acid |
| PT | = | Proton Transfer |
| RDF | = | Radial Distribution Function |
| ADF | = | Angular Distribution Function |
| VACF | = | Velocity Autocorrelation Function |
| <i>D_{coeff}</i> | = | Self-diffusion coefficient |
| MRT | = | Mean Residence Time |
| CN | = | Coordination Number |

LIST OF ABBREVIATIONS (Continued)

| | | |
|---|---|---|
| ps | = | Pico second |
| fs | = | Femto second |
| Expt. | = | Experiment |
| ° | = | Degree |
| Å | = | Angström |
| kcal mol ⁻¹ | = | Kilocalorie / mole |
| cm ² s ⁻¹ | = | Square centimeter per second |
| rad ² s ⁻¹ | = | Square radian per second |
| E_{tot} | = | Total interactions energy |
| E_{MM} | = | Interaction energy within MM region |
| E_{QM-MM} | = | Interaction energy between QM and MM regions |
| $\langle \Psi_{QM} \hat{H} \Psi_{QM} \rangle$ | = | Interactions within QM region |
| F_i | = | Forces acting on each particle |
| $S_m(r)$ | = | Smoothing function |
| F_{QM} | = | QM Force |
| F_{MM} | = | MM Force |
| r_l | = | Distance characterizing the start of QM region |
| r_0 | = | Distance characterizing the end of QM region |
| E_a | = | Activation energy |
| E_{bond} | = | Bond energy |
| $\Delta E_{NH_4^+ - H_2O}$ | = | Pair potential energy between NH ₄ ⁺ and H ₂ O |

LIST OF ABBREVIATIONS (Continued)

| | | |
|----------------------------|---|--|
| $\Delta E_{H_3O^+ - H_2O}$ | = | Pair potential energy between H_3O^+ and H_2O |
| q | = | Point charge |
| r_{ij} | = | Distances between the i -th site and the j -th site atoms |
| $g_{\alpha\beta}(r)$ | = | Site-site pair correlation functions |
| $N_{\alpha\beta}(r)$ | = | Average of β site located in the shell ($r, r+\Delta r$) centered on α site |
| $n_{\alpha\beta}(r)$ | = | Site-site integration number |
| ρ_β | = | Average number density of β site in the liquid |
| $C(t)$ | = | Time correlation function |
| t_{sim} | = | Simulation time |
| N_{ex} | = | Number of exchange events |
| $R_x, R_y,$ and R_z | = | Rotational motions along $x, y,$ and x axis |
| D_R | = | Rotational diffusion constant |
| $\theta(t)$ | = | An angle formed by a vector in the body-fixed frame at with its initial direction ($\theta=0$ at $t=0$) |
| C_{2v} | = | Symmetry of C_{2v} point group (rotation around C_{2v} axis) |
| C_{3v} | = | Symmetry of C_{3v} point group (rotation around C_{3v} axis) |
| A | = | Associative exchange mechanism |
| I | = | Interchange mechanism |
| D | = | Dissociative exchange mechanism |

LIST OF ABBREVIATIONS (Continued)

| | | |
|---------------------|---|---|
| I_a | = | Associative interchange mechanism |
| I_d | = | Dissociative interchange mechanism |
| $\tau_{H_2O}(H_i)$ | = | MRT of water molecules at each of hydrogen atoms of NH_4^+ (or H_3O^+) |
| $\tau_{H_2O}(H_2O)$ | = | MRT of water molecules in the bulk |

CHAPTER I

INTRODUCTION

1.1 Development of computer simulations

During the past decades, classical statistical mechanics simulations have been employed extensively in the study of pure liquids and solutions, often revealing valuable details of the composition and structure of these systems. The well-established tools for the simulations of atomic or molecular liquids are Monte Carlo (MC) and Molecular Dynamics (MD) methods. While the MC method mainly produces structural and energetic features of a model system, the MD simulation in addition supplies time-dependent properties such as reaction dynamics and vibrational spectra.

According to classical simulations, the basic approach to both MC and MD methods is a separation of interactions between all particles present in the system into contributions of pair, three-body, four-body up to n -body,

$$V_{total} = \sum_{i>j} V(i, j) + \sum_{i>j>k} V(i, j, k) + \dots + \sum_{i>j>k>\dots>n} V(i, j, k, \dots, n) \quad (1.1)$$

Basically, only the first term on the right-hand side has been taken into account, whereas the contributions of the higher n -body interactions are always assumed to be small and by no means negligible. However, it has been well recognized that the higher terms can play a significant role and are not negligible, even for rare gas fluids

(Beaumont, Chihara, and Morrison, 1961; Ermakova, Solca, Huber, and Marx, 1995). Consequently, methodical development to correct the effects of the higher terms has been of interest. In particular for a realistic view of liquids and solutions, it has been shown that the model interaction potential must include polarizability and many-body nonadditive contributions. With regards to this point, various models have been proposed, for example, the Polarizable Continuum Model (PCM) (Tomasi and Persico, 1994), which incorporates the many-body interactions in an average way, or a direct approach, by calculating the energy hypersurface of many-body interactions and then fitting them to an analytical function (Hannongbua, 1997; Probst, Spohr, Heinzinger, and Bopp, 1991). Both exemplary models can provide significant improvement of the results. However, for the PCM model, a major weakness is that it can not reproduce specific interaction with the surrounding solvent, such as hydrogen bonds (Erras-Hanauer, Clark, and Eldik, 2003). For the direct approach, the construction of many-body potentials represents a difficult task, and is hardly feasible for large molecular systems, because of their complicated orientation dependence (Hannongbua, 1997; Natália, Cordeio, and Gomes, 1993). Another approach to implement the contributions of n -body interactions is the first-principle simulation method introduced by Car, and Parrinello (CP) (Car, and Parrinello, 1985). This method has been applied on relatively small systems of 30-50 particles, evaluating forces by means of a simple combination of Becke's 1988 exchange functional and correlation functional by Lee, Yang, and Parr (BLYP) approach. Nevertheless, severe limitation of the CP-MD applicability for the treatment of electrolyte solutions has been well-documented (Ohtaki and Radnai, 1993; Schwenk, Loeffler, and Rode, 2001).

In general, a correct treatment of multiple intermolecular interactions could be obtained by means of *ab initio* quantum mechanics method. However, the full *ab initio* calculation for a condensed-phase system consisting of a large number of molecules is still beyond the current computational feasibility. Consequently, an alternative way is to apply the so-called combined Quantum Mechanical and Molecular Mechanical (QM/MM) method (Atkins, 1994; Bernal and Fowler, 1933; Brancato and Tuckerman, 2005; Conway, 1964; Day et al., 2002; Drukker, de Leeuw, and Hammes-Schiffer, 1998; Eigen, 1964; Hermida-Ramón and Karlström, 2004; Hückel, 1928; Izvekov and Vóth, 2005; James and Wales, 2005; Kebarle, 1977; Kim et al., 2002; Pomès and Roux, 1996; Robinson and Stokes, 1959; von Grothuss, 1806). In recent years, several hybrid QM/MM models, in combination with, for example, semiempirical (Cummins and Gready, 1997; Field, Bash, and Karplus, 1990; Gao, 1996; Warshel, and Levitt, 1976), density functional (Stanton, Hartsough, and Merz, 1995), valence bond (Åqvist and Warshel, 1993; Bernardi, Olivucci, and Robb, 1992), or even *ab initio* Hartree-Fock (HF) (Muller and Warshel, 1995; Singh and Kollman, 1986) methodology with commonly used force fields, have been proposed and successfully applied to various condensed-phase systems. A “Born-Oppenheimer *ab initio* QM/MM-MD” technique has been lately proposed and employed for studying structural and dynamical properties of various ions in solutions (Brooks, Bruccoleri, and Olafson, 1983; Intharathap, Tongraar, and Sagarik, 2005; Kerdcharoen, Liedl, and Rode, 1996; Tongraar, Liedl, and Rode, 1997; Tongraar, Liedl, and Rode, 1998; Tongraar, Sagarik, and Rode, 2001; Tongraar, Sagarik, and Rode, 2002; Tongraar and Rode, 2005; Rode, Schwenk, and Tongraar, 2004; Schwenk, Loeffler, and Rode, 2001; Xenides, Randolph, and Rode, 2005). This

technique treats the active site region, *e.g.*, the solvation shell around ion, quantum mechanically, while the environment consisting of solvent molecules is described by classical pair or pair plus three-body potentials. By this scheme, the complicated many-body contributions within the solvation sphere of the ion can be reliably included. The QM/MM results have clearly shown the important role of non-additive contributions and that inclusion of higher-order interaction terms is essential for the correct description of the solvated ions, even for monovalent metal ions in which many-body interactions could be expected to be weaker than in the case of di- and trivalent ions (Tongraar, Liedl, and Rode, 1998a; Tongraar, Liedl, and Rode, 1998b; Tongraar and Rode, 1999; Tongraar and Rode, 2001; Tongraar and Rode, 2003). For instance, it has been demonstrated that the “structure-breaking” behavior of K^+ in water is only revealed by the QM treatment of the first hydration shell (Tongraar, Liedl, and Rode, 1998a). This finding proved the essential importance for the interpretation of the functionality of the potassium-specific ion channels in cell membranes (Armstrong, 1998; Tongraar, Liedl, and Rode, 1998a).

1.2 Subjects of interest: *Ab initio* QM/MM-MD simulations of NH_4^+ and H_3O^+ in water

Since the QM/MM method has been successfully applied to various ions in aqueous solutions, it is of particular interest to employ this technique to more complicated cations, in particular the ammonium (NH_4^+) and hydronium (H_3O^+) ions, in aqueous solution. The NH_4^+ ion represents an important chemical species which provides a simple model for solvated amides (Perrin and Gipe, 1984; Perrin and Gipe, 1986). In addition, in compactly folded ribonucleic acids (RNAs), coordination or

hydrogen bonding of this ion in specific sites is crucial for its ability to stabilize the RNA fragment structure (Wang, Lu, and Draper, 1993). The detailed interpretation on the structure and dynamics of NH_4^+ in aqueous solution has been studied extensively (Böhm and McDonald, 1984; Brugé, Bernasconi, and Parrinello, 1999a; Brugé, Bernasconi, and Parrinello, 1999b; Chang and Dang, 2003; Dang, 1993; Hewish and Neilson, 1981; Jiang, Chang, Lee, and Lin, 1999; Jorgensen and Gao, 1986; Karim and Haymet, 1990; Kassab, Evleth, and Hamou-Tahra, 1990; Pálinkás, Radnai, Szász, and Heinzinger, 1981; Perrin and Gipe, 1987; Szász and Heinzinger, 1979). Of particular interest, recent Nuclear Magnetic Resonance (NMR) measurements (Perrin and Gipe, 1986; Perrin and Gipe, 1987) have shown that NH_4^+ rotates quite fast in aqueous solution, despite the expected strong hydrogen bonding between the NH_4^+ ion and its surrounding water molecules. To explain such surprising phenomenon, several rotational mechanisms have been proposed based on either *ab initio* geometry optimizations (Brugé et al., 1999a; Jiang et al., 1999; Kassab et al., 1990) as well as MC (Jorgensen and Gao, 1986) and MD simulations (Böhm, and McDonald, 1984; Brugé et al., 1999a; Chang and Dang, 2003; Dang, 1993; Karim and Haymet, 1990; Pálinkás et al., 1981; Szász and Heinzinger, 1979). Most of the previous studies have provided useful information on the dynamical properties of the hydrated NH_4^+ , in particular its fast diffusive rotational motion. However, the agreement on the structure of the first solvation shell of NH_4^+ , which is a necessary prerequisite for understanding its rotational mechanism, is still far from satisfactory. On the structural viewpoint of NH_4^+ in aqueous solution, the most representative picture of the coordination to emerge is of two groups of water molecules. There is a first group of four, which is strongly oriented so as to create nearly linear N-H \cdots O interactions. This

structural aspect is supported by experimental X-ray diffraction (XRD) and neutron diffraction (ND) studies (Hewish and Neilson, 1981; Pálinkás et al., 1981). The second group of water molecules is much less strongly oriented than the first and its structure is a source of major disagreement between the theoretical observations, consisting of 1 to 8 water molecules (Böhm and McDonald, 1984; Brugé et al., 1999a; Chang and Dang, 2003; Dang, 1993; Jorgensen and Gao, 1986; Karim and Haymet, 1990; Pálinkás et al., 1981; Szász and Heinzinger, 1979). Hence, the comprehensive knowledge of how NH_4^+ interacts with water molecules remains incomplete.

Recently, PCM-MD simulation (Chang and Dang, 2003) has been performed, providing a qualitative prediction on the rotational dynamics of NH_4^+ in water which is in good agreement with experimental observations. However, it has been demonstrated that the contributions of the ion's polarizability are not directly obtainable since there is no direct measurement of this quantity in aqueous solution, and the available data are usually extrapolations from ionic crystal and salt solutions (Coker, 1976; Jungwirth and Tobias, 2002; Pyper, Pike, and Edwards, 1992; Tobias, Jungwirth, and Parrinello, 2001). Another attempt to obtain a reliable picture of NH_4^+ in water is based on CP-MD simulation (Brugé et al., 1999b). However, this CP-MD simulation has been performed with respect to density functional theory (DFT) at the BLYP level and has been applied on a relatively small system of one NH_4^+ and 63 water molecules, which has been documented as a severe limitation of the CP-MD applicability for the treatment of electrolyte solutions (Schwenk, Loeffler, and Rode, 2001; Rode, Schwenk, and Tongraar, 2004). In addition, although both PCM- and CP-MD approaches can provide quite reasonable detailed information on the rotational dynamics of NH_4^+ in water, the observed corresponding coordination numbers of 5.8

(Chang and Dang, 2003) and 5.3 (Brugé et al., 1999b) are considerably low when compared to the results from XRD measurement (Pálinkás et al., 1981).

Besides the NH_4^+ ion, H_3O^+ is also one of most fundamental ions, which has been widely used as a model system for understanding proton (H^+) migration in liquid water (Agmon, 1995; Brancato and Tuckerman, 2005; Brodskaya, Lyubartsev, and Laaksonen, 2002; Cheng, 1998; Christie and Jordan, 2001; Day, Soudackov, Čuma, Schmitt, and Voth, 2002a; Hermida-Ramón and Karlström, 2004; Izvekov and Voth, 2005; James and Wales, 2005; Karlström, 1988; Kim, Schmitt, Gruetzmacher, Voth, and Scherer, 2002; Kochanski, 1985; Lapid, Agmon, Petersen, and Voth, 2005; Lobaugh and Voth, 1996; Marx, Tuckerman, Hutter, and Parrinello, 1999; Ruff and Frierich, 1972; Sagnella and Tuckerman, 1998; Schmitt and Voth, 1998; Schmitt and Voth, 1999; Tuckerman, Laasonen, Sprik, and Parrinello, 1995a; Tuckerman, Laasonen, Sprik, and Parrinello, 1995b; Tuckerman, Marx, Klein, and Parrinello, 1997; Vuilleumier and Borgis, 1997; Vuilleumier and Borgis, 1998a; Vuilleumier and Borgis, 1998b; Vuilleumier and Borgis, 1999; Wang and Voth, 2005; Wei and Salahub, 1994) as well as proton transfer (PT) in proteins embedded in membranes (Drukker, de Leeuw, and Hammes-Schiffer, 1998; Pomès and Roux, 1996). One particularly interesting issue comes from the anomalously high mobility of H^+ in aqueous solution, compared to other cations (Atkins, 1994; Robinson and Stokes, 1959). To describe such fast H^+ mobility, numerous PT mechanisms (Agmon, 1995; Bernal and Fowler, 1933; Conway, 1964; Eigen, 1964; Hückel, 1928; Tuckerman, Laasonen, Sprik, and Parrinello, 1995a; Tuckerman, Laasonen, Sprik, and Parrinello, 1995b; Tuckerman, Marx, Klein, and Parrinello, 1997) have been proposed. The mobility of H^+ in water has been generally regarded as a combination of H^+ jumping

between different water molecules and diffusion of the entire protonated water complexes through the hydrogen bond network. The former type of the PT process is much faster and known as the Grotthuss structural diffusion mechanism (von Grotthuss, 1806), in which the charge migration is characterized by successive jumps of H^+ from one oxygen site to the next, while in the latter type, the hydrated H_3O^+ complex diffuses through water in a way similar to other simple ions.

In experiments, attempts have been made to elucidate the microstructure as well as the dynamical properties of excess H^+ in water (Conway, 1964; Giguere, 1981; Kebarle, 1977). However, the behavior of the hydrated H^+ has not yet been clarified unambiguously, since it is rather difficult to prepare protonated water clusters for experimental observations. Furthermore, the structure of these clusters depends strongly on the neighboring water molecules (Headrick et al., 2005). Recently, the solvation structure of H_3O^+ in water has been examined experimentally using ND with hydrogen isotope substitution (Botti, Bruni, Imberti, Ricci, and Soper, 2005). It was suggested that each H^+ is part of a quite stable H_3O^+ ion which preferentially hydrogen-bonds to three nearest-neighbor water molecules. Fourth water molecule could be observed near the oxygen side of the H_3O^+ ion, exhibiting strong orientational correlations with the ion.

A number of theoretical studies have provided microscopic details on the nature of the H_3O^+ solvation, as well as on the mechanism of PT in water (Agmon, 1995; Brancato and Tuckerman, 2005; Brodskaya et al., 2002; Cheng, 1998; Christie and Jordan, 2001; Day et al., 2002; Hermida-Ramón and Karlström, 2004; Izvekov and Voth, 2005; James and Wales, 2005; Karlström, 1988; Kim et al., 2002; Kochanski, 1985; Lapid et al., 2005; Lobaugh and Voth, 1996; Marx et al., 1999; Ruff and

Frierich, 1972; Sagnella and Tuckerman, 1998; Schmitt and Voth, 1998; Schmitt and Voth, 1999; Tuckerman, Laasonen, Sprik, and Parrinello, 1995a; Tuckerman, Laasonen, Sprik, and Parrinello, 1995b; Tuckerman, Marx, Klein, and Parrinello, 1997; Vuilleumier and Borgis, 1997; Vuilleumier and Borgis, 1998a; Vuilleumier and Borgis, 1998b; Vuilleumier and Borgis, 1999; Wang and Voth, 2005; Wei and Salahub, 1994). Based on theoretical investigations, it has been postulated that the Eigen (H_9O_4^+) and Zundel (H_5O_2^+) complexes are the primarily important species in PT process. Early computer simulations (Kornyshev, Kuznetsov, Spohr, and Ulstrup, 2003; Tuckerman, Laasonen, Sprik, and Parrinello, 1995a; Tuckerman, Laasonen, Sprik, and Parrinello, 1995b; Vuilleumier and Borgis, 1998b; Vuilleumier and Borgis, 1999) indicated that the mechanism for the PT process in water involves a concerted double PT event, *e.g.*, a conversion of one H_5O_2^+ moiety into another directly, without a special involvement of H_3O^+ . In recent CP path-integral simulations (Tuckerman, Marx, Klein, and Parrinello, 1997), however, it was demonstrated that H^+ migration involves a concerted single PT event, *i.e.*, the more stable H_3O^+ is converted into the slightly less stable H_5O_2^+ and vice versa. This inter-conversion is coupled to hydrogen bond dynamics in the second solvation shell of H_3O^+ . With respect to the CP studies (Tuckerman, Laasonen, Sprik, and Parrinello, 1995a; Tuckerman, Laasonen, Sprik, and Parrinello, 1995b; Tuckerman, Marx, Klein, and Parrinello, 1997), some methodical drawbacks might come from the use of relatively small number of water molecules in the simulation and from the quality of the density functionals employed in the calculation of the electronic structure. An empirical approach to describe the structural diffusion mechanism of PT is based on multistate empirical valence bond (MS-EVB) models (Brancato and Tuckerman, 2005; Lapid et al., 2005; Lobaugh and

Voth, 1996; Schmitt and Voth, 1998; Schmitt and Voth, 1999; Vuilleumier and Borgis, 1997; Vuilleumier and Borgis, 1998a; Vuilleumier and Borgis, 1998b; Vuilleumier and Borgis, 1999; Wang and Voth, 2005), which provides H^+ delocalization among several water molecules in a classical force field. In most recent MS-EVB studies (Day et al., 2002; Schmitt and Voth, 1998; Schmitt and Voth, 1999), it has been shown that H_3O^+ is more stable (longer living) than $H_5O_2^+$, and thus the single PT event appears to be the most probable. However, there are some significant differences between the simulation results obtained from the MS-EVB potentials (Brodszkaya et al., 2002; Day et al., 2002; James and Wales, 2005; Lapid et al., 2005; Schmitt and Voth, 1998; Schmitt and Voth, 1999; Vuilleumier and Borgis, 1997; Vuilleumier and Borgis, 1998a; Vuilleumier and Borgis, 1998b; Vuilleumier and Borgis, 1999), due to the valence bond states employed in the models (Lapid et al., 2005).

Since previous theoretical and experimental studies have provided rather inhomogeneous picture of NH_4^+ and H_3O^+ in water, the motivation of this work was to obtain more reliable information on the structure and dynamics of these hydrated complexes. In the present study, the MD simulations based on *ab initio* QM/MM scheme were applied in the investigation of NH_4^+ and H_3O^+ in aqueous solution.

CHAPTER II

RESEARCH METHODOLOGY

2.1 QM/MM technique

By the QM/MM technique (Intharathep, Tongraar, and Sagarik, 2005; Kerdcharoen, Liedl, and Rode, 1996; Rode et al., 2004; Schwenk, Loeffler, and Rode, 2001; Tongraar, Liedl, and Rode, 1997; Tongraar, Liedl, and Rode, 1998a; Tongraar and Rode, 2004; Tongraar and Rode, 2005; Tongraar, Sagarik, and Rode, 2001; Tongraar, Sagarik, and Rode, 2002; Xenides, Randolph, and Rode, 2005), the system is partitioned into two parts, namely Quantum Mechanics (QM) and Molecular Mechanics (MM) regions (see Figure 2.1).

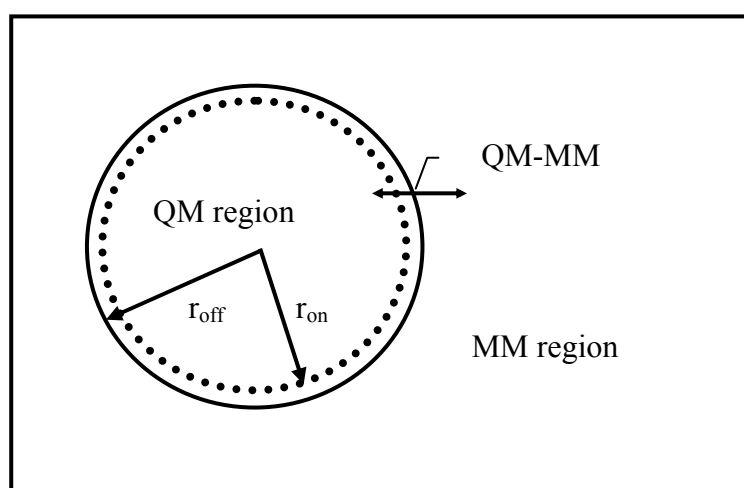


Figure 2.1 The QM/MM scheme

The QM region, the chemically most important region which includes a solute and its surrounding water molecules, is treated quantum mechanically, while the MM region is described by classical pair potentials. Accordingly, the total interaction energy of the system can be divided into three components,

$$E_{total} = \langle \Psi_{QM} | \hat{H} | \Psi_{QM} \rangle + E_{MM} + E_{QM-MM}, \quad (2.1)$$

where $\langle \Psi_{QM} | \hat{H} | \Psi_{QM} \rangle$ refers to the interactions within the QM region, while E_{MM} and E_{QM-MM} represent the interactions within the MM and between the QM and MM regions, respectively.

During the QM/MM simulation, exchange of water molecules between the QM and MM regions can occur frequently. With regards to this point, the forces acting on each particle in the system are switched according to which region the water molecule is entering or leaving and can be defined as

$$F_i = S_m(r)F_{QM} + (1 - S_m(r))F_{MM} \quad (2.2)$$

where F_{QM} and F_{MM} are QM and MM forces, respectively. $S_m(r)$ is a smoothing function (Brooks et al., 1983),

$$\begin{aligned} S_m(r) &= 1, & \text{for } r \leq r_1, \\ S_m(r) &= \frac{(r_0^2 - r^2)(r_0^2 + 2r^2 - 3r_1^2)}{(r_0^2 - r_1^2)^3}, & \text{for } r_1 < r \leq r_0, \\ S_m(r) &= 0, & \text{for } r > r_0, \end{aligned} \quad (2.3)$$

where r_1 and r_0 are distances characterizing the start and the end of the QM region, applied within an interval of 0.2 Å to ensure a continuous change of forces at the transition between the QM and MM regions.

2.2 MD simulation method

The MD technique is a very powerful tool for the study of complex matter systems, in a variety of states such as crystals, aqueous solution and in gas phase (Ciccotti, Frenkel, and McDonald, 1987; Ciccotti and Hoover, 1986; Halley, 1978; McCommon and Harvey, 1987). It provides a direct route from the microscopic details, which are not directly obtainable in real experiments, to macroscopic properties of experimental interest. This makes the MD simulation becomes very attractive for material science since realistic models of the structure and other properties of materials can be studied by this technique. The common scheme to perform the MD simulation is summarized in Figure 2.2. The actual simulation starts with reading in the starting configurations, velocities, accelerations and forces. The initial configuration has two simple forms, one using the random configurations and the other starting from a lattice. The essential condition of the simulation is that there are no explicitly time-dependent or velocity dependent forces that shall act on the system. In practice, the trajectories cannot be directly obtained from Newton's equation. Therefore, the time integration algorithm will be used to obtain the knowledge of positions, velocities and accelerations of two successive time steps. The energy of the system can be calculated using either the MM or QM method. The force on an atom can be calculated from the derivative of the energy with respect to the change in the atom's position. The particles will be moved by their new forces to the new configurations and the steps will be repeated until the system reaches equilibrium. Then the coordinates, velocities, accelerations, forces and so on are collected for

further structural and dynamical properties calculations. In general, only positions and velocities are usually stored since most of the important and interesting properties can be obtained from these two quantities.

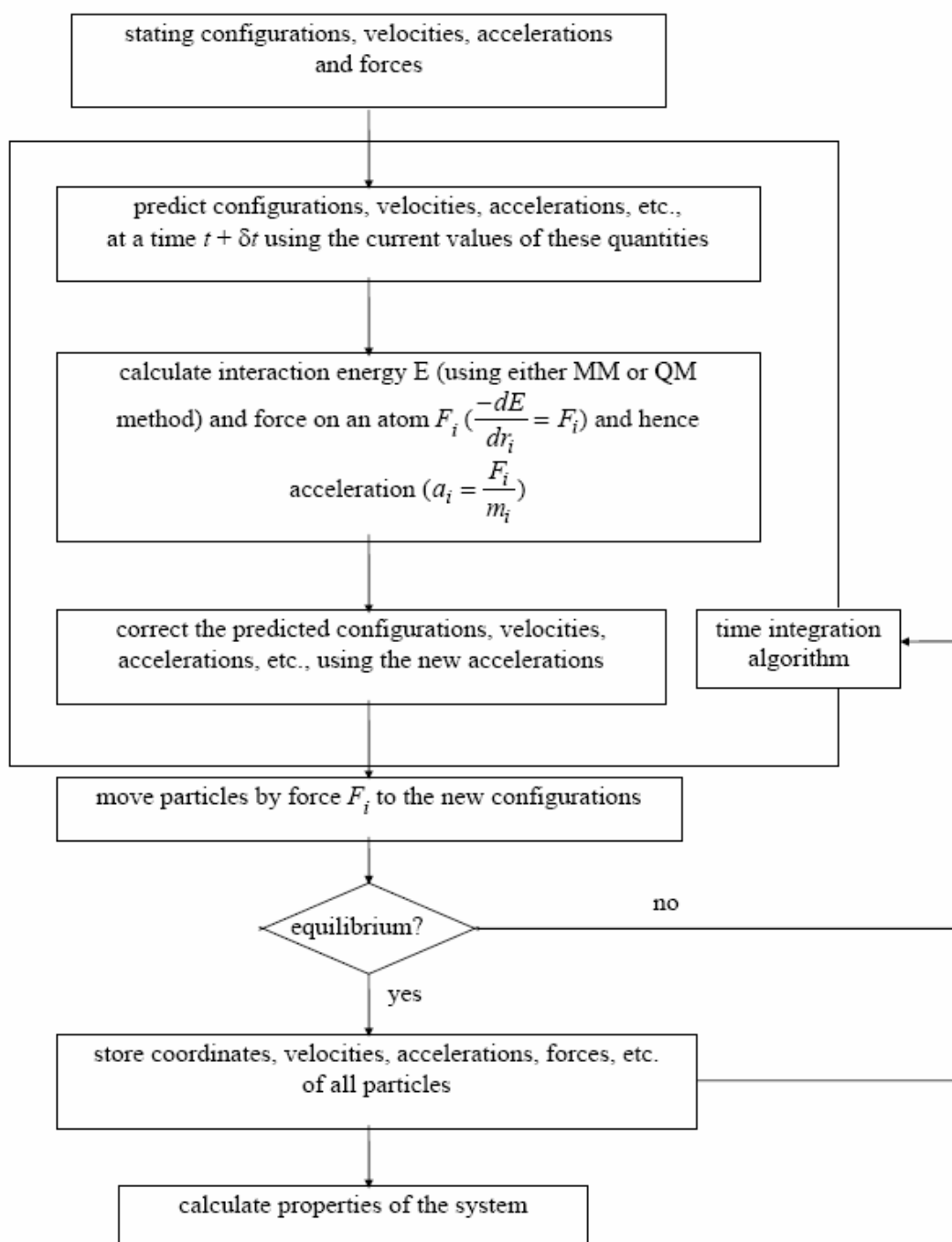


Figure 2.2 The MD scheme.

2.3 Effects of electron correlation

The reliability of the QM/MM results, besides the statistical requirement of a sufficiently long simulation trajectory for adequately sampling phase space, depends crucially on the QM level of theory, *i.e.*, whether or not electron correlation is taken into account, the choice of the basis set and the size of the QM region. In general, the inclusion of electron correlation in the QM calculations can substantially improve the quality of the results. In practice, however, this procedure is extremely time-consuming. In the case of NH_4^+ in water, in order to estimate the effects of electron correlation, geometry optimizations of the $\text{NH}_4^+(\text{H}_2\text{O})_4$ complexes were conducted using *ab initio* calculations at different levels of theory. The average binding energies with Basis Set Superposition Error (BSSE) correction (Boy and Bernardi, 1970), and the average $\text{N}_{\text{am}}\text{-H}_{\text{am}}\cdots\text{O}_{\text{w}}$ distances in the $\text{NH}_4^+(\text{H}_2\text{O})_4$ complex, calculated at the HF, DFT and higher correlated levels, such as second-order Møller-Plesset (MP2), Møller-Plesset theory to the 4th order in the space of double and quadruple substitutions (MP4-DQ), Coupled Cluster with Doubles excitations (CC-D) and Configuration Interaction with all Double substitutions (CI-D), using Double Zeta Valence (DZV) and Double Zeta plus Polarization function (DZP) (Dunning, and Hay, 1976) basis sets were summarized in Table 2.1. The QM calculations with the DZP basis set were carried out in order to provide a systematic comparison of the effects of electron correlation, as well as to critically evaluate the adequacy of the DZV basis set employed in the present QM/MM-MD simulation. In comparison to the results of the highly correlated methods, the neglect of electron correlation in the HF calculations yields slightly weaker binding energies with slightly larger $\text{N}_{\text{am}}\text{-H}_{\text{am}}\cdots\text{O}_{\text{w}}$ distances. In opposite direction, the DFT calculations, either with BLYP or B3LYP functional,

yield stronger binding energies and significantly short $N_{\text{am}}-H_{\text{am}}\cdots O_{\text{w}}$ distances, most probably caused by an overestimation of the correlation energy. This could be one of the reasons why the previous CP-MD study (Brugé et al., 1999b), using BLYP functional, yielded a rather high rigidity of the NH_4^+ hydrate complex. In general, the main advantage of the DFT, over the HF formalism, is that it uses the exchange-correlation operator instead of the exchange operator and so it partially includes electron correlation according to the $E_{\text{xc}}[\rho]$ (exchange-correlation energy) functional. However, since the extent of electron correlation included in the DFT calculations is not exactly known, lower coordination numbers and the overly rigid structures were frequently found when applying this method, especially for the treatment of ionic solutions (Hofer and Rode, 2004; Rode et al., 2004; Schwenk, Hofer, and Rode, 2004; Schwenk, Loeffler, and Rode, 2001; Schwenk and Rode, 2003). From the data obtained in Table 2.1, it could be assumed, therefore, that the effects of electron correlation would have a minor influence on the $\text{NH}_4^+-\text{H}_2\text{O}$ interactions, and that the *ab initio* calculations at the HF level using DZV basis set are accurate enough to produce reliable structure and dynamics details of the hydrated NH_4^+ . On the other hand, a comparison of the HF calculations with the DFT results with their inherent tendency towards lower coordination numbers and a too rigid hydration shell appeared also helpful in order to estimate the methodical boundaries.

Table 2.1 Average binding energies (in kcal mol⁻¹) and average $N_{am}-H_{am}\cdots O_w$ distances (in Å) of the optimized $NH_4^+-(H_2O)_4$ complex, calculated at HF, DFT and higher correlated methods.

| Method | DZV Basis set | | DZP Basis set | |
|--------|---|-----------------------------------|---|--------------------------------------|
| | E_{bond} (kcal mol ⁻¹) | $R_{N_{am}-H_{am}\cdots O_w}$ (Å) | E_{bond} (kcal mol ⁻¹) | $R_{N_{am}-H_{am}\cdots O_w}$ (Å) |
| HF | -19.40 | 1.83 | -16.19 | 1.90 |
| BLYP | -21.61 | 1.74 | -18.26 | 1.78 |
| B3LYP | -21.89 | 1.74 | -18.44 | 1.78 |
| MP2 | -19.69 | 1.82 | -17.25 | 1.81 |
| MP4-DQ | -19.68 | 1.81 | -16.78 | 1.84 |
| CC-D | -19.70 | 1.82 | -16.73 | 1.84 |
| CI-D | -19.57 | 1.81 | -16.58 | 1.85 |

E_{bond} = average binding energy of the $NH_4^+-(H_2O)_4$ complex

$R_{N_{am}-H_{am}\cdots O_w}$ = average distance between the hydrogen atoms of NH_4^+ and oxygen atoms of water molecules

Energies in kcal mol⁻¹ and distances in Å

For H_3O^+ in water, the optimized structures and binding energies of the H_3O^+ - $(\text{H}_2\text{O})_3$ complex, calculated at HF, B3LYP and higher correlated levels using DZP basis set (Dunning and Hay, 1976; Hay and Wadt, 1985) with BSSE correction, were summarized in Table 2.2. The DZP basis set was chosen since it was also employed in the present QM/MM simulation. In general, it is known that the use of larger basis set is a key factor for obtaining better results, *i.e.*, closer to experimental data. However, the use of large basis set in the QM calculations requires extensive central processing unit (CPU) time. In this work, the DZP basis set was considered to be large enough with respect to the available computational facility. In terms of the binding energies, an order of $\text{HF} > \text{MP4-DQ} \approx \text{CC-D} \approx \text{CI-D} > \text{MP2} > \text{B3LYP}$ was observed. In comparison with the results of the highly correlated methods, the neglect of electron correlation at the HF level results in a slight weakening of the binding energies. In contrast, the B3LYP calculations, although they provide reasonable geometries, predict too strong ion-water interactions, most probably due to an overestimation of the correlation energy (Intharathap et al., 2005; Rode et al., 2004). From the data displayed in Table 2.2, the contributions of the electron correlation to the binding energies were estimated to be about 5%. However, in light of the fact that the computational expense even for the simplest correlated method (MP2) is significant, it was decided to limit the calculations to the HF level and instead chose a larger size of the QM region. Moreover, it has been shown in a recent QM/MM simulation of pure water (Xenides et al., 2005), that the HF method with a sufficiently large QM region could provide detailed information of pure water in good agreement with the MP2-based simulation.

Table 2.2 Structures and binding energies of the optimized $\text{H}_3\text{O}^+(\text{H}_2\text{O})_3$ complex, calculated at HF, B3LYP and higher correlated methods using DZP basis set.

| Method | ΔE (kcal mol ⁻¹) | $\angle\text{H}_{\text{hy}}\text{-O}_{\text{hy}}\text{-H}_{\text{hy}}$ (°) | $\text{O}_{\text{hy}}\text{-H}_{\text{hy}}$ (Å) | $\text{O}_{\text{hy}}\cdots\text{O}_{\text{w}}$ (Å) |
|--------|--------------------------------------|--|---|---|
| HF | -76.917 | 112.90 | 1.03 | 2.56 |
| B3LYP | -90.365 | 114.19 | 1.02 | 2.54 |
| MP2 | -82.696 | 113.08 | 1.01 | 2.55 |
| MP4-DQ | -79.580 | 113.29 | 1.00 | 2.56 |
| CC-D | -79.403 | 113.25 | 1.00 | 2.56 |
| CI-D | -80.737 | 114.26 | 0.99 | 2.56 |

ΔE = binding energy

$\angle\text{H}_{\text{hy}}\text{-O}_{\text{hy}}\text{-H}_{\text{hy}}$ = average H-O-H bond angle of H_3O^+

$\text{O}_{\text{hy}}\text{-H}_{\text{hy}}$ = average O-H bond length of H_3O^+

$\text{O}_{\text{hy}}\cdots\text{O}_{\text{w}}$ = distance between oxygen atom of H_3O^+ and oxygen atoms of water molecules

Energies in kcal mol⁻¹ and distances in Å

2.4 MM interactions

For the interactions within the MM and between the QM and MM regions, flexible model, which describes intermolecular (*e.g.* the central force model version 2 (CF2) developed by Bopp, Jancsó, and Heinzinger, 1983), and intramolecular (*e.g.* the flexible Bopp, Jancsó, and Heinzinger (BJH) water model developed by Stillinger and Rahman, 1978) interactions, was employed for water. The use of flexible model is favored over any of the popular rigid water models, in order to ensure a compatibility and a smooth transition, when water molecules move from the QM region with their full flexibility to the MM region. For the NH_4^+ - H_2O interactions, the pair potential was newly constructed using augmented correlation consistent polarized valence triple zeta (aug-cc-pvtz) basis set (Dunning, 1989; Kendall, Dunning, and Harrison, 1992; Woon and Dunning, 1993). With respect to a symmetric tetrahedral geometry of the NH_4^+ ion, 878 HF interaction energy points for various NH_4^+ - H_2O configurations, obtained from Gaussian98 (Frisch et al., 1998) calculations, were fitted to an analytical form of

$$\Delta E_{\text{NH}_4^+-\text{H}_2\text{O}} = \sum_{i=1}^5 \sum_{j=1}^3 \left[\frac{A_{ij}}{r_{ij}^5} + \frac{B_{ij}}{r_{ij}^7} + C_{ij} \exp(-D_{ij} r_{ij}) + \frac{q_i q_j}{r_{ij}} \right] \quad (2.4)$$

where A , B , C and D are the fitting parameters (see Table 2.3), r_{ij} denotes the distances between the i -th atoms of NH_4^+ and the j -th atoms of water molecule. q_i and q_j are atomic net charges. The Mulliken charges on N and H of NH_4^+ were obtained from *ab initio* calculations using aug-cc-pvtz basis set, where those on O and H of water molecule were adopted from the CF2 model (Bopp et al., 1983). They were set to -0.5186 , 0.3796 , -0.6598 and 0.3299 , respectively.

Table 2.3 Optimized parameters of the analytical pair potential for the interaction of water with NH_4^+ (interaction energies in kcal mol^{-1} and distances in \AA).

| Pair | <i>A</i> ($\text{kcal mol}^{-1} \text{\AA}^5$) | <i>B</i> ($\text{kcal mol}^{-1} \text{\AA}^7$) | <i>C</i> (kcal mol^{-1}) | <i>D</i> (\AA^{-1}) |
|--|---|---|--|-----------------------------------|
| $\text{N}_{\text{am}}\text{-O}_{\text{w}}$ | 305.5759 | 3783.8268 | -1794.3299 | 2.1408 |
| $\text{N}_{\text{am}}\text{-H}_{\text{w}}$ | -3508.8159 | 1388.9633 | 10361.9735 | 2.5057 |
| $\text{H}_{\text{am}}\text{-O}_{\text{w}}$ | -349.7620 | 176.0625 | -9493.4261 | 3.7945 |
| $\text{H}_{\text{am}}\text{-H}_{\text{w}}$ | 27.0492 | 23.9161 | -31.5685 | 1.0399 |

With respect to the construction of pair potential for describing $\text{NH}_4^+\text{-H}_2\text{O}$ interactions, the procedure to generate $\text{NH}_4^+\text{-H}_2\text{O}$ configurations as well as samples of comparison between the stabilization energies obtained from the SCF calculations and from the fitted analytical function is given in Figure 2.3. This procedure is also employed for the construction of $\text{H}_3\text{O}^+\text{-H}_2\text{O}$ pair potential (see next paragraph).

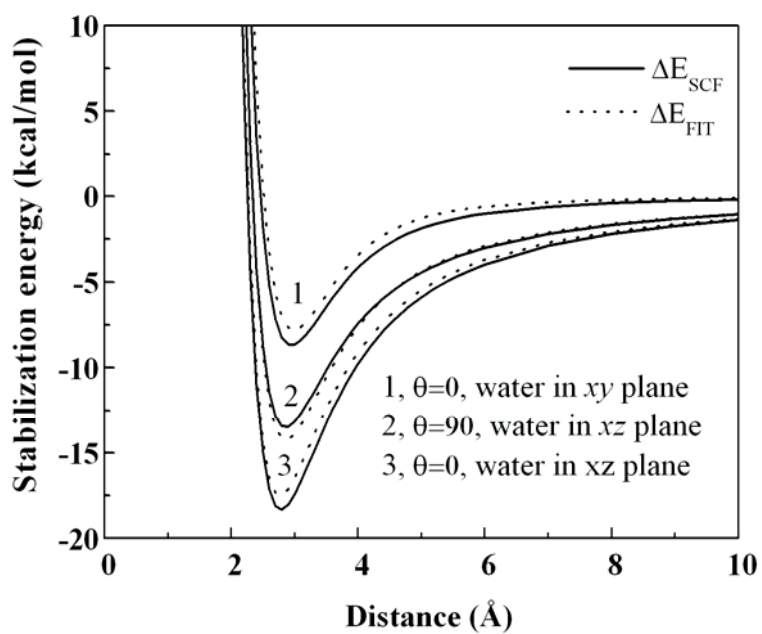
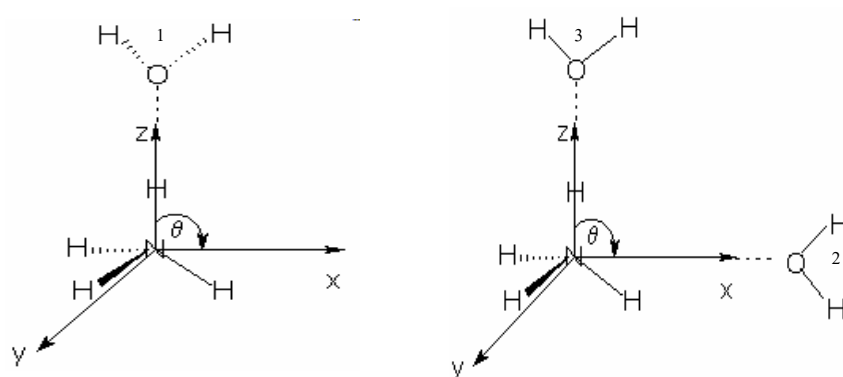


Figure 2.3 Comparison of the stabilization energies obtained from the SCF calculations and from the fitted analytical function of $\text{NH}_4^+ \text{-H}_2\text{O}$.

The pair potential function for describing the H_3O^+ - H_2O interactions was also newly constructed. The 4,056 MP2 interaction energy points for various H_3O^+ - H_2O configurations, obtained from Gaussian98 (Frisch et al., 1998) calculations using the aug-cc-pvtz basis set (Dunning, 1989; Kendall et al., 1992; Woon and Dunning, 1993), were fitted to a formula of

$$\Delta E_{\text{H}_3\text{O}^+ - \text{H}_2\text{O}} = \sum_{i=1}^4 \sum_{j=1}^3 \left[\frac{A_{ij}}{r_{ij}^6} + \frac{B_{ij}}{r_{ij}^8} + C_{ij} \exp(-D_{ij} r_{ij}) + \frac{q_i q_j}{r_{ij}} \right] \quad (2.5)$$

where A , B , C and D are fitting parameters (see Table 2.4). r_{ij} denotes the distances between the i -th atom of H_3O^+ and the j -th atom of water molecule. q_i and q_j are atomic net charges. The Mulliken charges on O and H of H_3O^+ were obtained from *ab initio* calculations using aug-cc-pvtz basis set, whereas the charges on O and H of water were taken from the flexible water model (Bopp et al., 1983; Stillinger and Rahman, 1978). They were set to -0.0861 , 0.3617 , -0.6598 and 0.3299 , respectively. The use of Mulliken charges, for the Coulombic terms in the construction of potential function, is one of acceptable procedures employed in almost all of such investigations published over the past decades (Intharathep et al., 2005; Kerdcharoen et al., 1996; Rode et al., 2004; Schwenk, Loeffler, and Rode, 2001; Tongraar, Liedl, and Rode, 1997; Tongraar, Liedl, and Rode, 1998a; Tongraar, Liedl, and Rode, 1998b; Tongraar and Rode, 2004; Tongraar and Rode, 2005; Tongraar, Sagarik, and Rode, 2001; Tongraar, Sagarik, and Rode, 2002; Xenides et al., 2005). It is known that through the ion-water interactions, these values change, but this effect will partially be compensated by the other terms in the potential during fitting to the *ab initio* energy surfaces.

Table 2.4 Optimized parameters of the analytical pair potential for the interaction of water with H_3O^+ (interaction energies in kcal mol^{-1} and distances in \AA).

| Pair | A ($\text{kcal mol}^{-1} \text{\AA}^6$) | B ($\text{kcal mol}^{-1} \text{\AA}^8$) | C (kcal mol^{-1}) | D (\AA^{-1}) |
|--|--|--|-----------------------------------|------------------------------|
| $\text{O}_{\text{hy}}\text{-O}_{\text{w}}$ | 13765.0507 | -24306.2865 | -1855.9251 | 1.5601 |
| $\text{H}_{\text{hy}}\text{-O}_{\text{w}}$ | 262.9355 | -138.8278 | -2112.6279 | 2.9810 |
| $\text{O}_{\text{hy}}\text{-H}_{\text{w}}$ | 149.5560 | -128.6074 | -2.9463 | 0.5078 |
| $\text{H}_{\text{hy}}\text{-H}_{\text{w}}$ | -30.9738 | 16.3171 | 1212.4652 | 3.8320 |

2.5 Simulation protocol

All QM/MM MD simulations were performed in a canonical ensemble at 298 K. The temperature of the ensemble was kept constant using the Berendsen algorithm (Berendsen, Postma, van Gunsteren, DiNola, and Haak, 1984), with a relaxation time of 0.1 ps. The cubic box, with a box length of 18.17 \AA , contains one ion (NH_4^+ or H_3O^+) and 199 water molecules with periodic boundary conditions. The Newtonian equations of motion were treated by a general predictor-corrector algorithm and the time step was set to 0.2 fs, which allowed for explicit movement of hydrogen atoms of NH_4^+ , H_3O^+ and water. The reaction-field method (Adams, Adams, and Hills, 1979) was employed for the calculation of long-range interactions.

Since the QM region is the most expensive computational part, selection of QM size is a crucial point. To estimate the size of the QM region, the systems were initially equilibrated by performing classical MD simulations, *i.e.*, the simulations

which employed only pair potentials. According to the pair potential simulations (data not shown), the first minimum of the $N_{\text{am}}\text{-O}_w$ and $\text{O}_{\text{hy}}\text{-O}_w$ peaks with respect to $N_{\text{am}}\text{-O}_w$ (for NH_4^+ -water system) and $\text{O}_{\text{hy}}\text{-O}_w$ (for H_3O^+ -water system) radial distribution functions (RDFs, see section 2.6), are located at distance around 3.8 Å. Therefore, a QM region with a diameter of 7.6 Å was chosen, assuming to be large enough to ensure a smooth convergence of the QM forces to the pair potential forces beyond the QM region. There are about 10-14 water molecules within these regions. The QM/MM simulations were started with the system's re-equilibration for 30,000 time steps, followed by another 80,000 (for NH_4^+ -water system) and 100,000 (for H_3O^+ -water system) time steps to collect configurations every 10th step.

2.6 Structural data

The structure of hydrated NH_4^+ and H_3O^+ will be discussed in terms of set of site-site pair correlation functions,

$$g_{\alpha\beta}(r) = N_{\alpha\beta}(r)/(4\pi r^2 \Delta r \rho_\beta) \quad (2.6)$$

where $N_{\alpha\beta}(r)$ is the average number of β sites located in the shell $(r, r + \Delta r)$ centered on site α , and $\rho_\beta = \frac{N_\beta}{V}$ is the average number density of β sites in the liquid. This function is well-known as radial distribution functions (RDFs) and the corresponding integration number is defined as

$$n_{\alpha\beta}(r) = 4\pi\rho_\beta \int_0^r g_{\alpha\beta}(r') r'^2 dr' \quad (2.7)$$

In addition, the detailed information on the ion-water hydrogen-bond interactions as well as the orientation of water molecules surrounding the ions can be explained in terms of angular distribution functions (ADFs).

2.7 Dynamical data

2.7.1 Velocity Autocorrelation Functions (VACFs)

Dynamic properties, such as translational, librational and vibrational frequencies of the species in the systems can be described by evaluation of VACFs.

The normalized VACFs is defined by

$$C(t) = \frac{\sum_i^{N_t} \sum_j^{N} \vec{v}_j(t_i) \vec{v}_j(t_i + t)}{N_t N \sum_i^{N_t} \sum_j^{N} \vec{v}_j(t_i) \vec{v}_j(t_i)} = \frac{\langle \vec{v}_j(0) \vec{v}_j(t) \rangle}{\langle \vec{v}_j(0)^2 \rangle} \quad (2.8)$$

where \vec{v}_j is the instantaneous velocity; t is the correlation length; N is the number of particles; N_t is the number of time origin t_i . $\langle \rangle$ donates the ensemble average. The correlation length was usually set to 2 ps and a gap of 10-50 time steps between time origins was chosen. To compare with experiments, the time-correlation function ($C(t)$) is transformed to produce a spectrum ($\hat{C}(\omega)$) using Fourier transformation,

$$\hat{C}(\omega) = \int_{-\infty}^{+\infty} C(t) \exp(-i\omega t) dt = \int_{-\infty}^{+\infty} C(t) \cos \omega t dt = 2 \int_0^{\infty} C(t) \cos \omega t dt \quad (2.9)$$

For more details, see Appendix D in “Computer Simulation of Liquids” (Allen and Tildesley, 1990).

2.7.2 Mean Residence Times (MRTs) and solvent exchange reactions

During the *ab initio* QM/MM MD simulations, trajectories of each of species in the systems were monitored. The rate of water exchange processes at the ions was evaluated through the mean residence time (MRT) of the water molecules. In this work, the MRT values were calculated using a “direct” method (Hofer, Tran, Schwenk, and Rode, 2004). By this method, the whole trajectories were scanned for movements of ligands, either leaving or entering a coordination shell. Whenever a ligand crosses the boundaries of this shell, its further path is followed, and if its new placement outside/inside the shell lasts for more than t^* , the event is accounted as “real” exchange process. MRT is computed as

$$MRT(\tau) = \frac{CN \times t_{sim}}{N_{ex}} \quad (2.10)$$

where CN is the product of the average number of ligand in that shell; t_{sim} is the duration of the simulation; N_{ex} equals to the number of events. For weakly interacting systems, the parameters t^* were usually set to 0.0 and 0.5 ps. The former value is used to follow the lifetime of hydrogen bonds and the rate of their breaking, while the latter is suitable to account for exchanges of ligands in the immediate neighborhood of a given molecule, leaving the coordination shell for a minimal period of 0.5 ps.

The water exchange reaction between the first coordination shell around a central reference ion and bulk is the simplest ligand substitution reaction,



where H_2O^* represents the exchanged water ligands.

The mechanistic classification accepted for ligand substitution reactions was proposed by Langford and Gray in 1965 (Figure 2.3) (Langford and Gray, 1965). They divided substitution reactions into three categories of stoichiometric mechanisms: associative (*A*), where an intermediate of increased coordination number can be detected, dissociative (*D*) where an intermediate of reduced coordination number can be detected, and interchange (*I*) where there is no kinetically detectable intermediate. Furthermore, they distinguished two major categories of intimate mechanisms: those with an associative activation mode (*a*), where the reaction rate is approximately as sensitive to variation of the entering group as to variation of the leaving group, and those with a dissociative mode (*d*), where the reaction rate is much more sensitive to the variation of the leaving group than to variation of the entering group. Evidently all *D* mechanisms must be dissociatively activated and all *A* mechanisms must be associatively activated. The *I* mechanisms include a continuous spectrum of transition states where the degree of bond-making between the incoming ligand and the complex ranges from very substantial (*I_a* mechanism) to negligible (*I_d* mechanism) (Merbach, 1982; Merbach, 1987). For the solvent exchange process, the forward and backward reaction coordinates must be symmetrical. Thus, for an *I_d* mechanism, with negligible bond-making of the entering group, the leaving group is also necessarily weakly bound. Inversely, for an *I_a* mechanism, both the entering and the leaving group must have a considerable bonding to the central ion (Merbach, 1982).

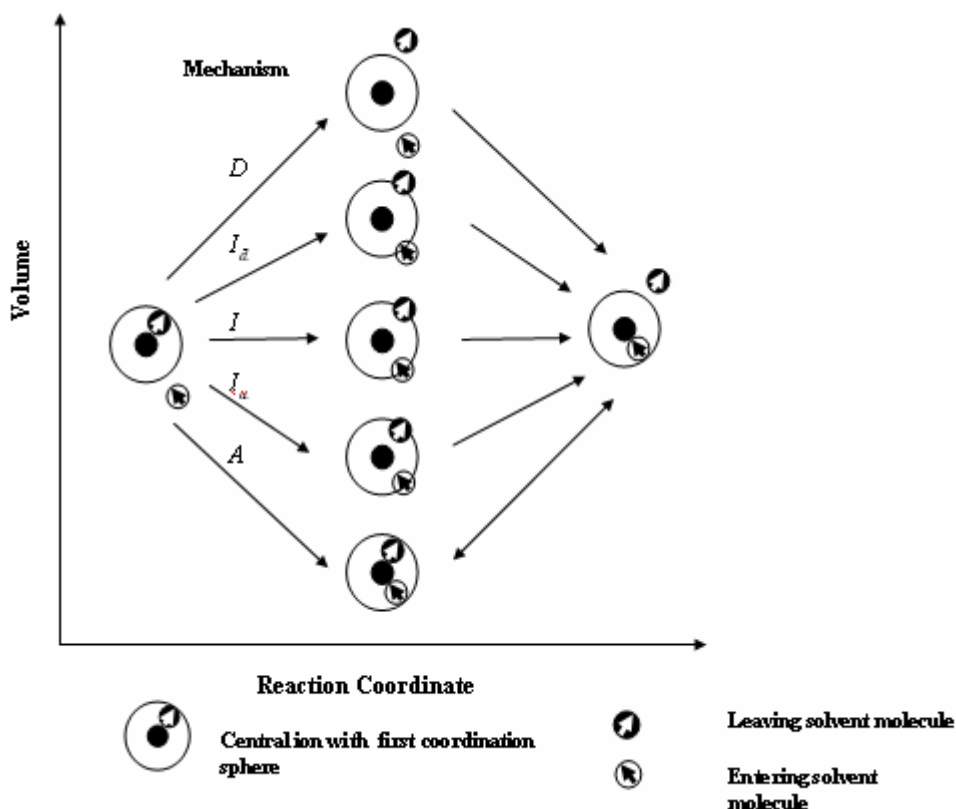


Figure 2.4 Representation of the transition states for the spectrum of solvent of symmetrical ligand exchange process.

2.8 Computer softwares and facilities

In the present study, all calculations were performed at the School of Chemistry, Institute of Science, Suranaree University of Technology (SUT). The computational facility and standard computational chemistry softwares are as followed:

- COMPAQ Alpha 2000 and COMPAQ Alpha Workstation XP1000/667 MHz
- Linux Personal Computer (Redhat Linux, 2.0 GHz Pentium IV, 512 MB RAM)
- Gaussian 98 package of program (Frisch et al., 1998)
- QM/MM-MD code (developed from an original QM/MM-MD version applied for simple ions in aqueous solution).

CHAPTER III

RESULTS AND DISCUSSION

3.1 *Ab initio* QM/MM dynamics of NH_4^+ in water

3.1.1 Structural properties

The hydration structure of NH_4^+ is characterized by means of $N_{\text{am-O}_w}$, $N_{\text{am-H}_w}$, $H_{\text{am-O}_w}$ and $H_{\text{am-H}_w}$ RDFs and their corresponding integration numbers, as shown in Figure 3.1. The QM/MM simulation reveals a broad unsymmetrical first $N_{\text{am-O}_w}$ peak at 2.84 Å, together with considerable tailing up to around 4.7 Å. In comparison to the $O_w\text{-O}_w$ RDF of bulk water, as depicted in Figure 3.2, the shape of $N_{\text{am-O}_w}$ RDF indicates a high flexibility of the NH_4^+ -water complex, as well as a high mobility of first shell water molecules. In addition, the first minimum of the $N_{\text{am-O}_w}$ peak is not well separated from the bulk, suggesting that water molecules surrounding the NH_4^+ ion are quite labile, and are loosely held by the ion. The observed hydration structure of NH_4^+ is significantly different to those obtained by most recent MD simulations (Brugé, 1999b; Chang and Dang, 2003), which reported rather well defined the first and even the second solvation shells of the NH_4^+ ion (see Figure 3.3, i.e., $r=3.1$ Å, $n=5.3$ (Brugé, 1999b) and $r=3.2$ Å, $n=5.8$ (Chang and Dang, 2003)). In the present QM/MM simulation, the minimum position of the $N_{\text{am-O}_w}$ RDF may be roughly estimated to be 3.5 Å, where an integration up to this $N_{\text{am-O}_w}$ range gives coordination number of 6.5 ± 0.2 . Compared to the experimentally observed CN of 8

(Pálinkás et al., 1981), good agreement can then be achieved. In fact, comparison between experiments and theories is not always straightforward since most of the experimental methods for structural analysis have to be performed with solutions of relatively high concentrations, while the theoretical approaches mostly refer to very dilute solutions. As a consequence, a CN determined experimentally for high concentration solutions can be affected by coexisting counterions. Rapid ligand exchange poses another problem for the interpretation of experimental data, as it often leads to the simultaneous coexistence of several solvate species with different geometry and the CN value. When trying to fit a single (averaged) model to the spectroscopic data of such a system, errors will necessarily be introduced.

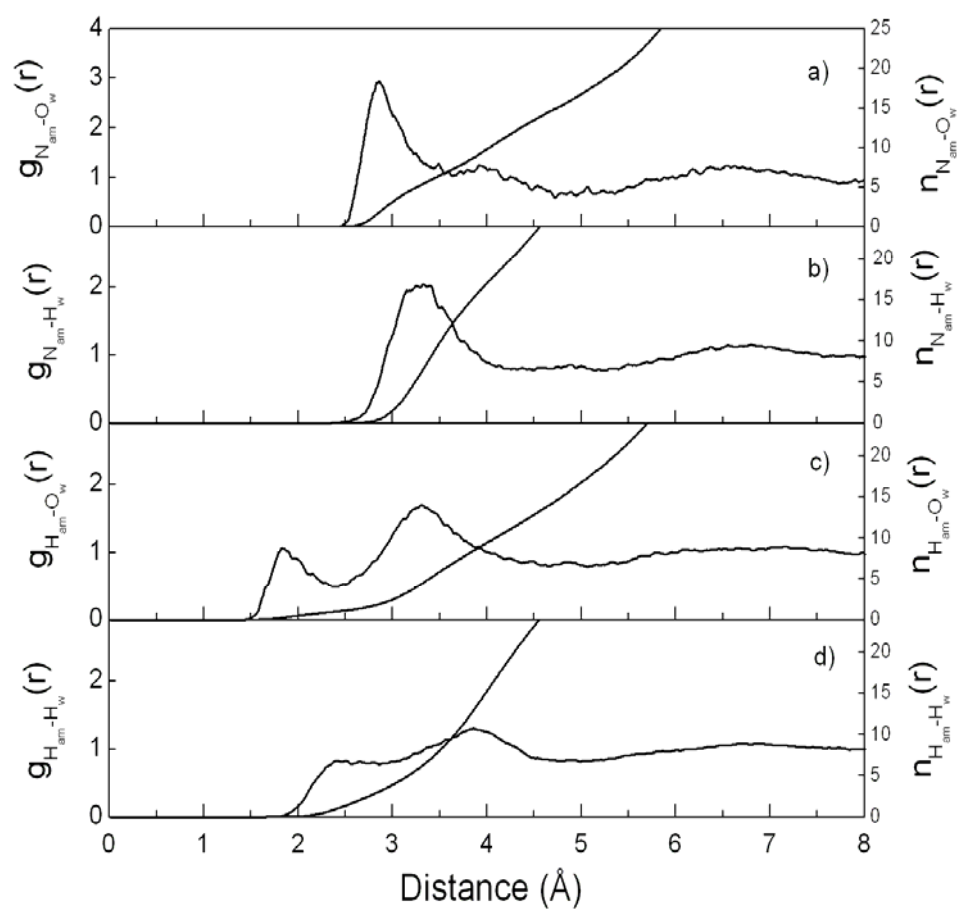


Figure 3.1 a) $N_{\text{am}}\text{-O}_w$, b) $N_{\text{am}}\text{-H}_w$, c) $H_{\text{am}}\text{-O}_w$ and d) $H_{\text{am}}\text{-H}_w$ RDFs and their corresponding integration numbers.

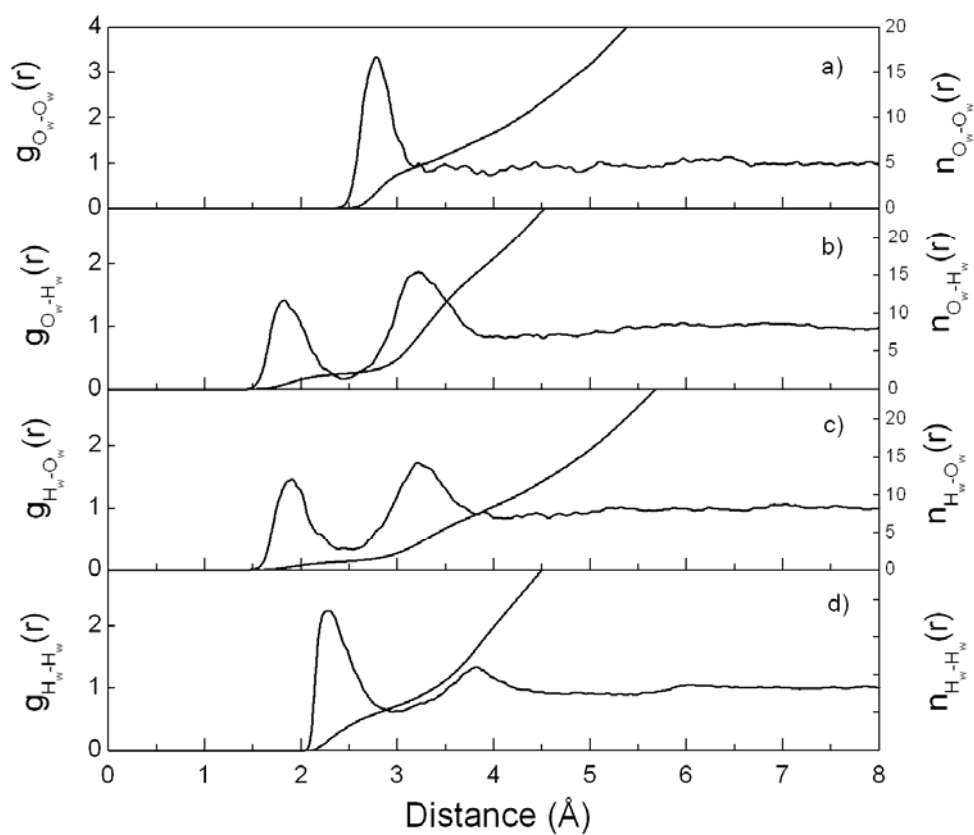


Figure 3.2 a) O_w-O_w , b) O_w-H_w , c) H_w-O_w and d) H_w-H_w RDFs and their corresponding integration numbers. The first atom of each pair refers to the atoms of the water molecule, whose oxygen position was defined as center of the QM region during the QM/MM simulation.

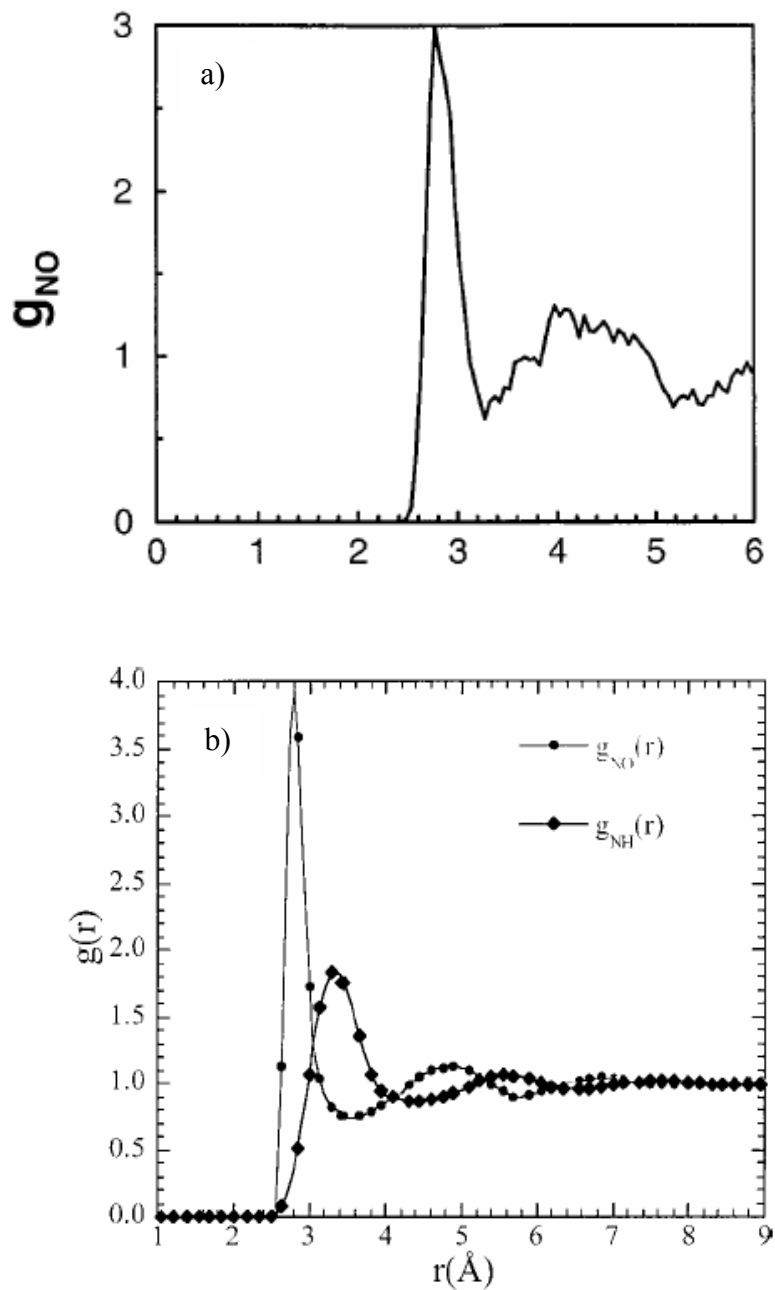


Figure 3.3 Simulated radial pair correlation function a) for nitrogen-oxygen obtained from CP MD simulation and b) for nitrogen-oxygen and nitrogen-hydrogen obtained from PCM MD simulation.

Figure 3.4 shows the probability distributions of the number of surrounding water molecules, calculated within the $N_{\text{am}}\cdots\text{O}_w$ distances of 3.0, 3.5 and 4.0 Å, respectively. With respect to the $N_{\text{am}}\cdots\text{O}_w$ distance of 3.5 Å, a preferred CN of 6 is observed, followed by 7, 5 and 8 in smaller amounts. Apparently, numerous possible species of hydrated NH_4^+ exist, varying from 4- to 10-fold coordinated complexes. In fact, a small shift of $N_{\text{am}}\cdots\text{O}_w$ minimum will have significant impact on the CN value. For example, at a slight larger $N_{\text{am}}\cdots\text{O}_w$ distance of 4.0 Å, the most frequent observed number of water molecules increases rapidly from 6 to 10. The QM/MM results demonstrate that numerous water molecules can mutually play a role in the hydrogen bond formation of NH_4^+ in water.

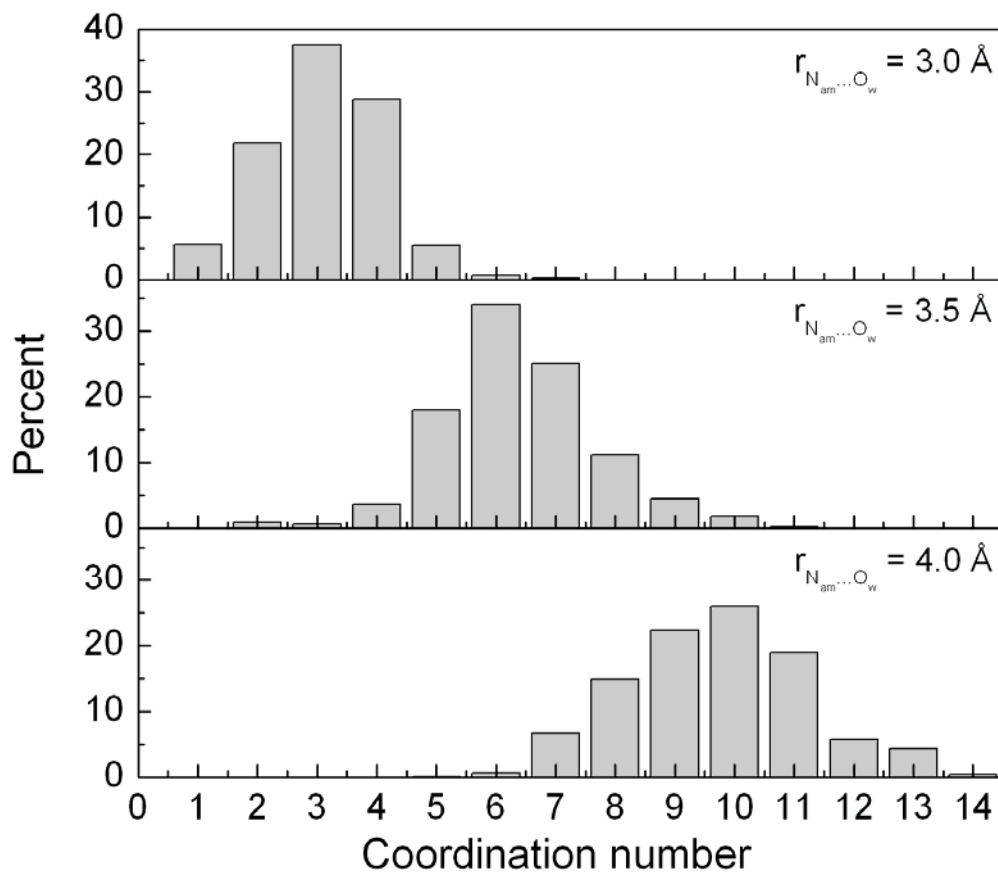


Figure 3.4 CN distributions, calculated up to the $N_{am} \dots O_w$ distances of 3.0, 3.5 and 4.0 Å, respectively.

The hydrogen bonding between NH_4^+ and water can be interpreted via the $\text{H}_{\text{am}}\text{-O}_w$ and $\text{H}_{\text{am}}\text{-H}_w$ RDFs, as depicted in Figures 3.1c and d, respectively. The first $\text{H}_{\text{am}}\text{-O}_w$ peak is centered at 1.84 Å, which is an indicative of hydrogen bonds between the hydrogen atoms of NH_4^+ and their nearest neighbor water molecules. Integrating up to the first $\text{H}_{\text{am}}\text{-O}_w$ minimum yields about 1.1 waters, indicating that each of the hydrogen atoms of NH_4^+ coordinates to single water molecule. Compared to the $\text{O}_w\text{-H}_w$ and $\text{H}_w\text{-O}_w$ RDFs of pure water (Figures 3.2b and c), the first $\text{H}_{\text{am}}\text{-O}_w$ peak is not well separated from the second one, pointing at a more frequent and easy exchange of water molecules between the first shell and the outer region. Together with a rather broad $\text{N}_{\text{am}}\text{-H}_w$ RDF, the QM/MM results clearly show that the hydrogen bonds between NH_4^+ and water is not extremely strong, in contrast to the recent MD simulations (Brugé et al., 1999b; Chang and Dang, 2003), which suggested that the first four water molecules formed a tight first solvation shell around the NH_4^+ ion. From the QM/MM simulation, the hydration enthalpy of the NH_4^+ ion can be approximated by calculation of the energy difference between the ion-water and the water-water interactions of the solution and the water-water interaction energy of the pure water, under the identical conditions. In this work, the hydration enthalpy of NH_4^+ is estimated to be $-85.7 \text{ kcal mol}^{-1}$, which is in good agreement with the experimental values of between -84 and $-89 \text{ kcal mol}^{-1}$ (Arnett et al., 1972; Aue, Webb, and Bowers, 1976; Klots, 1981).

Figure 3.5 displays the $\text{O}_w\cdots\text{N}_{\text{am}}\cdots\text{O}_w$ angular distributions, calculated up to the $\text{N}_{\text{am}}\cdots\text{O}_w$ distances of 3.0, 3.5 and 5.0 Å, respectively. At short $\text{N}_{\text{am}}\cdots\text{O}_w$ distances, a tetrahedral cage structure of the hydrated NH_4^+ is recognizable by a pronounced large peak between 80-120°. The slight distortion from the ideally

tetrahedral arrangement can be understood due to the interference between the first four water molecules that are directly hydrogen bonded to NH_4^+ , with the other nearest-neighbor water molecules. It is obvious that some other nearest-neighbor water molecules can also position closely to the ion, even at a short $\text{N}_{\text{am}} \cdots \text{O}_{\text{w}}$ distance of 3.0 Å, as can be seen from a slight pronounced peak around 60° . This phenomenon is understandable since water molecules are quite small, and many of them can form cluster around the NH_4^+ ion. As a consequence, water molecules are involved in the hydrogen bond formation with the ion, and thus, providing the flexible structure of the NH_4^+ -water complex.

Figure 3.6 illustrates the characteristics of the hydrogen bonds between NH_4^+ and water by means of the distributions of $\text{N}_{\text{am}}\text{-H}_{\text{am}} \cdots \text{O}_{\text{w}}$ angle, calculated within the $\text{H}_{\text{am}} \cdots \text{O}_{\text{w}}$ distances of 1.8, 2.0 and 2.5 Å, respectively. At the short $\text{H}_{\text{am}} \cdots \text{O}_{\text{w}}$ distances of 1.8 and 2.0 Å, the $\text{N}_{\text{am}}\text{-H}_{\text{am}} \cdots \text{O}_{\text{w}}$ hydrogen bonds are nearly linear, with peak maxima around $160\text{-}170^\circ$. Considering at the $\text{H}_{\text{am}} \cdots \text{O}_{\text{w}}$ distance of 2.5 Å, which corresponds to the first $\text{H}_{\text{am}}\text{-O}_{\text{w}}$ RDF minimum, the probability of finding linear hydrogen bonds apparently decreases, while the pronounced peak between $90\text{-}140^\circ$ becomes more significant. The latter peak implies the presence of multiple, non-linear hydrogen bonds within the first solvation shell of each of the hydrogen atoms of NH_4^+ . The observed multiple coordination can be analyzed by plotting the $\text{H}_{\text{am}}\text{-N}_{\text{am}} \cdots \text{O}_{\text{w}}$ angular distributions, calculated within the $\text{N}_{\text{am}} \cdots \text{O}_{\text{w}}$ distance of 3.5 Å, as depicted in Figure 3.7. The two pronounced peaks around $0\text{-}30^\circ$ and $90\text{-}120^\circ$ correspond to the distributions of the four nearest-neighbor water molecules that form nearly linear hydrogen bonds to each of the NH_4^+ hydrogens. Apart from the water molecules that are directly hydrogen-bonded to the NH_4^+ ion, it seems that other nearest-neighbor

water molecules prefer to form bifurcated complex between two hydrogen atoms of NH_4^+ . The preferred bifurcated structure of the non-hydrogen bonding waters over the trifurcated one can be recognizable from a more pronounced shoulder peak around $50\text{-}80^\circ$, compared to that of around $150\text{-}180^\circ$. The QM/MM results are in contrast to that reported in the CP-MD simulation (Brugé et al., 1999b), in which only one non-directional hydrogen bonding water molecule was observed within the defined first solvation shell and this water molecule was found to occupy a position near the center of a triangular face of the tetrahedron.

To provide additional insights into the hydrogen bonds between NH_4^+ and water, the water orientation within the $\text{H}_{\text{am}} \cdots \text{O}_w$ distance of 2.5 \AA is plotted and shown in Figure 3.8. The orientation of water molecules is described in terms of the distribution of the angle θ , as defined by the $\text{H}_{\text{am}} \cdots \text{O}_w$ axis and the dipole vector of the water molecule. The QM/MM simulation indicates clear dipole-oriented arrangements of the hydrogen bonding waters towards the NH_4^+ ion, by a pronounced peak around $100\text{-}170^\circ$. A slight pronounced peak around $30\text{-}70^\circ$ could be attributed to the dipole-oriented arrangements of the nearest-neighbor non-hydrogen bonding water molecules that are less induced by the NH_4^+ ion. In stead, they seem to be influenced by other surrounding water molecules which located within and/or beyond the $\text{H}_{\text{am}} \cdots \text{O}_w$ distance of 2.5 \AA .

Because the QM/MM approach allows the charge distributions on NH_4^+ and its surrounding water molecules to vary dynamically during the simulation process, the polarizability of water molecules surrounding the ion, as well as the effects of charge-transfer in the ion-water complex, which affect the structure of the

hydrated NH_4^+ , are automatically included. In the QM/MM simulation, the average Mulliken charge on NH_4^+ is +0.893 and those on O and H of water molecules surrounding the ion are -0.921 and $+0.465$, respectively. Although the use of polarizable models can provide qualitative predictions for such circumstance (Chang and Dang, 2003), the present QM/MM results suggest that it could never reach the quality of the QM/MM approach, where all charges are corrected dynamically according to the structural changes of the hydrated NH_4^+ .

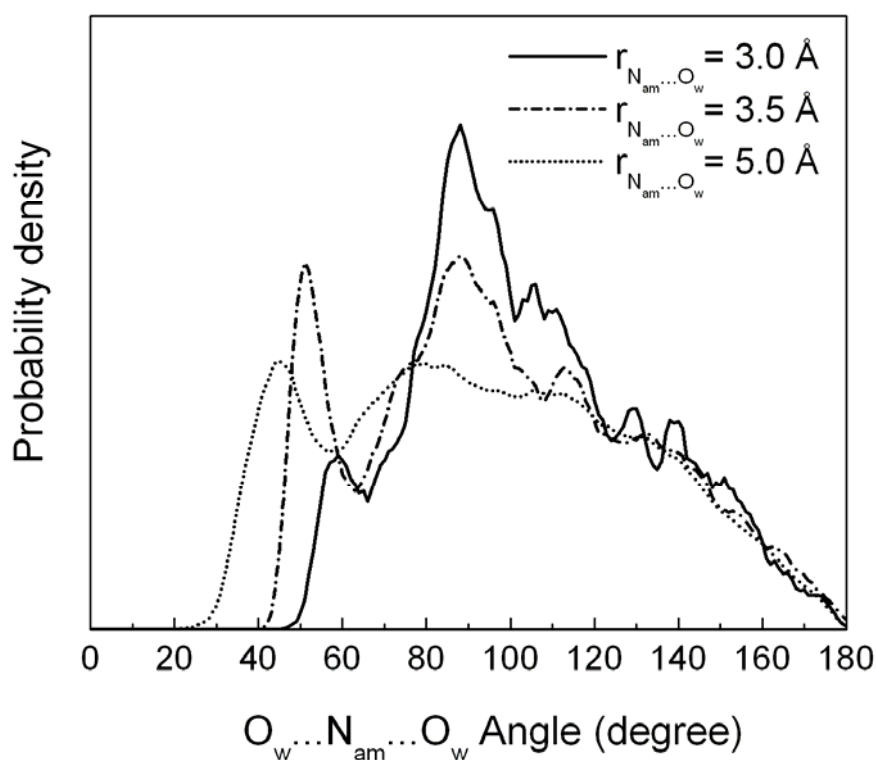


Figure 3.5 $\text{O}_w \cdots \text{N}_{am} \cdots \text{O}_w$ angular distributions, calculated up to the $\text{N}_{am} \cdots \text{O}_w$ distances of 3.0, 3.5 and 5.0 Å, respectively.

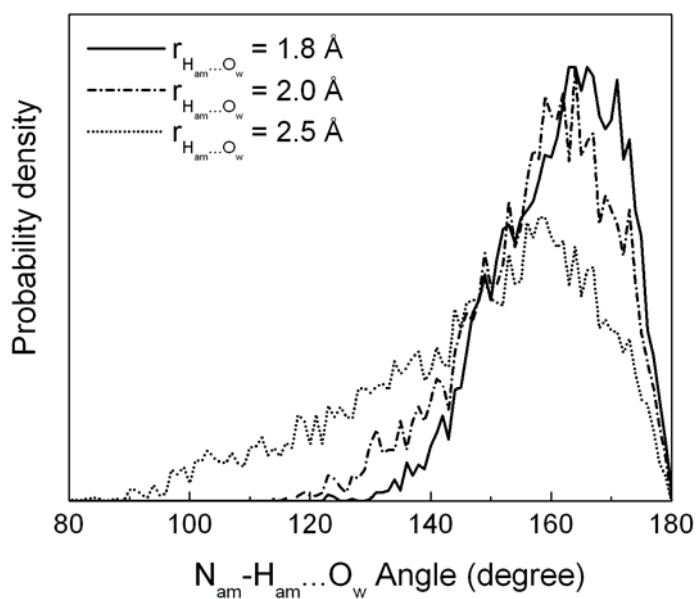


Figure 3.6 $N_{am}-H_{am}\cdots O_w$ angular distributions, calculated up to the $H_{am}\cdots O_w$ distances of 1.8, 2.0 and 2.5 Å, respectively.

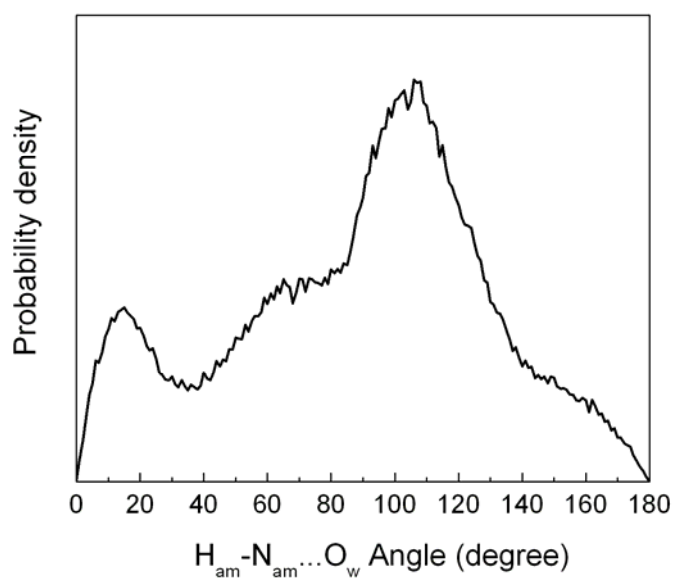


Figure 3.7 $H_{am}-N_{am}\cdots O_w$ angular distributions, calculated within the $N_{am}\cdots O_w$ distance of 3.5 Å.

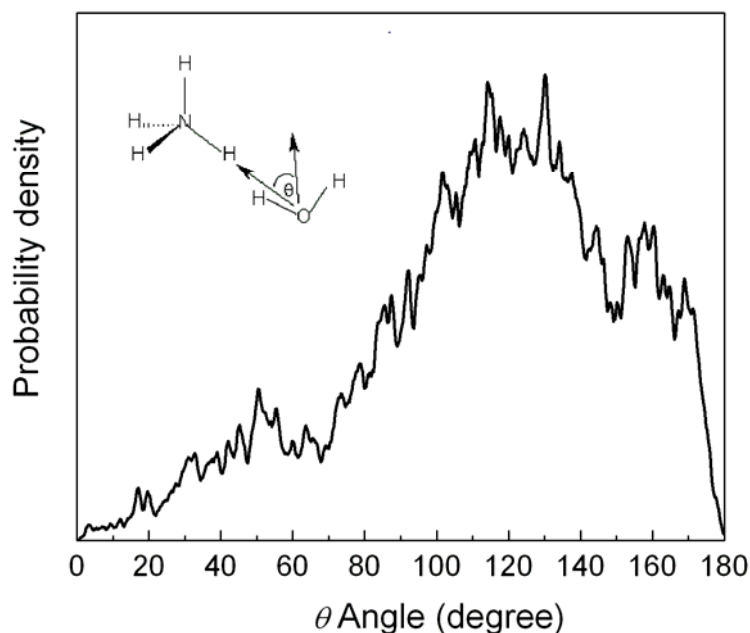


Figure 3.8 Distributions of θ , calculated within the $N_{\text{am}} \cdots O_{\text{w}}$ distance of 3.5 Å.

3.1.2 Dynamical Properties

3.1.2.1 Translational motions

Due to a relatively short time of the QM/MM simulation, the dynamical properties of hydrated NH_4^+ reported in this work are discussed with care and will not be over-interpreted. The self-diffusion coefficients (D_{coeff}) for NH_4^+ as well as for water molecules surrounding the ion and those in the bulk (Tongraar and Rode, 2004) were calculated from the Green-Kubo relation (McQuarrie, 1976),

$$D_{\text{coeff}} = \frac{1}{3} \lim_{t \rightarrow \infty} \int_0^t C_v(t) dt \quad (3.1)$$

where $C_v(t)$ denotes the center-of-mass VACFs. All of the calculated D_{coeff} values are summarized in Table 3.1. Based on our QM/MM simulation, the D_{coeff} value for NH_4^+

in water is estimated to be $3.46 \times 10^{-5} \text{ cm}^2 \text{ s}^{-1}$, which is about 2-3 times larger than the experimental values (Wishaw and Stokes, 1954). It should be noted that discrepancy between experiment and theory is often found since the experimentally observed dynamics parameters are usually determined for high concentration solutions, in which the counterion effects can influence the results, while the values obtained in this work correspond to a very dilute solution. In comparison to bulk water (Tongraar and Rode, 2004), the QM/MM results indicate that NH_4^+ diffuses quite fast, while water molecules in the solvation shell of the ion diffuse on a time scale comparable to that of the bulk. The observed fast diffusive translation of NH_4^+ can be described due to the flexible NH_4^+ solvation, and thus, allowing the NH_4^+ ion to translate more freely without carrying any of nearest-neighbor waters with it.

Table 3.1 Self-diffusion constants for NH_4^+ and water.

| Species | D_{coeff} ($\times 10^{-5} \text{ cm}^2 \text{ s}^{-1}$) | Method/Ref. |
|--|---|-------------------------------------|
| NH_4^+ in water | 3.46 | QM/MM-MD (this work) |
| | 0.82 | MD (Karim, and Haymet, 1990) |
| | ~ 2.7 | MD (Chang, and Dang, 2003) |
| | 1-2 | Expt. (Wishaw, and Stokes, 1954) |
| H_2O around NH_4^+ ($N_{am} \cdots O_w$ distance = 3.5 Å) | 3.23 | QM/MM-MD (this work) |
| Pure H_2O | 3.31 | QM/MM-MD (Tongraar, and Rode, 2004) |

$N_{am} \cdots O_w$ distance = distance between NH_4^+ nitrogen and oxygen atom of water

Spectral densities, corresponding to the hindered translations of NH_4^+ and of water molecules, were analyzed by Fourier transformations of the center-of-mass VACFs, as shown in Figure 3.9. For bulk water (Tongraar and Rode, 2004), a pronounced peak with maximum at about 60 cm^{-1} and a broad band around $150\text{-}300 \text{ cm}^{-1}$ are identified as hindered translational motions of the center-of-mass parallel and perpendicular to the dipole vector of water molecules, which have been attributed to the hydrogen bond bending and the $O_w \cdots O_w$ stretching motions, respectively (Sceats and Rice, 1980). In comparison to bulk water, the power spectra of water molecules in the hydration sphere of NH_4^+ are not significant different to that of the pure water, indicating a small influence of this ion on the translational motions of its surrounding water molecules. For the translational motion of NH_4^+ itself, the Fourier transforms

show a maximum at zero frequency, which correspond to the high probability of translation of this ion in the environment of water molecules.

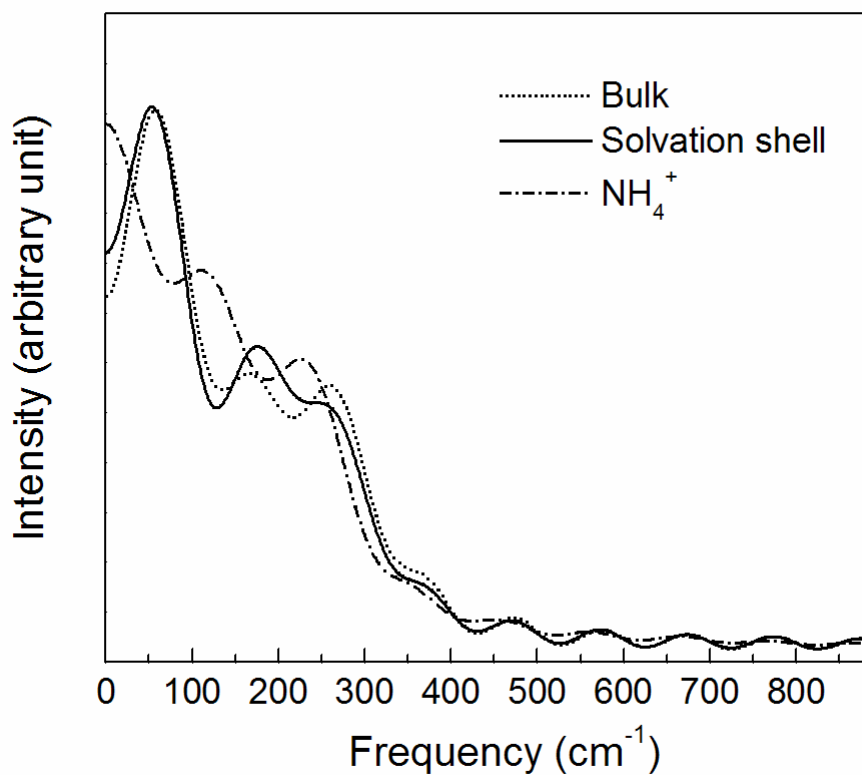


Figure 3.9 Power spectra of the translational motions of NH_4^+ and of water molecules in the bulk and in the hydration shell of the ion, calculated from the center-of-mass VACFs of the ion and water.

3.1.2.2 Librational motions

Based on the normal-coordinate analyses (Bopp, 1986), the power spectra of the librational motions of water molecules, calculated within the $H_{am} \cdots O_w$ distance of 2.5 Å, and of NH_4^+ (only for a rotation around C_{3v} axis) are displayed in Figure 3.10. In comparison to the frequencies of pure water (Tongraar and Rode, 2004), the librational frequencies, of the order of $R_z < R_x < R_y$, of water molecules surrounding the hydrogen atoms of NH_4^+ are all blue-shifted. The shift to higher frequencies can be attributed to the steric hindrance in the NH_4^+ -water complex, in which water molecules form cluster with the ion. For the rotation of NH_4^+ in water, the rotational frequency of this ion around its C_{3v} axis is red-shifted, compared to the C_{2v} rotation of water molecules. The shift to lower frequency implies that NH_4^+ can rotate rather freely in an environment of water molecules. The rotational motion of NH_4^+ in water can be characterized by its rotational diffusion constant (D_R). Since NH_4^+ has an approximately symmetric tetrahedral geometry, all three principal moments of inertia are equivalent. Consequently, the D_R constant can then be obtained from the mean-square angle displacements,

$$\langle \theta(t)^2 \rangle = 4D_R t \quad (3.2)$$

where $\theta(t)$ denotes the angle formed by a vector in the body-fixed frame at with its initial direction ($\theta = 0$ at $t = 0$). The computed mean-square angle $\langle \theta(t)^2 \rangle$ as a function of time is displayed in Figure 3.11, and the D_R constant estimated from the slope was $0.088 \times 10^{12} \text{ rad}^2 \text{ s}^{-1}$, which is in good agreement with the experimental

value of about $0.075 \times 10^{12} \text{ rad}^2 \text{ s}^{-1}$ obtained by the NMR measurements (Perrin and Gipe, 1986; Perrin and Gipe, 1987).

The ease of NH_4^+ rotation can be ascribed due to the presence of numerous water molecules around the ion that facilitate the rotation. Based on the QM/MM results, the most probable rotational dynamics of the NH_4^+ ion in water can be considered as follow. Since the hydrogen bond between NH_4^+ and water is not extremely strong, its strength maybe somewhat comparable to that of between water and water. Hence, when a number of water molecules interact with the ion, the first four nearest-neighbor waters are temporarily immobilized at each edge of the tetrahedral NH_4^+ -water cage structure, while the others are more labile and are placed in bifurcated configurations between two hydrogen atoms of NH_4^+ . Thus, it is obvious that because of the bifurcated waters that significantly enhance the ease for each of the hydrogen atoms of NH_4^+ to break its original hydrogen bond (with its original water molecule) and then to form a new hydrogen bond with another (bifurcated) water molecule. With sufficient amount of bifurcated waters, possibly up to six water molecules (according to the rough estimated first hydration shell, see Figure 3.4), all possible re-established $\text{N}_{\text{am}}\text{-H}_{\text{am}}\cdots\text{O}_{\text{w}}$ hydrogen bonds can be easily occurred along any rotational pathway of the NH_4^+ ion. The QM/MM results support well a proposed multiple hydrogen bonding rotational mechanism (Perrin and Gipe, 1987) and are in good agreement with the NMR experiments (Perrin and Gipe, 1986), as well as in consistent with the reported rather low activation energy (E) for the reorientation of NH_4^+ in aqueous solution (Kassab et al., 1990; Perrin and Gipe, 1986; Brown, 1995).

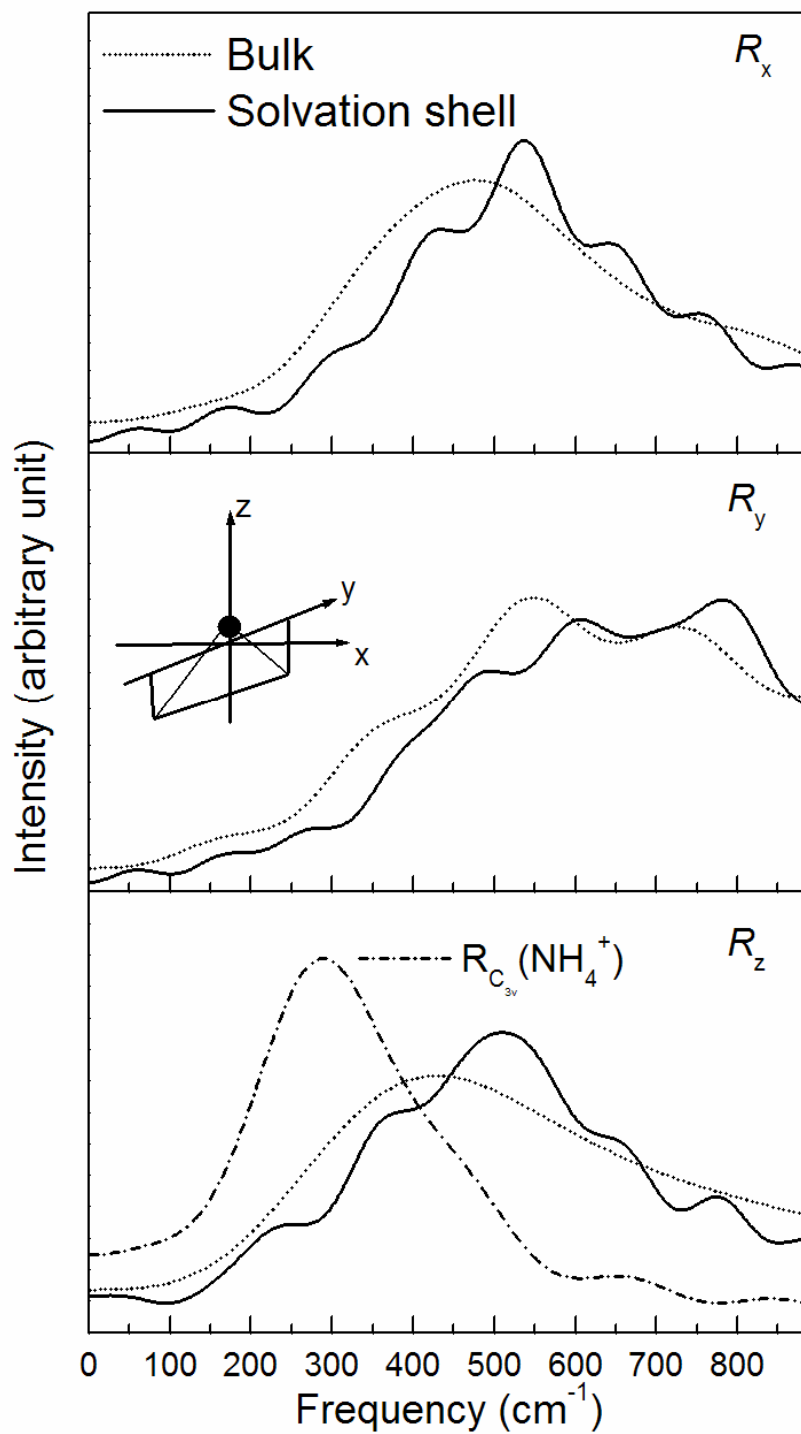


Figure 3.10 Power spectra of the librational motions of NH_4^+ and of water molecules in the bulk and in the hydration shell of the ion, as obtained by the QM/MM simulations.

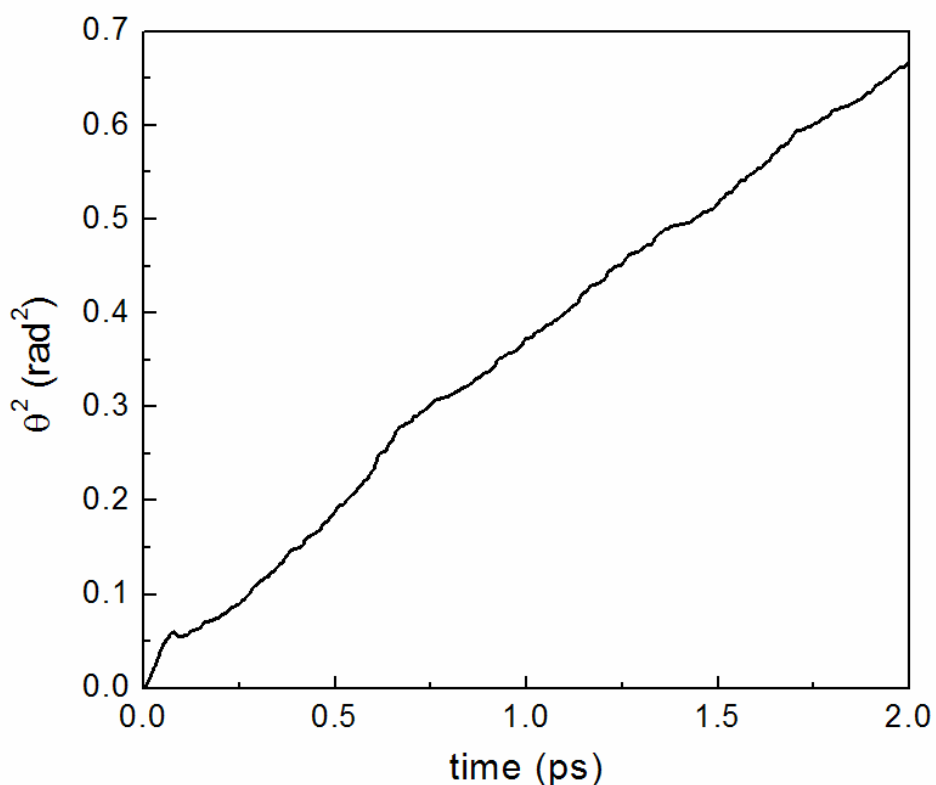


Figure 3.11 Mean-square angular displacements of NH_4^+ in water as a function of time.

3.1.2.3 Water exchange in the hydration shell of NH_4^+

Within the total simulation time of 16 ps, several water exchange processes occurred at each of the hydrogen atoms of NH_4^+ are observed. To focus more distinctly on the water exchange processes, the plot of $\text{H}_{\text{am}} \cdots \text{O}_w$ distance is zoomed within the $\text{H}_{\text{am}} \cdots \text{O}_w$ distance of 4.0 Å and for only the first 8 ps of the QM/MM simulation trajectory, as depicted in Figure 3.12. It is obvious that water molecules surrounding the hydrogen atoms of NH_4^+ can exchange by any of the proposed ‘classical’ types, such as the *A* and *D* as well as *I_a* and *I_d* mechanisms

(Langford and Gray, 1966). These data confirm the structural lability of the NH_4^+ ion in aqueous solution, corresponding to the appearance of various possible species of the hydrate complex formed in the solution.

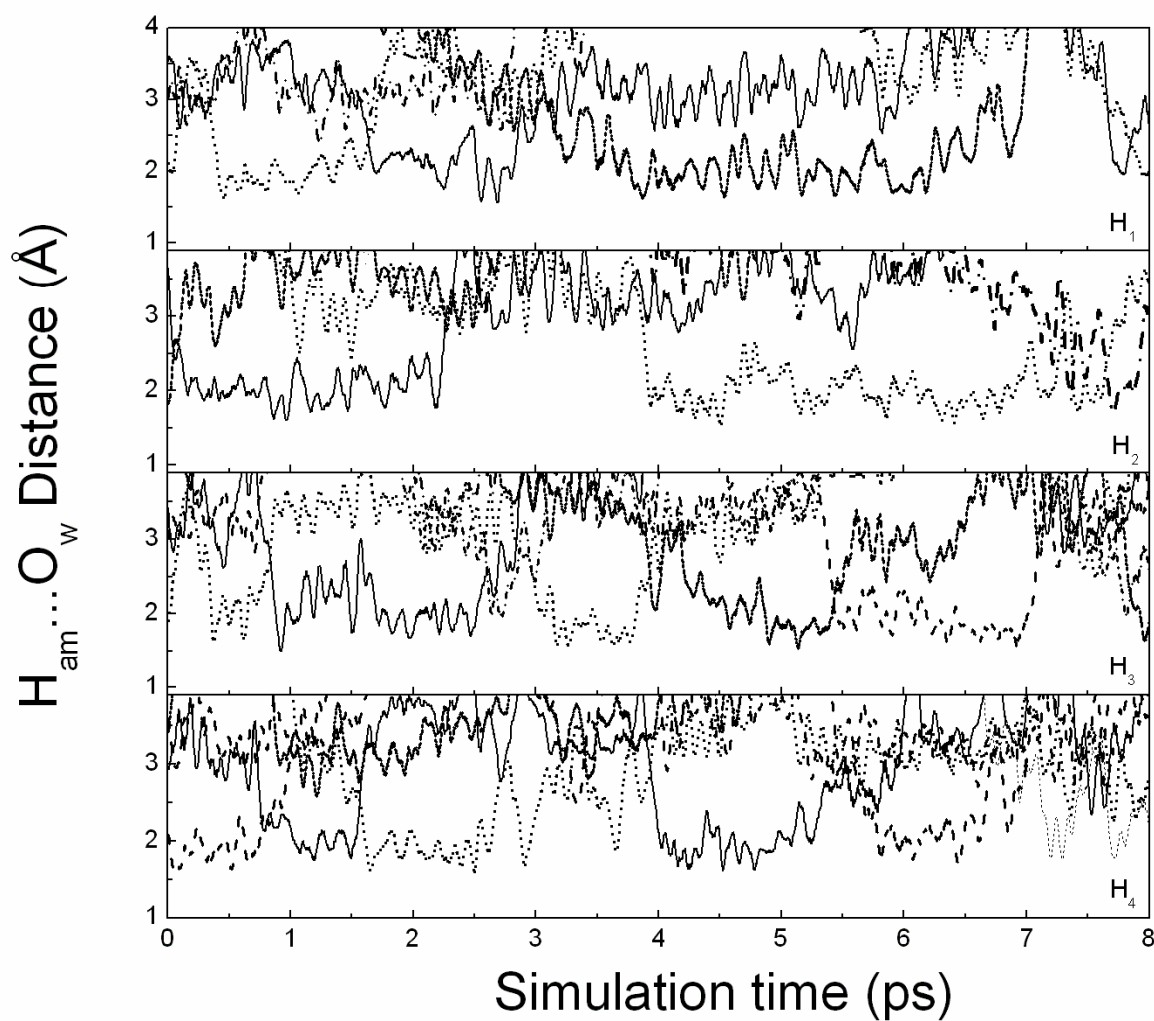


Figure 3.12 Water exchange in the first solvation shell of each of the hydrogen atoms of NH_4^+ , emphasizing for only the first 8 ps of the QM/MM simulation.

The rate of water exchange processes at each of the NH_4^+ hydrogens was evaluated by the MRT value of the water molecules. In this work, the MRT values were calculated using a ‘direct’ method (Hofer et al., 2004), being the product of the average number of nearest-neighbor water molecules located within the $\text{H}_{\text{am}} \cdots \text{O}_w$ distance of 2.5 Å with the duration of the QM/MM simulation, divided by the number of exchange events. Based on the direct accounting and setting various time parameter t^* , the MRT values are listed in Table 3.2. The time parameter t^* has been defined as a minimum duration of the ligand’s displacement from its original coordination shell. For such weakly hydrated NH_4^+ , the $t^* = 0.5$ ps was proposed to be the best choice (Hofer et al., 2004) as it corresponds to the mean lifetime of hydrogen bonds. With respect to this criterion, only the data obtained with $t^* = 0.0$ ps make sense for the estimation of H-bond lifetimes, while the MRT data obtained with $t^* = 0.5$ ps can be considered as a good measure for ligand exchange processes. In accordance with the $t^* = 0.5$ ps, an order of $\tau_{\text{H}_2\text{O}}(\text{H}_i) < \tau_{\text{H}_2\text{O}}(\text{H}_2\text{O})$ is observed. The QM/MM results clearly show that water molecules binding to each of the hydrogen atoms of NH_4^+ are quite labile, and that the hydrogen bond between NH_4^+ and water is not much strong, allowing numerous water exchange processes within the hydration sphere of the NH_4^+ ion to be frequently occurred. In addition, the MRT data also reveal the “structure-breaking” ability of the NH_4^+ ion in aqueous solution. The “structure-breaking” effect of the NH_4^+ ion can be recognized from its flexible hydration structure, as well as from the MRT values of water molecules surrounding the ion, which are smaller than that of the bulk. The QM/MM results suggest that the NH_4^+ ion can not form a well-defined ion-water complex, *i.e.*, its influence can be concerned mainly to disrupt the solvent’s hydrogen-bonded structure.

The detailed information on the solvation structure and dynamics of NH_4^+ in water is very crucial to fundamentally understand the reactivity of this ion in chemical and biological systems. For example, in the specific ion stabilization of the RNA structure, the potential of NH_4^+ to donate four hydrogen bonds in a tetrahedral geometry has been considered to responsible for its ability to stabilize the RNA fragment structure more effectively than the alkali metal cations (Wang et al., 1993). Furthermore, since the RNA fragment selectivity for NH_4^+ is the result of a match between a tetrahedral array of hydrogen bond acceptors in the RNA and NH_4^+ , the correct coordination or hydrogen bonding of NH_4^+ in specific sites is of particular importance in order to promote the correct conformation of the RNA.

Table 3.2 Mean residence times of water molecules in the bulk and in the first solvation shell of each of hydrogen atoms of NH_4^+ , calculated within the $H_{\text{am}} \cdots O_w$ distance of 2.5 Å.

| Atom/solute | CN | t_{sim} | $t^* = 0$ ps | | $t^* = 0.5$ ps | |
|---|------|------------------|-------------------|-----------------|-----------------------|---------------------|
| | | | N_{ex}^0 | $\tau_{H_2O}^0$ | $N_{\text{ex}}^{0.5}$ | $\tau_{H_2O}^{0.5}$ |
| H1 | 1.05 | 16.0 | 204 | 0.08 | 13 | 1.29 |
| H2 | 1.14 | 16.0 | 231 | 0.08 | 12 | 1.52 |
| H3 | 1.13 | 16.0 | 267 | 0.07 | 14 | 1.29 |
| H4 | 1.08 | 16.0 | 227 | 0.07 | 13 | 1.33 |
| Pure H_2O (Tongraar et al., 2004) | | | | | | |
| | 4.6 | 12.0 | 292 | 0.19 | 31 | 1.78 |

CN = average coordination number of the first hydration shell of water and of each of hydrogen atoms of NH_4^+ .

t^* = minimum duration of the ligand's displacement from its original coordination shell.

t_{sim} = simulation time in ps

$N_{\text{ex}}^{t^*}$ = number of exchange events

$\tau_{H_2O}^{t^*}$ = Mean residence time

3.2 *Ab initio* QM/MM dynamics of H_3O^+ in water

3.2.1 Structural properties

Since the detailed information on the solvation structure of hydrated H_3O^+ is crucial for understanding the proton transport dynamics, it is of particular interest to characterize the structural properties of the complex. The QM/MM results for the $\text{O}_{\text{hy}}\text{-O}_{\text{w}}$ and $\text{O}_{\text{hy}}\text{-H}_{\text{w}}$ RDFs, together with their corresponding integration numbers, are shown in Figures 3.13a and b, respectively. The QM/MM simulation shows a sharp first $\text{O}_{\text{hy}}\text{-O}_{\text{w}}$ peak with maximum at 2.6 Å. Integration of this peak up to the first $\text{O}_{\text{hy}}\text{-O}_{\text{w}}$ minimum yields an average coordination number of 3.4. This implies the prevalence of a well-defined H_9O_4^+ structure, which is occasionally distorted due to the presence of the fourth water molecule in the first hydration shell. The coordination number observed in this work is in good accord with the recent experiment (Botti et al., 2005), which demonstrated that, besides the three-coordinate nature of H_3O^+ , a fourth water molecule can be found occasionally in the vicinity of the oxygen atom of H_3O^+ (see Figure 3.14). Our first $\text{O}_{\text{hy}}\text{-O}_{\text{w}}$ peak is in contrast to the results from earlier CP-MD and MS-EVB MD simulations (Tuckerman, Laasonen, Sprik, and Parrinello, 1995a; Vuilleumier and Borgis, 1999), which reported a splitting of the first $\text{O}_{\text{hy}}\text{-O}_{\text{w}}$ peak due to the coexistence of the H_9O_4^+ and H_5O_2^+ complexes (see Figures 3.15 and 3.16, respectively). It has been well-established that the PT process is an extremely fast dynamics process (*e.g.* the inter-conversion period between the H_9O_4^+ and H_5O_2^+ hydration structure is only 1 ps or less), with the H_5O_2^+ form being the most important transition state complex. Interestingly, in the most recent CP-MD study (see Figure 3.17, Izvekov and Voth, 2005), no splitting was

found in the first peak of $O_{\text{hy}}-O_{\text{w}}$ RDF, which is consistent with the present QM/MM simulation. Thus, it is reasonable to conclude that the splitting of the first $O_{\text{hy}}-O_{\text{w}}$ peaks reported by Tuckerman, Laasonen, Sprik, and Parrinello (1995a) and Vuilleumier and Borgis (1999) could be an indication that the models employed overestimated the stability of $H_5O_2^+$. In other words, the $H_5O_2^+$ complex predicted by Tuckerman, Laasonen, Sprik, and Parrinello (1995a) and Vuilleumier and Borgis (1999) are too stable to represent a transition state complex in the PT process. According to the latter CP-MD study (Izvekov and Voth, 2005), however, the corresponding first $O_{\text{hy}}-O_{\text{w}}$ peak exhibited at a distance about 0.1 Å shorter than that observed in the present QM/MM simulation. In addition, the first solvation shell of H_3O^+ was predicted to be significantly more rigid, with the smaller coordination number of 3.1. In the QM/MM simulation, the first solvation shell, as seen in the $O_{\text{hy}}-O_{\text{w}}$ RDF, is not well separated from the bulk region, suggesting that the exchange of water molecules between the first solvation shell and the bulk takes place frequently (see below). The observed differences between the QM/MM and CP-MD results could be attributed partly to the neglect of the electron correlation effects at the HF level of theory. However, it could also be a consequence of the approximations and the parameterizations of the DFT methods, which is well-known to give slightly more rigid hydration shell of ions in solutions (Rode et al., 2004; Xenides et al., 2005). In Figure 3.13b, a small shoulder observed on the $O_{\text{hy}}-H_{\text{w}}$ peak around 2.7-2.8 Å suggests a weak $O_{\text{hy}}\cdots H_{\text{w}}$ hydrogen bond interaction on top of the H_3O^+ ion. The QM/MM results also demonstrate that H_3O^+ is not strongly shared in a local tetrahedral network of water.

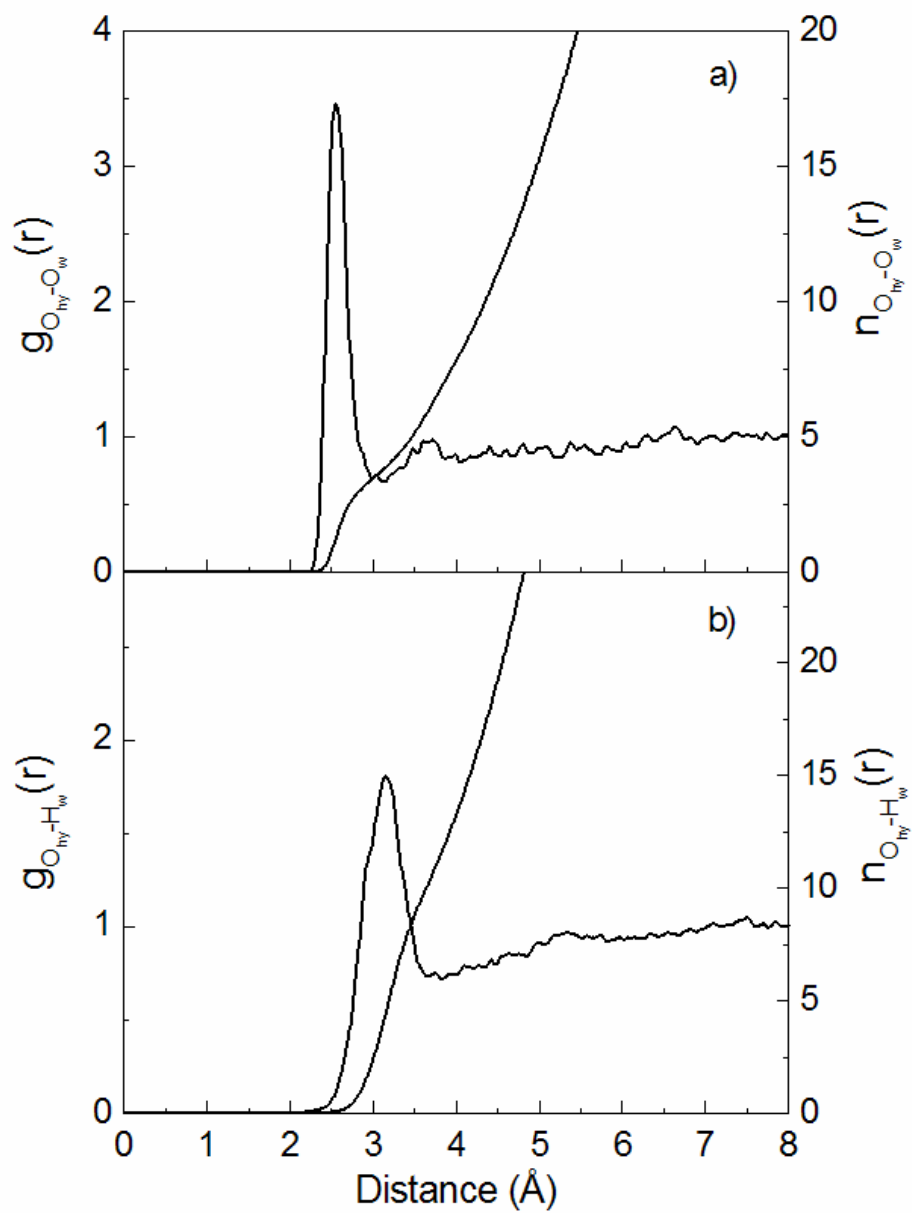


Figure 3.13 a) $O_{hy}-O_w$ and b) $O_{hy}-H_w$ RDFs and their corresponding integration numbers.

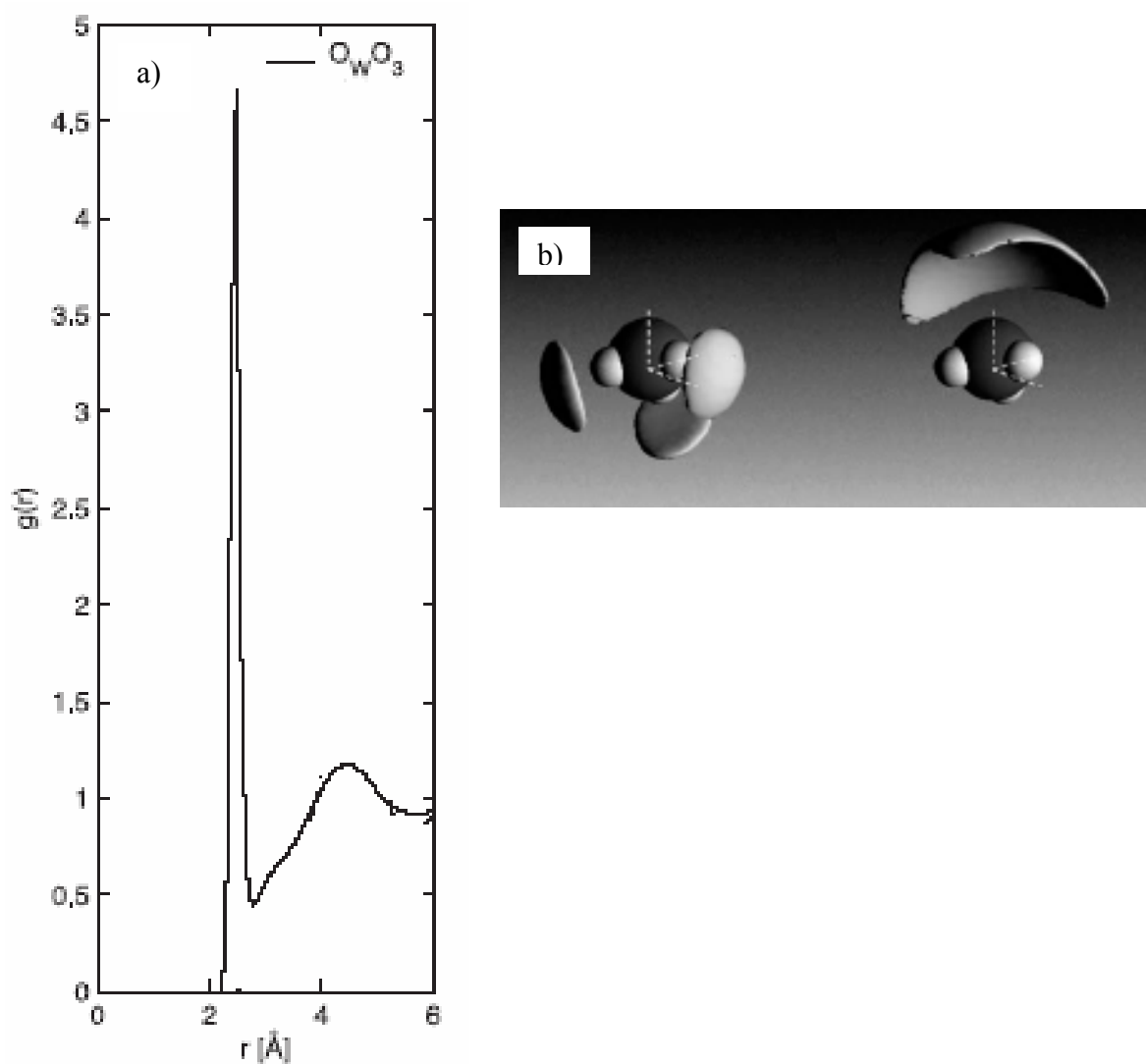


Figure 3.14 a) $O_{\text{hy}}-O_{\text{w}}$ radial distribution function and b) Left: the presence of three hydrogen-bonded water molecules; Right: the presence of a fourth neighboring water molecule obtained from the neutron diffraction experimental study.

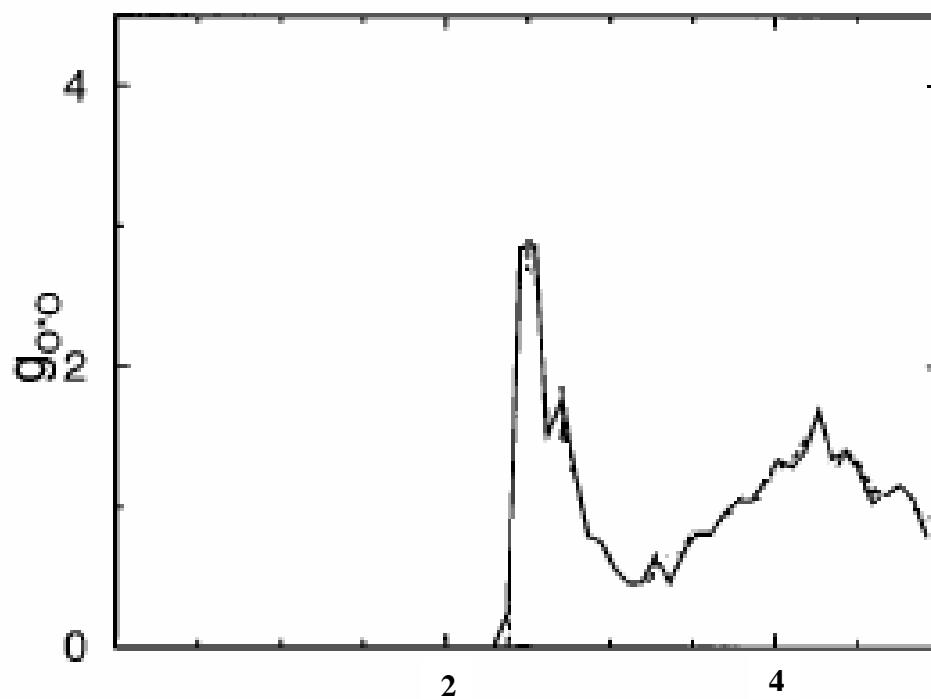


Figure 3.15 O^*-O radial distribution functions of the $H_9O_4^+$ and $H_5O_2^+$ structures of H^+ in water obtained from CP-MD simulation.

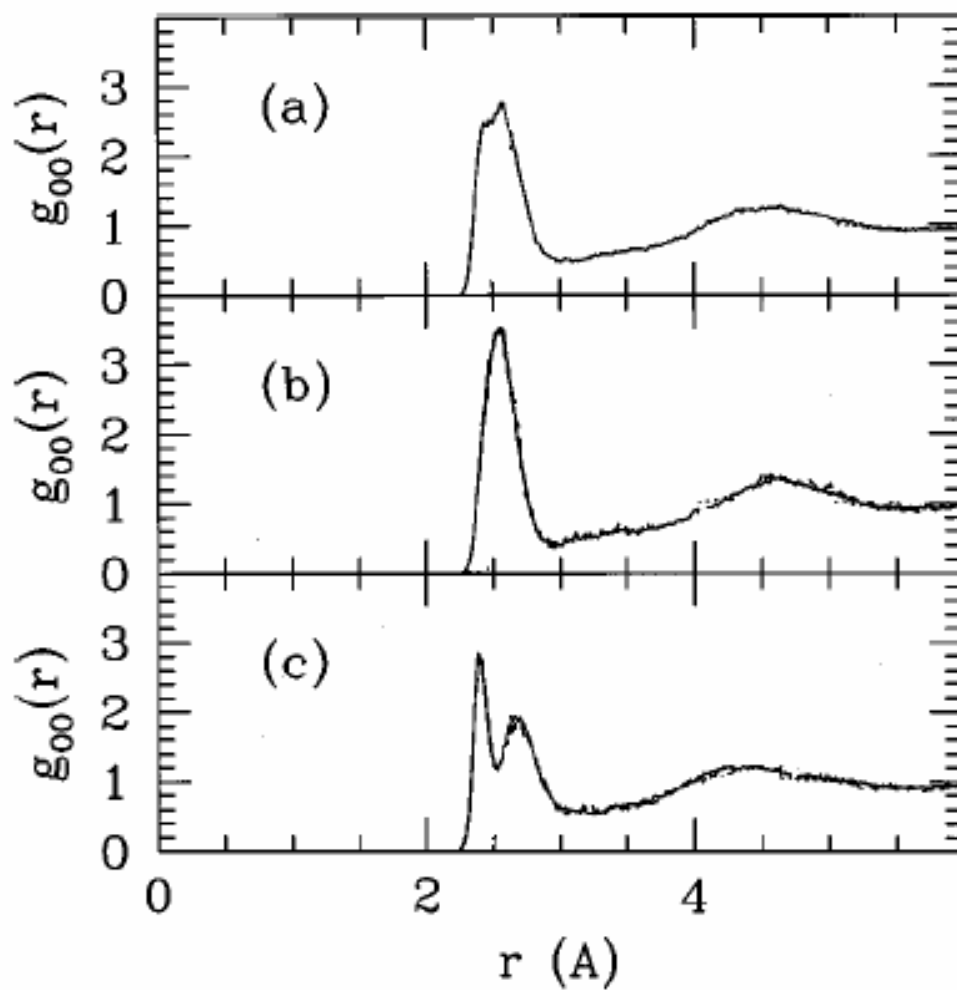


Figure 3.16 a) The radial distribution function $g_{\text{O}^*\text{O}}(r)$ centered around the oxygen O^* carrying the proton. b) The same but computed only for H_3O^+ structures. c) The same for H_5O_2^+ structures obtained from MS-EVB simulation.

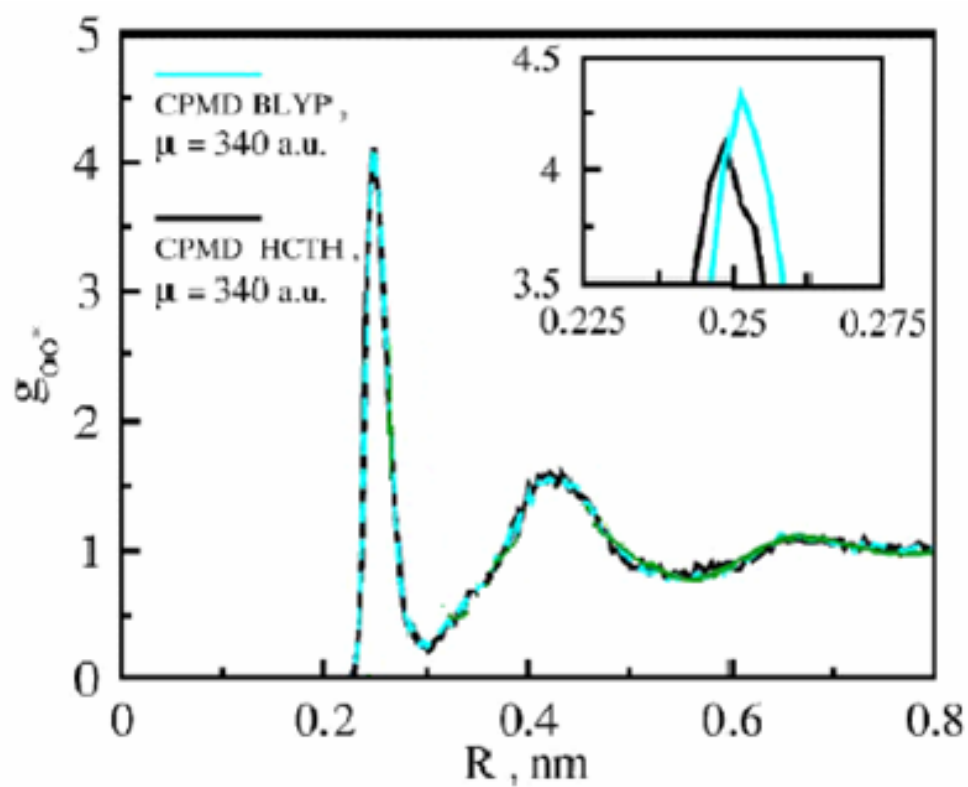


Figure 3.17 The water-hydronium RDF; g_{OO} from CP-MD simulations using the BLYP (bright blue solid line) and HCTH (black solid line) XC functionals.

Figure 3.18 shows the probability distribution of the number of surrounding water molecules, calculated up to the first minimum of the $O_{\text{hy}}-O_{\text{w}}$ RDF. The first hydration shell of H_3O^+ prefers a CN of 3. Nevertheless, it is obvious that about 1/3 of the configurations favor four nearest-neighbor water molecules. The ND and XRD experiments (Almlof, 1973; Triolo and Narten, 1975) also suggested the possibility of four nearest-neighbor water molecules for each H_3O^+ , in which the fourth water molecule might be found in two possible orientations: a proton-donor or a charge-dipole orientation.

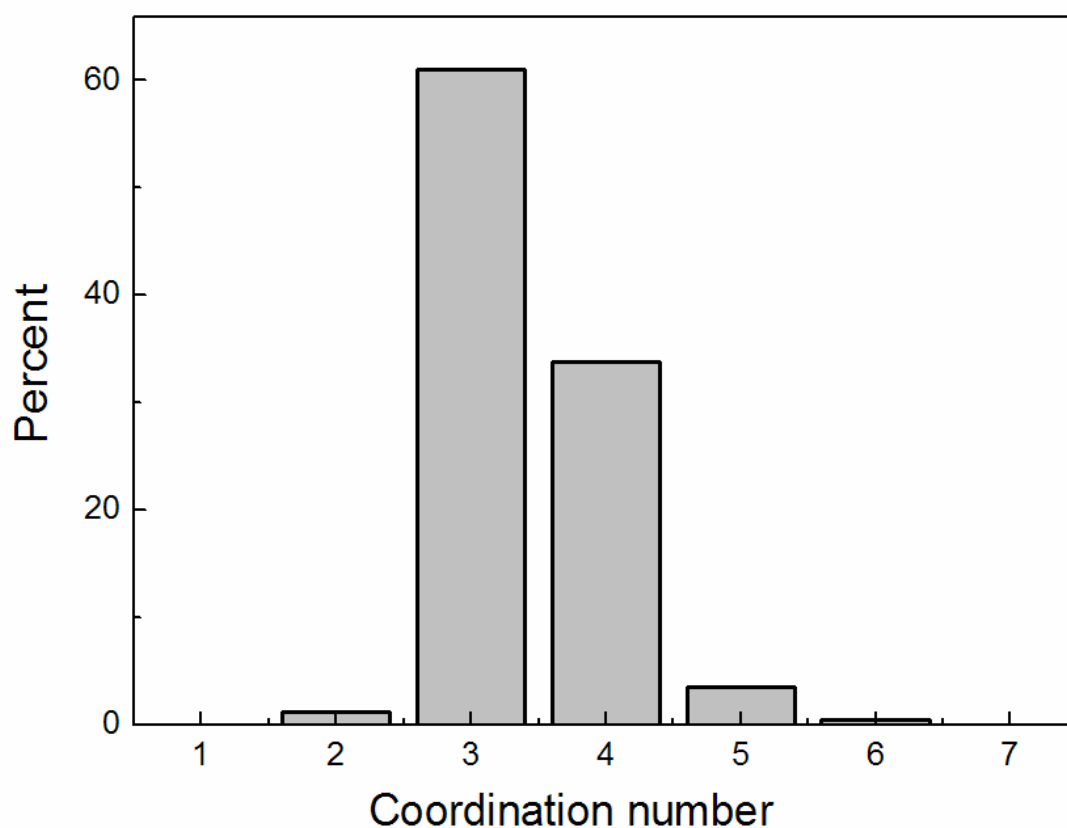


Figure 3.18 Distributions of CN, calculated up to an $O_{\text{hy}}\cdots O_{\text{w}}$ distance of 3.2 Å.

The distributions of water orientations around the ion are shown as the distribution of the cosine of the angle β between the $O_{\text{hy}}\cdots O_{\text{w}}$ distance vector and the dipole vector of the H_3O^+ ion (Figure 3.19). The QM/MM simulation shows a slight feature, almost constant distribution of orientations. This indicates again that the pyramidal H_3O^+ is not involved in a local tetrahedral structural motif and that the hydrogen bond structure is not particularly rigid. The absence of the fourth water molecule weakly bound in the lone pair direction of the H_3O^+ ion has been observed in the structures of the optimized $(\text{H}_2\text{O})_5\text{H}^+$ cluster (Wei and Salahub, 1994).

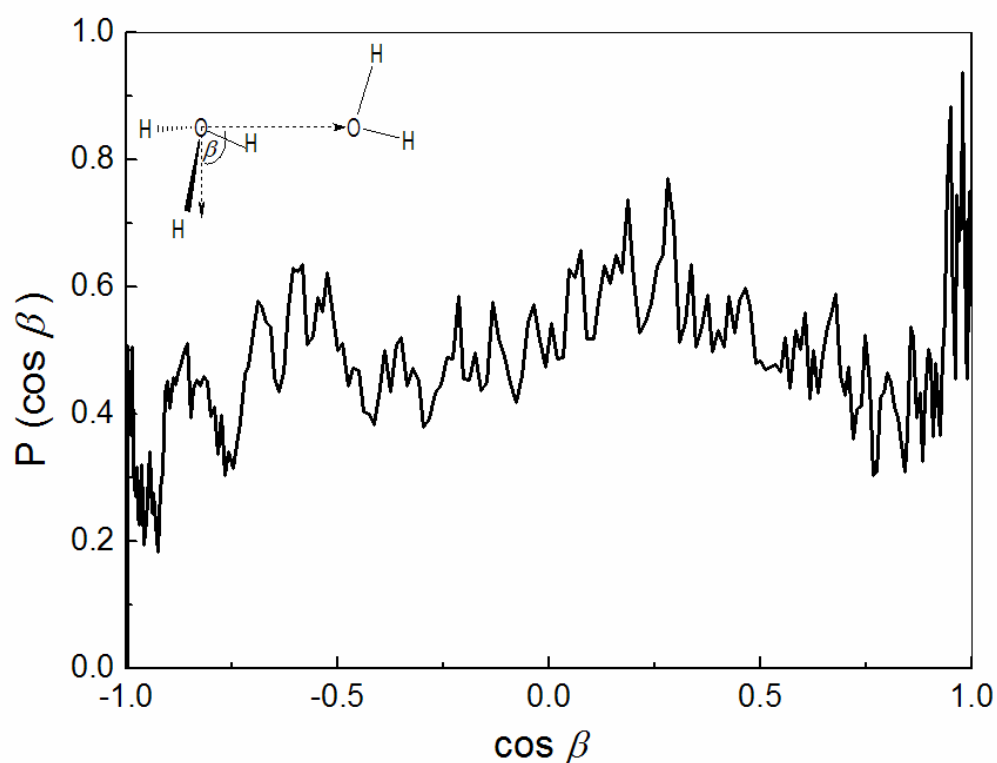


Figure 3.19 Distribution of the angle β between the instantaneous “symmetry” axis of H_3O^+ and the $O_{\text{hy}}\cdots O_{\text{w}}$ distance vector, for $O_{\text{hy}}\cdots O_{\text{w}}$ distances $\leq 3.2 \text{ \AA}$.

Information on the hydrogen bond characteristics between H_3O^+ and water can be obtained from the $\text{H}_{\text{hy}}\text{-O}_{\text{w}}$ and $\text{H}_{\text{hy}}\text{-H}_{\text{w}}$ RDFs, as shown in Figure 3.20. The QM/MM simulation shows the first $\text{H}_{\text{hy}}\text{-O}_{\text{w}}$ peak with a maximum at 1.53 Å, which is attributed to the hydrogen bonds between the hydrogen atoms of H_3O^+ and their nearest-neighbor water molecules. The integration up to the first minimum of the $\text{H}_{\text{hy}}\text{-O}_{\text{w}}$ RDF yields one (1.02) well-defined hydrogen bond between a water molecule and each hydrogen atom of the H_3O^+ ion. In the recent CP-MD study (Izvekov and Voth, 2005), the corresponding $\text{H}_{\text{hy}}\text{-O}_{\text{w}}$ peak exhibited, again, at a distance around 0.1 Å shorter than that observed in the QM/MM simulation. This discrepancy can be explained using the same arguments as in the case of $\text{O}_{\text{hy}}\text{-O}_{\text{w}}$ RDF. In Figure 3.20b, the $\text{H}_{\text{hy}}\text{-H}_{\text{w}}$ RDF shows a pronounced first peak at 2.14 Å, which is consistent with the resulting $\text{H}_{\text{hy}}\text{-O}_{\text{w}}$ RDF.

For more detailed analysis of hydrogen bonding between H_3O^+ and water molecules, the probability distributions of the cosine of the $\text{O}_{\text{hy}}\text{-H}_{\text{hy}}\cdots\text{O}_{\text{w}}$ angle, calculated from the subset of configurations with $\text{H}_{\text{hy}}\cdots\text{O}_{\text{w}}$ distances smaller than 2.0 (dashed line) and smaller than 2.5 Å (full line), respectively, are plotted in Figure 3.21. The overall short $\text{H}_{\text{hy}}\cdots\text{O}_{\text{w}}$ distances of less than 2.2 Å (the first minimum of the $\text{H}_{\text{hy}}\text{-O}_{\text{w}}$ RDF in Figure 3.20) are consistent with almost linear $\text{O}_{\text{hy}}\text{-H}_{\text{hy}}\cdots\text{O}_{\text{w}}$ hydrogen bonds. Comparing between the two curves, deviation of the curve at slight longer $\text{H}_{\text{hy}}\cdots\text{O}_{\text{w}}$ distance of 2.5 Å can be attributed to the presence of the next nearest-neighbor, *e.g.* the fourth water molecule.

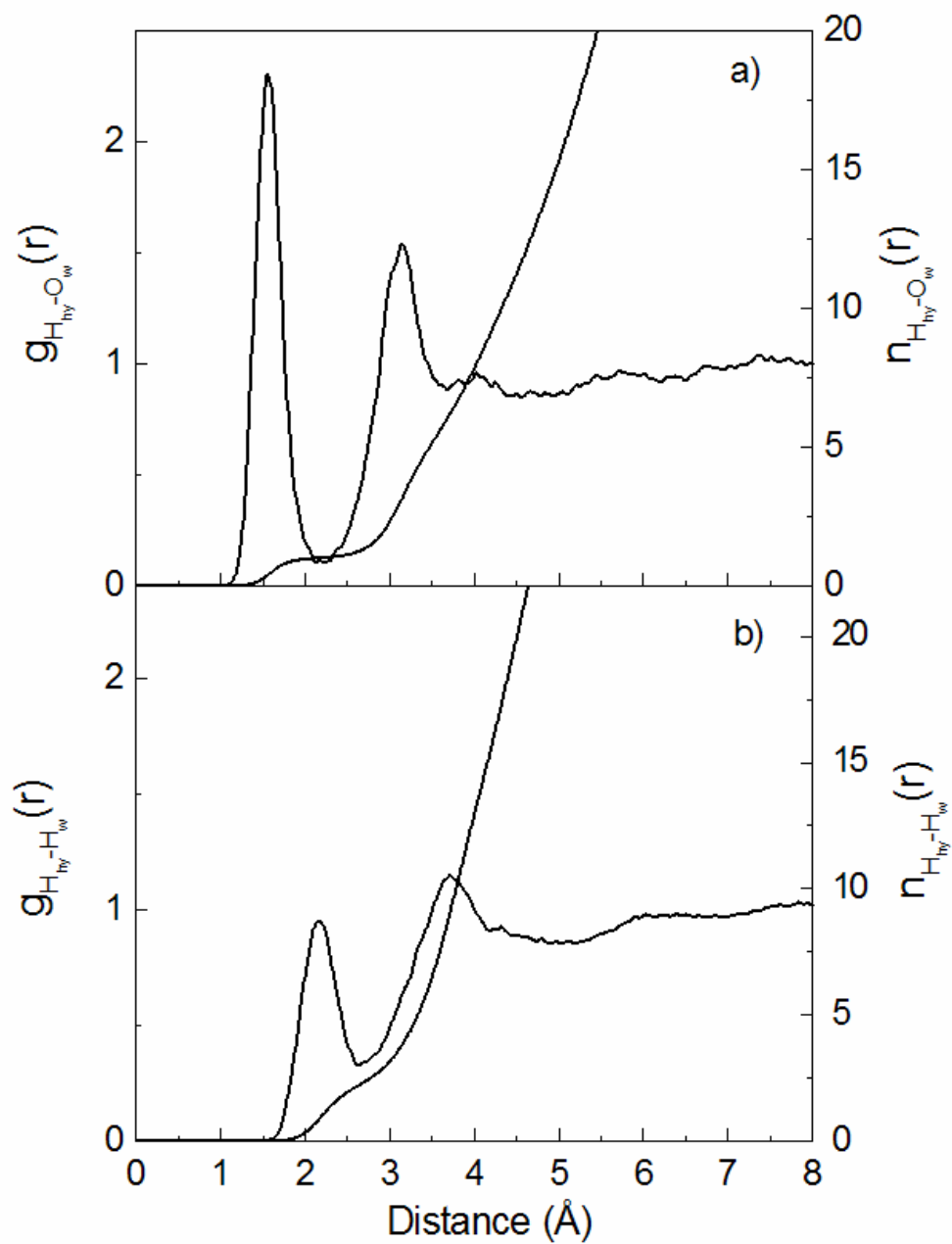


Figure 3.20 a) $H_{hy}-O_w$ and b) $H_{hy}-H_w$ RDFs and their corresponding integration numbers.

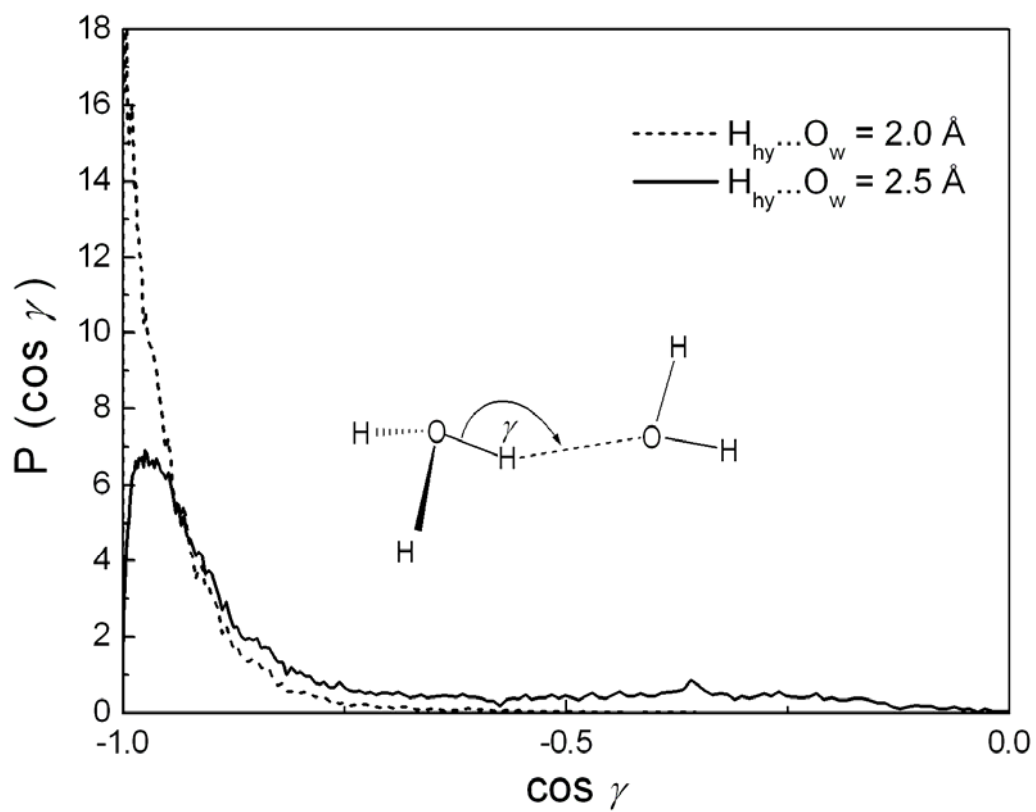


Figure 3.21 $O_{hy}-H_{hy} \cdots O_w$ angular distributions as indicated, calculated for $H_{hy} \cdots O_w$ distances ≤ 2.0 and $\leq 2.5 \text{ \AA}$, respectively.

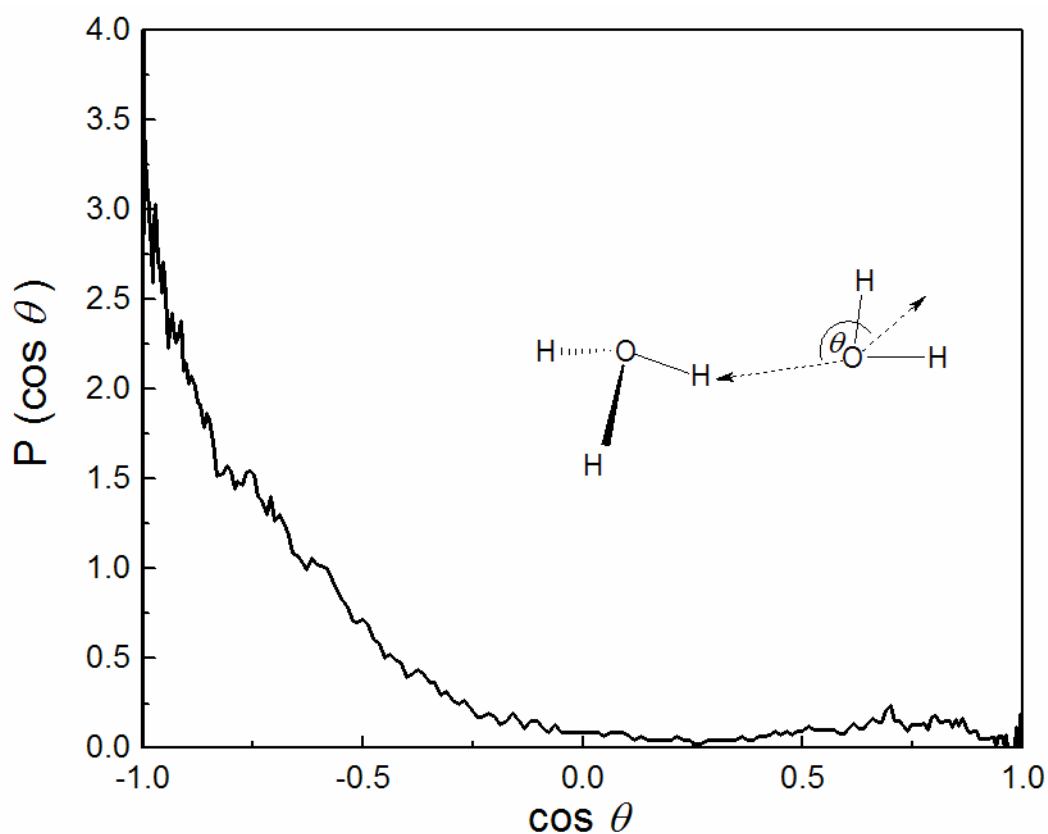


Figure 3.22 Distributions of the angle θ , between the intramolecular $O_{\text{hy}}\text{-H}_{\text{hy}}$ vector and the water dipole vector, for $O_{\text{hy}}\cdots O_{\text{w}}$ distances ≤ 3.2 Å.

Figure 3.22 shows the distribution of the cosine of the angle θ between the $H_{\text{hy}}\text{-O}_{\text{w}}$ vector and the dipole vector of the hydration water molecules. The QM/MM simulation shows a clear dipole-oriented arrangement of nearest-neighbor water molecules towards H_3O^+ . In addition, a small maximum is observed around $\cos \theta = 0.7$, which could be attributed to the correlations between the next nearest-neighbor water molecules and the lone pair direction.

3.2.2 Intramolecular geometry

The intramolecular geometry of the H_3O^+ ion and of the first shell water molecules is described by the distributions of their O-H bond lengths and H-O-H angles in Figure 3.23. Both the O-H bond lengths and H-O-H angles distributions of H_3O^+ are broader than those of the first shell water molecules. This is an indication of the partial formation of H_5O_2^+ , in which the intramolecular $\text{O}_{\text{hy}}\text{-H}_{\text{hy}}$ bond is fully extended at the expense of a short $\text{O}_{\text{w}}\cdots\text{H}_{\text{hy}}$ distance.

Figure 3.24 shows the corresponding probability distributions of the *longest* intramolecular $\text{O}_{\text{hy}}\text{-H}_{\text{hy}}$ bond distance (full line) which is obtained by choosing the longest $\text{O}_{\text{hy}}\text{-H}_{\text{hy}}$ bond in each analyzed configuration. It shows a maximum peak around 1.1 Å, which is very close to the corresponding distance of the symmetrical H_5O_2^+ ion, and ranges up to 1.3 Å. At the same time, the distribution of the shortest intermolecular $\text{O}_{\text{w}}\cdots\text{H}_{\text{hy}}$ distance also shows a maximum at 1.45 Å and ranges down to 1.15 Å. The overlap of the two distributions corresponds to (almost) the symmetrical H_5O_2^+ ions. Note that, due to the structure of H_3O^+ adopted at the beginning of the simulation, the completely symmetric H_5O_2^+ structures are not allowed.

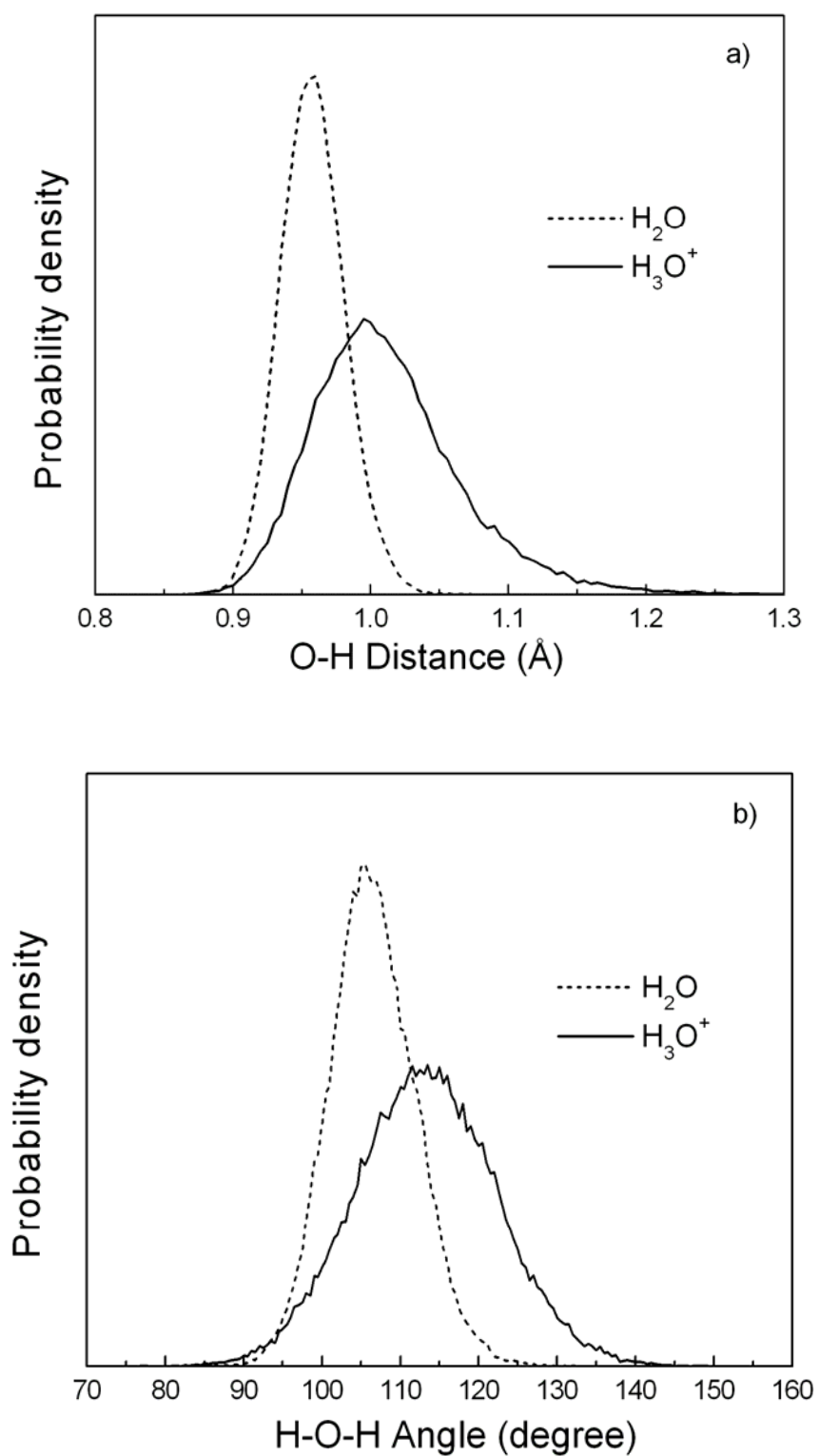


Figure 3.23 Distributions of a) bond lengths and b) bond angles between H_3O^+ and the nearest-neighbor water molecules.

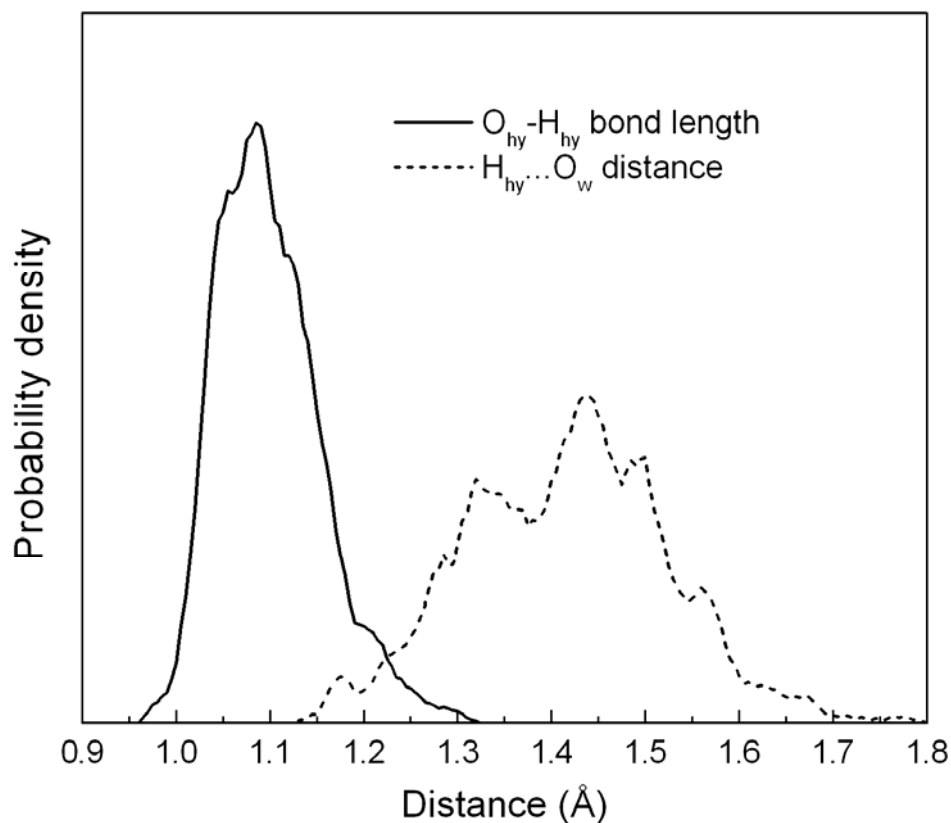


Figure 3.24 Distributions of the longest intramolecular $O_{hy}-H_{hy}$ bond length (full line) and of the shortest intermolecular $H_{hy}\cdots O_w$ distance (dashed line).

3.2.3 Dynamical properties

3.2.3.1 Translational motions

The D_{coeff} value was calculated from the center-of-mass VACF ($C_v(t)$) for H_3O^+ using the Green-Kubo relation (McQuarrie, 1976), (see Equation (3.1)). Integrating the VACF over 2.0 ps yields an estimate for D_{coeff} of $9.9 \times 10^{-5} \text{ cm}^2 \text{ s}^{-1}$. This value (at ‘infinite’ dilution) seems to be in good agreement with the experimentally observed proton diffusion coefficient of $9.3 \times 10^{-5} \text{ cm}^2 \text{ s}^{-1}$ (at high concentration and in the presence of counterions (Agmon, 1995)). By the way,

remarks should be made on the D_{coeff} value obtained by the present QM/MM simulation. It is recognized that the total proton conductivity (vehicle mechanism (Kreuer, Rabenau, and Weppner, 1982)) in aqueous solution results mainly from the diffusion of the protonated water (H_3O^+) and the Grotthuss mechanism. However, the relative contribution between the “vehicle” and “structure” diffusions seems not easy to identify (Kreuer, Paddison, Spohr, and Schuster, 2004). In addition, due to the use of restricted QM region, the proton can oscillate between the H_3O^+ ion and water molecules in the first and some parts of the second hydration shells. Such an oscillation can occur at a much faster rate (*e.g.* because of the very low barrier of proton transfer reaction) than the Grotthuss transport that requires the protonic charge penetration coupling between the first and the second shell water molecules. Since the Grotthuss mechanism, together with the nuclear quantum effects, is not taken into account in the present QM/MM simulation, it is anticipated that the observed D_{coeff} value could be somewhat overestimated.

The power spectrum, which corresponds to the hindered translation of H_3O^+ in water, was obtained by Fourier transformation of the center-of-mass VACF using the correlation length of 2.0 ps, with 2,000 averaged time origins, and is shown in Figure 3.25. The Fourier transformation shows two maxima. The first maximum at zero frequency signifies fast translational motion of the ion in water, while the second one at 360 cm^{-1} could be attributed to the fast H_3O^+ subunit motion during the formation and destruction of the transient $H_5O_2^+$ complex which is largely oscillatory in nature (see details in section 3.2.3.3 below).

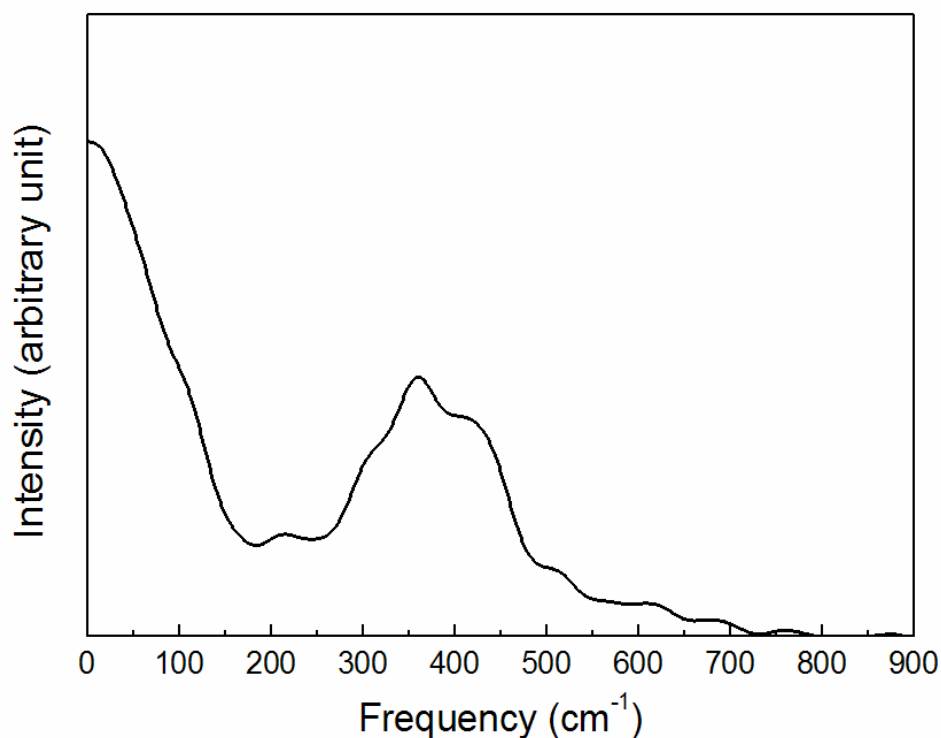


Figure 3.25 Fourier transformation of the translational VACF of the H_3O^+ ion in water.

3.2.3.2 Water exchange in the hydration shell of H_3O^+

The exchange processes of water molecules near each of the hydrogen atoms of H_3O^+ can be best visualized by the plots of the $\text{H}_{\text{hy}} \cdots \text{O}_w$ distances against simulation time, as shown in Figure 3.26. In the course of the QM/MM simulation, several water exchange processes were observed at the hydrogen atoms of H_3O^+ , most of which are the A and I_a mechanisms. These types of exchange process are indicative of strong ion-water interactions.

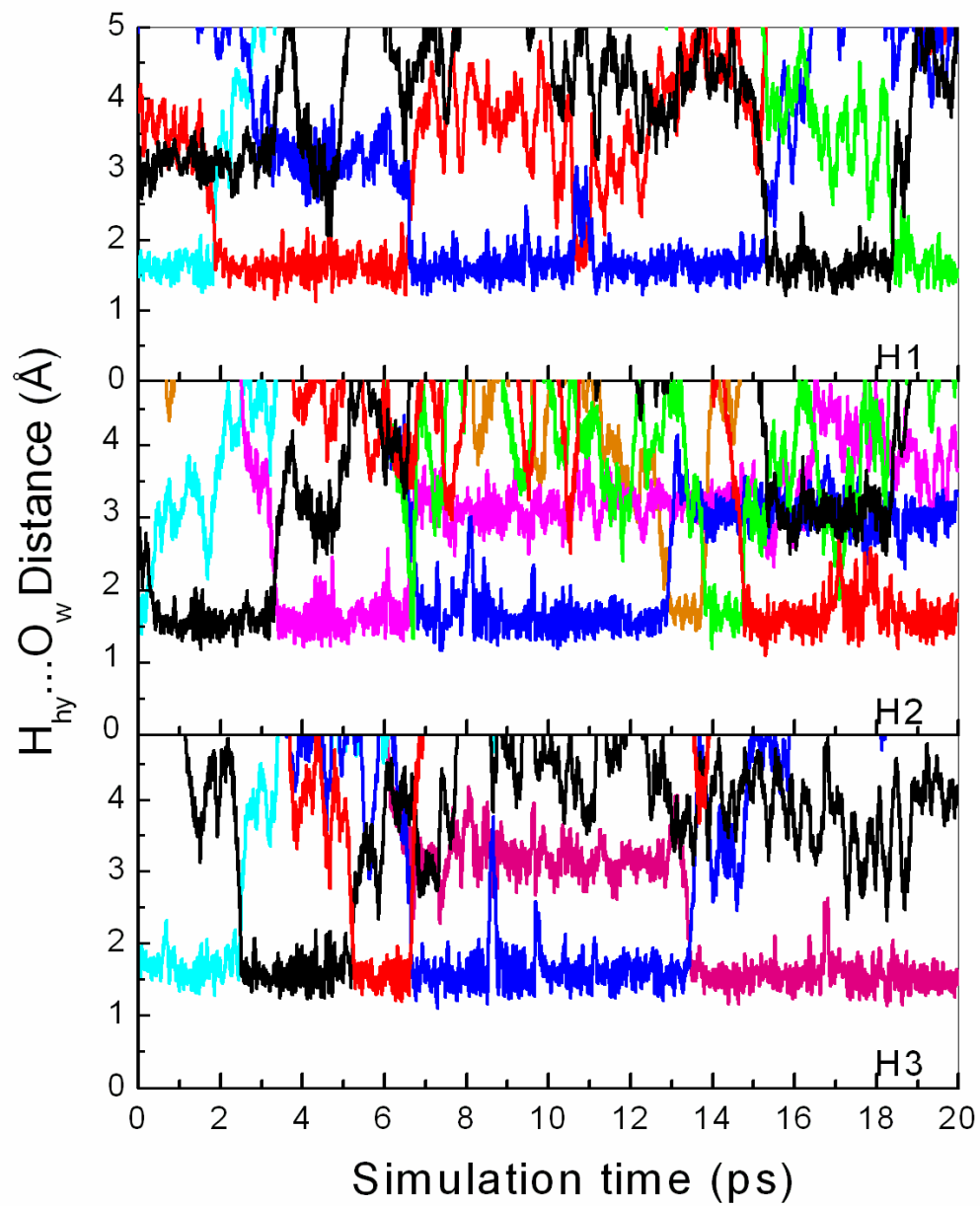


Figure 3.26 Time dependence of $H_{hy} \dots O_w$ distances.

The rate of water exchange processes at the H_3O^+ hydrogens was evaluated through the MRT of the water molecules. In this work, the MRT data were calculated using the direct method (Hofer et al., 2004) with t^* values of 0.0 and 0.5 ps and the results are summarized in Table 3.3. For $t^* = 0.0$ ps, the QM/MM simulation leads to widely varying MRT values, which are of the same order of magnitude as for pure water (Xenides et al., 2005), yet significantly distinct for each of the three hydrogen atoms, indicating the limitations of the QM/MM simulation with respect to the short simulation time. It could, however, imply an imbalance of the hydrogen-bond strength at each of the hydrogen atoms of H_3O^+ , due to the temporary formation of the H_5O_2^+ complexes. Comparing the bulk and the hydration shell dynamics of water molecules on the basis of the MRT value is quite meaningful, since the MRT data for pure water were available based on a similar QM/MM simulation. Using $t^* = 0.5$ ps, the QM/MM simulation clearly shows an order of $\tau_{\text{H}_2\text{O}}(\text{H}_i) > \tau_{\text{H}_2\text{O}}(\text{H}_2\text{O})$ for all three hydrogen atoms of H_3O^+ . In comparison to the MRT data for pure water (Xenides et al., 2005), the QM/MM simulation thus clearly indicates a “structure-making” ability of the H_3O^+ ion in aqueous solution. In this work, it should be noted that the QM/MM data of pure water employed for comparison with our QM/MM results are obtained from the compatible QM/MM simulations, i.e., the pure waters were treated quantum mechanically at similar QM level of accuracy using the same basis sets.

Table 3.3 Mean residence time of water molecules in the bulk and in the first hydration shell of each of hydrogen atoms of H_3O^+ , calculated within the first minimum of $\text{H}_{\text{hy}} \cdots \text{O}_w$ RDF.

| Atom/solute | CN | t_{sim} | $t^* = 0.0$ ps | | $t^* = 0.5$ ps | |
|--|-----|------------------|-------------------|-------------------------------|-----------------------|-----------------------------------|
| | | | N_{ex}^0 | $\tau_{\text{H}_2\text{O}}^0$ | $N_{\text{ex}}^{0.5}$ | $\tau_{\text{H}_2\text{O}}^{0.5}$ |
| H1 | 1.0 | 20.0 | 65 | 0.31 | 8 | 2.50 |
| H2 | 1.0 | 20.0 | 113 | 0.18 | 11 | 1.82 |
| H3 | 1.0 | 20.0 | 47 | 0.42 | 8 | 2.50 |
| Pure H_2O (Xenides et al., 2005) | 4.2 | 40.0 | - | 0.33 | - | 1.51 |

CN = average coordination number of the first hydration shell of water and of each of hydrogen atoms of NH_4^+ .

t^* = minimum duration of the ligand's displacement from its original coordination shell.

t_{sim} = simulation time in ps

$N_{\text{ex}}^{t^*}$ = number of exchange events

$\tau_{\text{H}_2\text{O}}^{t^*}$ = Mean residence time

3.2.3.3 Proton transfer dynamics

To study “chemical reactions” such as the PT process in the solution of H_3O^+ in water, bond breaking and forming within the hydrated H_3O^+ complex has to be accurately described. In aqueous solution, it is well-established that the H_9O_4^+ and H_5O_2^+ complexes are the most important species. H_9O_4^+ is formed when the three hydrogen atoms in H_3O^+ are equivalently hydrated, forming three analogous hydrogen bonds with three nearest-neighbor water molecules. H_5O_2^+ is formed when one H^+ ion is symmetrically shared between two water molecules. The properties of H_5O_2^+ have been investigated in quantum mechanical calculations of isolated $(\text{H}_2\text{O})_n\text{H}^+$ clusters (Cheng, 1998; Karlström, 1988; Kochanski, 1985; Wei and Salahub, 1994), as well as in previous *ab initio* simulations (Tuckerman, Laasonen, Sprik, and Parrinello, 1995a; Tuckerman, Laasonen, Sprik, and Parrinello, 1995b; Tuckerman, Marx, Klein, and Parrinello, 1997).

In order to obtain some information on the frequency of the H_5O_2^+ formation, threshold values for the $\text{O}_{\text{hy}} \cdots \text{O}_{\text{w}}$ distances (R_{max}) are established to monitor the H_5O_2^+ ion. The H_5O_2^+ complex is considered to be “formed” when the $\text{O}_{\text{hy}} \cdots \text{O}_{\text{w}}$ distance in the original H_9O_4^+ complex is smaller than R_{max} . For $R_{\text{max}} = 2.4 \text{ \AA}$ (e.g. the equilibrium $\text{O} \cdots \text{O}$ distance of $\text{H}_2\text{O} \cdots \text{H}^+ \cdots \text{OH}_2$ in the gas-phase (Agmon, 1995)), the QM/MM simulation reveals that approximately 10% of the MD configurations consists of the H_5O_2^+ structure. Increasing R_{max} to 2.5 \AA , the proportion of H_5O_2^+ in solution rapidly increases to 45%. In addition, configurations such as H_7O_3^+ (e.g., a complex in which two of the $\text{O}_{\text{hy}} \cdots \text{O}_{\text{w}}$ distances of the original H_9O_4^+ are $\leq 2.5 \text{ \AA}$), can also be observed, in about 10% of the cases. In fact, the H_5O_2^+ and

H_7O_3^+ structures belong to the same fluctuating complex (H_9O_4^+), *e.g.*, small shift of the H_3O^+ hydrogen atoms along their $\text{O}_{\text{hy}}\text{-H}_{\text{hy}}$ bonds converts the original H_9O_4^+ into either H_7O_3^+ or H_5O_2^+ structures, and vice versa.

During the simulation, charges of all particles within the QM region can vary dynamically. Consequently, transient inter-conversions between the H_3O^+ -centered, the H_9O_4^+ complex, and the H_5O_2^+ -centered, the H_5O_2^+ form, are accompanied by charge fluctuations. Figure 3.27 displays the variations of $\text{O}_{\text{hy}}\text{-H}_{\text{hy}}$ bond length and $\text{H}_{\text{hy}}\cdots\text{O}_{\text{w}}$ distance over a short time span of 4 ps. There are only few situations in which the intramolecular $\text{O}_{\text{hy}}\text{-H}_{\text{hy}}$ and the intermolecular $\text{H}_{\text{hy}}\cdots\text{O}_{\text{w}}$ distances are equal. Thus the symmetric H_5O_2^+ structure is expected to be not very stable (short-lived) in the current simulation, *e.g.*, once the H_5O_2^+ complex is formed, it rapidly reverts back to the original H_9O_4^+ complex. As a consequence, the first maximum of the $\text{O}_{\text{hy}}\text{-O}_{\text{w}}$ RDF (Figure 3.13a) is not split or significantly broadened. Interestingly, as can be seen from the trajectory around 2.5 ps, a water exchange process can simultaneously take place near one hydrogen (H3) as a consequence of an intermediate formation of the H_5O_2^+ around another hydrogen (H2). A similar process seems to occur at around 3.4 ps (H2 and H1).

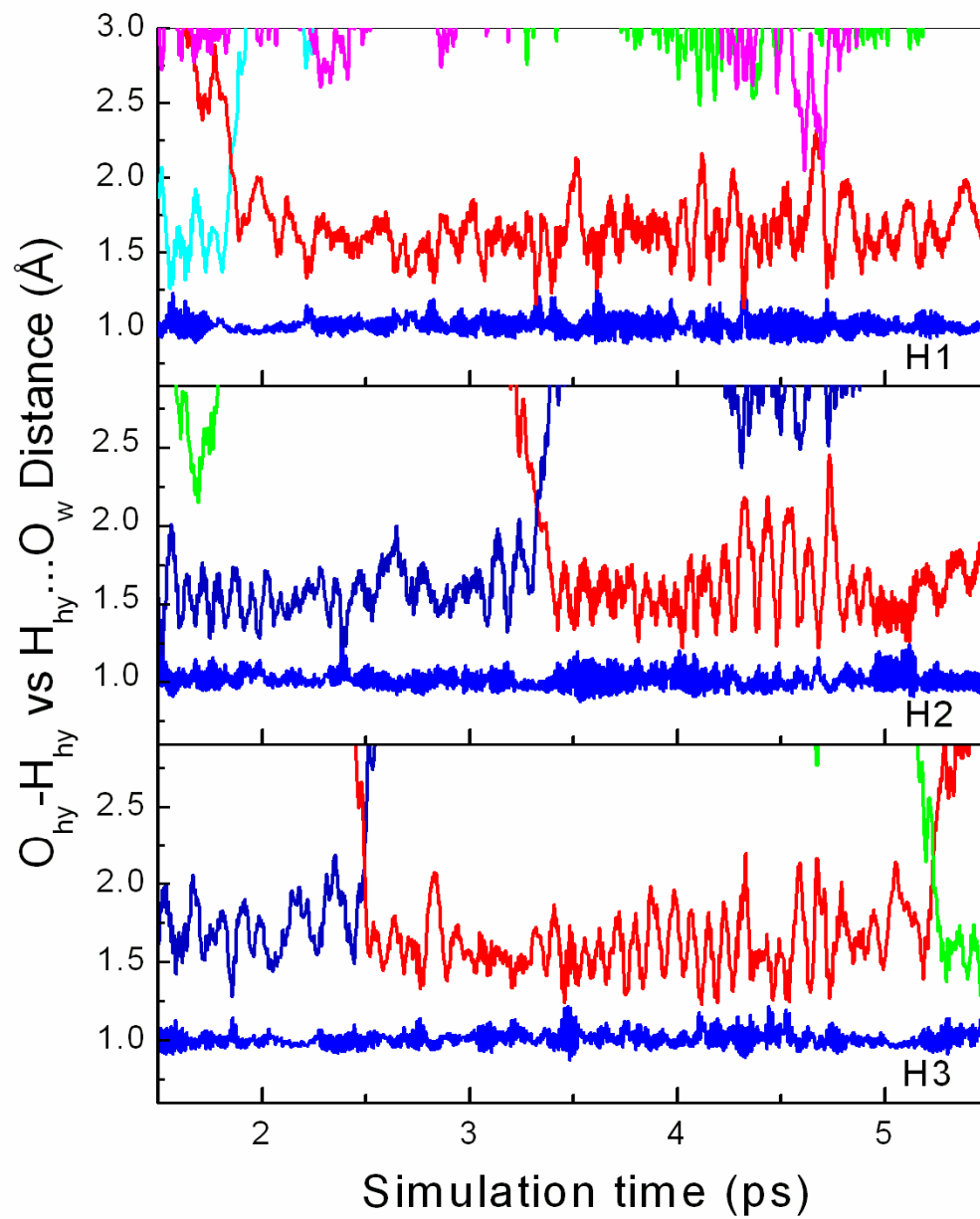


Figure 3.27 Time dependence of $O_{hy}-H_{hy}$ bond lengths and $H_{hy}\cdots O_w$ distances, selecting only for a 4 ps period.

Based on the QM/MM results, the structure and dynamics of the hydrated H_3O^+ can be summarized as follow. Starting from a quite stable H_3O^+ ion, *e.g.*, a structure in which the positive charge is localized at the center of the ion with three equivalent neighbouring water molecules each of which forming a hydrogen bond, the H_9O_4^+ complex is formed. When the next nearest-neighbor water (*e.g.*, the fourth water molecule) approaches the central oxygen atom of H_9O_4^+ , it exchanges with one of the water molecules of the complex (at 2 ps in Figure 3.27), leading to a perturbation of the charge distribution in the complex; which subsequently causes an imbalance of the partial charges at each of the hydrogen atoms of H_3O^+ , and finally, to an imbalance of the $\text{H}_{\text{hy}}\cdots\text{O}_{\text{w}}$ hydrogen-bond distances. Under this circumstance, the strongest $\text{O}_{\text{hy}}\text{--H}_{\text{hy}}\text{--O}_{\text{w}}$ bond (*e.g.*, the one with the shortest $\text{O}_{\text{hy}}\cdots\text{O}_{\text{w}}$ distance) in the H_9O_4^+ complex transiently converts to the H_5O_2^+ intermediate and suddenly back to the H_9O_4^+ form.

CHAPTER IV

CONCLUSION

In this work, the MD simulations based on combined QM/MM method have been performed to investigate the solvation structure and dynamics of NH_4^+ and H_3O^+ in water. Based on the QM/MM-MD scheme, the active site region, *i.e.*, the solvation sphere of NH_4^+ and H_3O^+ , was treated by QM method, while the rest of the system consisting of further solvent molecules is described by classical MM potentials. This QM/MM-MD technique can be seen as a very promising tool for studying such systems since it reliably includes the complicated many-body contributions, as well as the polarization effects within the solvation shell of the ions. It is demonstrated that the reliability of the QM/MM results, besides the statistical requirement of a sufficiently long simulation trajectory for adequately sampling phase space, depends crucially on the QM level of theory, *e.g.*, whether or not electron correlation is taken into account, on the choice of the basis set, and on the size of the QM region. In general, the inclusion of electron correlation in the QM calculations can substantially improve the quality of the results. In practice, however, this procedure is extremely time-consuming, even at the simple MP2 correlated level. Therefore, it was assumed that the correlation effect is small enough to be neglected. Thus, the QM treatment employed in the present study was limited to the HF level of accuracy, with a sufficiently large QM region. This can be considered as a suitable compromise between the quality of the simulation results and the requirement of CPU time.

For the system of NH_4^+ in water, the QM/MM results have revealed a flexible and more labile hydration structure of NH_4^+ , in which numerous species of hydrated NH_4^+ appear, varying possible from 4- to 10-fold coordinated complexes. The hydrogen bonding between NH_4^+ and water is found to be not extremely strong, especially when compared to that of water-water interactions. The hydration enthalpy of NH_4^+ is estimated to be $-85.7 \text{ kcal mol}^{-1}$, which is in good agreement with the experimental values of between -84 and $-89 \text{ kcal mol}^{-1}$. In terms of dynamical properties, the D_{coeff} value for NH_4^+ in water is estimated to be $3.46 \times 10^{-5} \text{ cm}^2 \text{ s}^{-1}$. Compared to the corresponding data of bulk water, the QM/MM results clearly indicate fast translation and rotation of NH_4^+ in water. This phenomenon has been ascribed to the observed multiple coordination, which drives the NH_4^+ ion to translate and rotate quite freely within its surrounding water molecules. In addition, a “structure-breaking” behavior of the NH_4^+ ion is well reflected by the detailed analysis on the water exchange process and the MRTs data of water molecules surrounding the ion.

For the system of H_3O^+ in water, the H_9O_4^+ complex is found to be the most prevalent species in the aqueous solution, partly due to the selection scheme of the center of the QM region. Besides the three nearest-neighbor water molecules directly hydrogen-bonded to H_3O^+ , other neighbor waters, such as a fourth water molecule which interacts preferentially with the oxygen atom of the H_3O^+ ion, are found occasionally near the ion. Nevertheless, it was observed that this fourth water molecule is not strongly shared in a local tetrahedral network of water, *e.g.*, it weakly bound in the lone pair direction of the H_3O^+ ion. Analyses of the water exchange processes and the MRTs value of water molecules in the ion’s hydration shell indicate

that such next-nearest neighbor water molecules participate in the rearrangement of the hydrogen-bond network during fluctuative formation of the H_5O_2^+ ion, and thus contribute to the Grotthuss mechanism of H^+ .

During the QM/MM simulation, it is observed that the H_9O_4^+ complex frequently converts back and forth into the H_5O_2^+ structure, *e.g.*, the small shift of the H_3O^+ hydrogen atoms along their $\text{O}_{\text{hy}}\text{-H}_{\text{hy}}$ bonds converts the original H_9O_4^+ into either the H_7O_3^+ or H_5O_2^+ structures, and vice versa. The D_{coeff} value of H_3O^+ is estimated to be $9.9 \times 10^{-5} \text{ cm}^2 \text{ s}^{-1}$. This value (at ‘infinite’ dilution) seems to be in good agreement with the experimentally observed proton diffusion coefficient of $9.3 \times 10^{-5} \text{ cm}^2 \text{ s}^{-1}$ (at high concentration and in the presence of counterions). However, it should be noted that the total proton conductivity (vehicle mechanism) in aqueous solution results mainly from the diffusion of the protonated water (H_3O^+) and the Grotthuss mechanism, where the relative contribution between the “vehicle” and “structure” diffusions seems not easy to identify.

A final remark should be made on the QM/MM results of H_3O^+ in water. By the QM/MM-MD scheme, the use of restricted QM region allows H^+ to oscillate only between the H_3O^+ ion and water molecules in the first and some part of the second hydration shells, thus no actual PT is allowed during the QM/MM simulation. In this context, the results obtained by the QM/MM simulation can provide detailed information with respect to the structure and dynamics of the hydrated H_3O^+ complex at the state “before” and/or “after” the actual PT process, rather than to visualize the PT pathway.

REFERENCES

REFERENCES

- Adams, D. J., Adams, E. H., and Hills, G. J. (1979). **Molecular Physics**. 38: 387.
- Agmon, N. (1995). The Grotthuss mechanism. **Chemical Physics Letters**. 244: 456-462.
- Allen, M. P., and Tildesley, D. J. (1990). Computer simulation of liquids, Clarendon Press, Oxford.
- Almlof, J. (1973). **Chemica Scripta**. 3: 73.
- Åqvist, J., and Warshel, A. (1993). Simulation of enzyme reactions using valence bond force fields and other hybrid quantum/classical approaches. **Chemical Reviews**. 93: 2523-2544.
- Armstrong, C. (1998). The vision of the pore. **Science**. 280: 56-57.
- Arnett, E. M., et al. (1972). Complete thermodynamic analysis of the "anomalous order" of amine basicities in solution. **Journal of the American Chemical Society**. 94: 4724-4726.
- Atkins, P. W. (1994). **Physical Chemistry**. 5th ed. New York: Freeman.
- Aue, D. H., Webb, H. M., and Bowers, M. T. (1976). A thermodynamic analysis of solvation effects on the basicities of alkylamines. An electrostatic analysis of substituent effects. **Journal of the American Chemical Society**. 98: 318-329.
- Beaumont, R. H., Chihara, H., and Morrison, J. A. (1961). Thermodynamic properties of krypton. Vibrational and other properties of solid argon and solid krypton. **Proceedings of the Physical Society**. 78: 1462-1481.

- Bernal, J. D., and Fowler, R. H. (1933). A Theory of water and ionic solution, with particular reference to hydrogen and hydroxyl ions. **The Journal of Chemical Physics**. 1: 515-548.
- Bernardi, F., Olivucci, M., and Robb, M. A. (1992). Simulation of MC-SCF results on covalent organic multi-bond reactions: Molecular mechanics with valence bond (MM-VB). **Journal of the American Chemical Society**. 114: 1606-1616.
- Bohm, H., and McDonald, I. R. (1984). **Molecular Physics**. 80: 887.
- Bopp, P. (1986). A study of the vibrational motions of water in an aqueous CaCl_2 solution. **Chemical Physics**. 106: 205-212.
- Bopp, P., Jancsó, G., and Heinzinger, K. (1983). An improved potential for non-rigid water molecules in the liquid phase. **Chemical Physics Letters**. 98: 129-133.
- Botti, A., Bruni, F., Imberti, S., Ricci, M. A., and Soper, A. K. (2005). Solvation shell of H^+ ions in water. **Journal of Molecular Liquids**. 117: 77-79.
- Boys, S. F., and Bernardi, F. (1970). **Molecular Physics**. 19: 553.
- Brancato, G., and Tuckerman, M. E. (2005). A polarizable multistate empirical valence bond model for proton transport in aqueous solution. **The Journal of Chemical Physics**. 122: 224507-1 - 224507-11.
- Brodskaya, E., Lyubartsev, A. P., and Laaksonen, A. (2002). Investigation of water clusters containing OH^- and H_3O^+ ions in atmospheric conditions. A molecular dynamics simulation study. **The Journal of Physical Chemistry B**. 106: 6479-6487.

- Brooks, B. R, Bruccoleri, R. E., Olafson, B. D., States, D. J., Swaminathan, S., and Karplus, M. (1983). CHARMM: A program for macromolecular energy, minimization, and dynamics calculations. **Journal of Computational Chemistry**. 4: 187-217.
- Brown, R. J. C. (1995). Hydrogen bonding of the ammonium ion. **Journal of Molecular Structure**. 345: 77-81.
- Brugé, F., Bernasconi, M., and Parrinello, M. (1999a). *Ab initio* simulation of rotational dynamics of solvated ammonium ion in water. **Journal of the American Chemical Society**. 121: 10883-10888.
- Brugé, F., Bernasconi, M., and Parrinello, M. (1999b). Density-functional study of hydration of ammonium in water clusters. **The Journal of Chemical Physics**. 110: 4734-4736.
- Car, R., and Parrinello, M. (1985). Unified approach for molecular dynamics and density-functional theory. **Physical Review Letters**. 55: 2471-2474.
- Chang, T-M., and Dang, L. X. (2003). On rotational dynamics of an NH_4^+ ion in water. **Journal of Chemical Physics**. 118: 8813-8820.
- Cheng, H. (1998). Water clusters: Fascinating hydrogen-bonding networks, solvation shell structures, and proton motion. **The Journal of Physical Chemistry A**. 102: 6201-6204.
- Christie, R. A., and Jordan, K. D. (2001). Theoretical investigation of the $\text{H}_3\text{O}^+(\text{H}_2\text{O})_4$ cluster. **The Journal of Physical Chemistry A**. 105: 7551-7558.
- Ciccotti, G., Frenkel, D., and McDonald, I. R. (1987). **Simulation of Liquids and Solids**. North-Holland.

- Ciccotti, G., Hoover, W.G. (1986). **Molecular Dynamics Simulation of Statistical-mechanical Systems**. North-Holland.
- Coker, H. (1976). Empirical free-ion polarizabilities of the alkali metal, alkaline earth metal, and halide ions. **The Journal of Physical Chemistry**. 80: 2078-2084.
- Conway, B. E. (1964). **Modern Aspects of Electrochemistry**. London: Butterworths.
- Cummins, P. L., and Gready, J. E. (1997). Coupled semiempirical molecular orbital and molecular mechanics model (QM/MM) for organic molecules in aqueous solution. **Journal of Computational Chemistry**. 18: 1496-1512.
- Dang, L. X. (1993). Solvation of ammonium ion. A molecular dynamics simulation with nonadditive potentials. **Chemical Physics Letters**. 213: 541-546.
- Day, T. J. F., Soudackov, A. V., Čuma, M., Schmitt, U. W., and Voth, G. A. (2002). A second generation multistate empirical valence bond model for proton transport in aqueous systems. **The Journal of Chemical Physics**. 117: 5839-5849.
- Drukker, K., de Leeuw, S. W., and Hammes-Schiffer, S. (1998). Proton transport along water chains in an electric field. **The Journal of Chemical Physics**. 108: 6799-6808.
- Dunning, T. H., Jr. (1989). Gaussian basis sets for use in correlated molecular calculations. I. The atoms boron through neon and hydrogen. **The Journal of Chemical Physics**. 90: 1007-1023.
- Dunning, T. H., Jr., and Hay, P. J. (1976). **Modern Theoretical Chemistry**. New York: Plenum III.

- Eigen, M. (1964). Proton transfer, acid-base catalysis, and enzymatic hydrolysis. Part I: ELEMENTARY PROCESSES. **Angewandte Chemie International Edition**. 3: 1-19.
- Ermakova, E., Solca, J., Huber, H., and Marx, D. (1995). Many-body and quantum effects in the radial distribution function of liquid neon and argon. **Chemical Physics Letters**. 246: 204-208.
- Erras-Hanauer, H., Clark, T., and Eldik, R. (2003). Molecular orbital and DFT studies on water exchange mechanisms of metal ions. **Coordination Chemistry Reviews**. 238-239: 233-253.
- Field, M. J., Bash, P. A., and Karplus, M. (1990). A combined quantum mechanical and molecular mechanical potential for molecular dynamics simulations. **Journal of Computational Chemistry**. 11: 700-733.
- Frank, H. S. (1956). **Chemical Physics of Ionic Solutions**. New York: John Wiley & Sons.
- Frisch, M. J., Trucks, G. W., Schlegel, H. B., Scuseria, G. E., Robb, M. A., Cheeseman, J. R., Zakrewski, V. G., Montgomery, J. A., Stratmann, R. E., Burant, J. C., Dapprich, S., Millam, J. M., Daniels, A. D., Kudin, K. N., Strain, M. C., Farkas, O., Tomasi, J., Barone, V., Cossi, M., Cammi, R., Mennucci, B., Pomelli, C., Adamo, C., Clifford, S., Ochterski, J., Peterson, G. A., Ayala, P. Y., Cui, Q., Morokuma, K., Malick, D. K., Rabuck, A. D., Raghavachari, K., Foresman, J. B., Cioslowski, J., Ortiz, J. V., Stefanov, B. B., Liu, G., Liashenko, A., Piskorz, P., Komaromi, I., Gomperts, R., Martin, R. L., Fox, D. J., Keith, T., Al-Laham, M. A., Peng, C. Y., Nanayakkara, A., Gonzalez, C., Challacombe, M., Gill, P. M. W., Johnson,

- B. G., Chen, W., Wong, M. W., Andres, J. L., Head-Gordon, M., Replogle, E. S., Pople, J. A. (1998). **Gaussian 98** package (revision A.7) [Computer Software]. Pittsburgh, PA, USA: Gaussian.
- Gao, J. (1996). Methods and applications of combined quantum mechanical and molecular mechanical potentials. **Reviews in Computational Chemistry**. 7: 119-185.
- Giguere, P. A. (1981). Comment on " H_3O^+ and OH^- , the real ions in aqueous acids and bases". **Chemical Physics**. 60: 421-423.
- Halley, J. W. (1978). **Correlation Functions and Quasi-Particle interactions in condensed Matter**. New York: Plenum.
- Hannongbua, S. (1997). The role of nonadditive effects in the first solvation shell of Na^+ and Mg^{2+} in liquid ammonia: Monte Carlo studies including three-body corrections. **The Journal of Chemical Physics**. 106: 6076-6081.
- Hay, P. J., and Wadt, W. R. (1985). *Ab initio* effective core potentials for molecular calculations. Potentials for the transition metal atoms Sc to Hg. **The Journal of Chemical Physics**. 82: 270-283.
- Headrick, J. M., et al. (2005). Spectral signatures of hydrated proton vibrations in water clusters. **Science**. 308: 1765-1769.
- Hermida-Ramón, J. M., and Karlström, G. (2004). Study of the hydronium ion in water. A combined quantum chemical and statistical mechanical treatment. **Journal of Molecular Structure: THEOCHEM**. 712: 167-173.
- Hewish, N. A., and Neilson, G. W. (1981). Ammonium ion coordination in concentrated aqueous ammonium chloride. **Chemical Physics Letters**. 84: 425-427.

- Hofer, T. S., and Rode, B. M. (2004). The solvation structure of Pb(II) in dilute aqueous solution: An *ab initio* quantum mechanical/molecular mechanical molecular dynamics approach. **The Journal of Chemical Physics**. 121: 6406-6411.
- Hofer, T. S., Tran, H. T., Schwenk, C. F., and Rode, B. M. (2004). Characterization of dynamics and reactivities of solvated ions by *ab initio* simulations. **Journal of Computational Chemistry**. 25: 211-217.
- Hückel, E. (1928). **Elektrochem**. 34: 546.
- Intharathep, P., Tongraar, A., and Sagarik, K. (2005). Structure and dynamics of hydrated NH_4^+ : An *ab initio* QM/MM molecular dynamics simulation. **Journal of Computational Chemistry**. 26: 1329-1338.
- Izvekov, S., and Voth, G. A. (2005). *Ab initio* molecular-dynamics simulation of aqueous proton solvation and transport revisited. **The Journal of Chemical Physics**. 123: 044505-1 - 044505-9.
- James, T., and Wales, D. J. (2005). Protonated water clusters described by an empirical valence bond potential. **The Journal of Chemical Physics**. 122: 134306-1 – 134306-11.
- Jiang, J. C., Chang, H., Lee, Y. T., and Lin, S. H. (1999). *Ab initio* studies of $\text{NH}_4^+(\text{H}_2\text{O})_{1-5}$ and the influence of hydrogen-bonding nonadditivity on geometries and vibrations. **The Journal of Physical Chemistry A**. 103: 3123-3135.
- Jorgensen, W. L., and Gao, J. (1986). Monte Carlo simulations of the hydration of ammonium and carboxylate ions. **The Journal of Physical Chemistry**. 90: 2174-2182.

- Jungwirth, P., and Tobias, D. J. (2002). Chloride anion on aqueous clusters, at the air-water interface, and in liquid water: Solvent effects on Cl^- polarizability. **The Journal of Physical Chemistry A**. 106: 379-383.
- Karim, O. A., and Haymet, A. D. J. (1990). Dynamics of an ammonium ion in water: Molecular dynamics simulation. **The Journal of Chemical Physics**. 93: 5961-5966.
- Karlström, G. (1988). Proton transport in water modeled by a quantum chemical dielectric cavity model. **The Journal of Physical Chemistry**. 92: 1318-1322.
- Kassab, E., Evleth, E. M., and Hamou-Tahra, Z. D. (1990). Theoretical characterization of the rotational motion of ammonium ion in water clusters. **Journal of the American Chemical Society**. 112: 103-108.
- Kerdcharoen, T., Liedl, K. R., and Rode, B. M. (1996). A QM/MM simulation method applied to the solution of Li^+ in liquid ammonia. **Chemical Physics**. 211: 313-323.
- Kebarle, P. (1977). Ion thermochemistry and solvation from gas phase ion equilibria. **Annual Review of Physical Chemistry**. 28: 445-476.
- Kendall, R. A., Dunning, T. H., Jr., and Harrison, R. J. (1992). Electron affinities of the first-row atoms revisited. Systematic basis sets and wave functions. **The Journal of Chemical Physics**. 96: 6796-6806.
- Kim, J., Schmitt, U. W., Gruetzmacher, J. A., Voth, G., and Scherer, N. E. (2002). The vibrational spectrum of the hydrated proton: Comparison of experiment, simulation, and normal mode analysis. **The Journal of Chemical Physics**. 116: 737-746.

- Klots, C. E. (1981). Solubility of protons in water. **The Journal of Physical Chemistry**. 85: 3585-3588.
- Kochanski, E. (1985). Theoretical studies of the system $\text{H}_3\text{O}^+(\text{H}_2\text{O})_n$ for $n = 1, 9$. **Journal of the American Chemical Society**. 107: 7869-7873.
- Kornyshev, A. A., Kuznetsov, A. M., Spohr, E., and Ulstrup, J. (2003). Kinetics of proton transport in water. **The Journal of Physical Chemistry B**. 107: 3351-3366.
- Kreuer, K. D., Paddison, S. J., Spohr, E., and Schuster, M. (2004). Transport in proton conductors for fuel-cell applications: Simulations, elementary reactions, and phenomenology. **Chemical Review**. 104: 4637-4678.
- Kreuer, K. D., Rabenau, A., and Weppner, W. (1982). Vehicle mechanism, a new model for the interpretation of the conductivity of fast proton conductors. **Angewandte Chemie International Edition**. 21: 208-209.
- Lapid, H., Agmon, N., Petersen, M. K., and Voth, G. A. (2005). A bond-order analysis of the mechanism for hydrated proton mobility in liquid water. **The Journal of Chemical Physics**. 122: 014506-1 – 014506-11.
- Lobaugh, J., and Voth, G. A. (1996). The quantum dynamics of an excess proton in water. **The Journal of Chemical Physics**. 104: 2056-2069.
- Langford, C. H., and Gray, H. B. (1965). **Ligand Substitution Process**. New York: Benjamin.
- Marx, D., Tuckerman, M. E., Hutter, J. G., and Parrinello, M. (1999). Functional waters in intraprotein proton transfer monitored by FTIR difference spectroscopy. **Nature**. 397: 601-604.

- McComman, J. A., and Harvey, S. C. (1987). **Dynamics of Proteins and Nuclei Acids**. London: Cambridge University Press.
- McQuarrie, D. A. (1976). **Statistical Mechanics**. New York: Harper & Row.
- Merbach, A. E. (1982). **Pure and Applied Chemistry**. 54: 1479.
- Merbach, A. E. (1987). Use of high pressure kinetic studies in determining inorganic substitution mechanisms. **Pure and Applied Chemistry**. 59: 161-172.
- Muller, R. P., and Warshel, A. (1995). *Ab initio* calculations of free energy barriers for chemical reactions in solution. **The Journal of Physical Chemistry**. 99: 17516-17524.
- Natália, M., Cordeiro, D. S., and Gomes, J. A. N. F. (1993). *Ab initio* copper-water interaction potential for the simulation of aqueous solutions. **Journal of Computational Chemistry**. 14: 629-638.
- Ohtaki, H., and Radnai, T. (1993). Structure and dynamics of hydrated ions. **Chemical Review**. 93: 1157-1204.
- Pálinkás, G., Radnai, T., Szász, G. I., and Heinzinger, K. (1981). The structure of an aqueous ammonium chloride solution. **The Journal of Chemical Physics**. 74: 3522-3526.
- Perrin, C. L., and Gipe, R. K. (1984). Deuterium fractionation factor for unhydrated hydronium ion. Deuterium isotope effects on proton-transfer equilibria in acetonitrile. **Journal of the American Chemical Society**. 96: 5631-5634.
- Perrin, C. L., and Gipe, R. K. (1986). Rotation, solvation, and hydrogen bonding of aqueous ammonium ion. **Journal of the American Chemical Society**. 108: 1088-1089.
- Perrin, C. L., and Gipe, R. K. (1987). **Science** 238: 1393.

- Pomès, R., and Roux, B. (1996). Theoretical study of H^+ translocation along a model proton wire. **The Journal of Physical Chemistry**. 100: 2519-2527.
- Probst, M. M., Spohr, E., Heinzinger, K., and Bopp, P. (1991). A molecular dynamics simulation of an aqueous beryllium chloride solution. **Simulation**. 7: 43.
- Pyper, N. C., Pike, C. G., and Edwards, P. P. (1992). **Molecular Physics**. 76: 353.
- Robinson, R. A., and Stokes, R. H. (1959). **Electrolyte Solutions**. 2nd ed. London: Butterworths.
- Rode, B. M., Schwenk, C. F., and Tongraar, A. (2004). Structure and dynamics of hydrated ions—new insights through quantum mechanical simulations. **Journal of Molecular Liquid**. 110: 105-122.
- Ruff, I., and Frierich, V. J. (1972). Transfer diffusion. IV. Numerical test of the correlation between prototrope mobility and proton exchange rate of H_3O^+ and OH^- ions with water. **The Journal of Physical Chemistry**. 76: 2954-2957.
- Schmitt, U. W., and Voth, G. A. (1998). Multistate empirical valence bond model for proton transport in water. **The Journal of Physical Chemistry B**. 102: 5547-5551.
- Schmitt, U. W., and Voth, G. A. (1999). The computer simulation of proton transport in water. **The Journal of Chemical Physics**. 111: 9361-9381.
- Schwenk, C. F., Loeffler, H. H., and Rode, B. M. (2001). Molecular dynamics simulations of Ca^{2+} in water: Comparison of a classical simulation including three-body corrections and Born–Oppenheimer *ab initio* and density functional theory quantum mechanical/molecular mechanics simulations. **The Journal of Chemical Physics**. 115: 10808-10813.

- Schwenk, C. F., Hofer, T. S., and Rode, B. M. (2004). "Structure breaking" effect of hydrated Cs^+ . **The Journal of Physical Chemistry A**. 108: 1509-1514.
- Schwenk, C. F., and Rode, B. M. (2003). Extended *ab initio* quantum mechanical/molecular mechanical molecular dynamics simulations of hydrated Cu^{2+} . **The Journal of Chemical Physics**. 119: 9523-9531.
- Singh, U. C., and Kollman, P. A. (1986). A combined *ab initio* quantum mechanical and molecular mechanical method for carrying out simulations on complex molecular systems: Applications to the $\text{CH}_3\text{Cl} + \text{Cl}^-$ exchange reaction and gas phase protonation of polyethers. **Journal of Computational Chemistry**. 7: 718-730.
- Stanton, R. V., Hartsough, D. S., and Merz, K. M., Jr. (1995). An examination of a density functional/molecular mechanical coupled potential. **Journal of Computational Chemistry**. 16: 113-128.
- Stillinger, F. H., and Rahman, A. (1978). Revised central force potentials for water. **The Journal of Chemical Physics**. 68: 666-670.
- Szász, G. I., and Heinzinger, K. (1979). **Zeitschrift fur Naturforschung**. 34a: 840.
- Sagnella, D. E., and Tuckerman, M. (1998). An empirical valence bond model for proton transfer in water. **The Journal of Chemical Physics**. 108: 2073-2083.
- Sceats, M. G., and Rice, S. A. (1980). The water-water pair potential near the hydrogen bonded equilibrium configuration. **The Journal of Chemical Physics**. 72: 3236-3247.

- Tobias, D. J., Jungwirth, P., and Parrinello, M. (2001). Surface solvation of halogen anions in water clusters: An *ab initio* molecular dynamics study of the Cl^- $(\text{H}_2\text{O})_6$ complex. **The Journal of Chemical Physics**. 114: 7036-7044.
- Tongraar, A., Liedl, K. R., and Rode, B. M. (1997). Solvation of Ca^{2+} in Water Studied by Born-Oppenheimer *ab Initio* QM/MM Dynamics. **The Journal of Physical Chemistry A**. 101: 6299-6309.
- Tongraar, A., Liedl, K. R., and Rode, B. M. (1998a). Born-Oppenheimer *ab initio* QM/MM dynamics simulations of Na^+ and K^+ in water: From structure making to structure breaking effects. **The Journal of Physical Chemistry A**. 102: 10340-10347.
- Tongraar, A., Liedl, K. R., and Rode, B. M. (1998b). The hydration shell structure of Li^+ investigated by Born-Oppenheimer *ab initio* QM/MM dynamics. **Chemical Physics Letters**. 286: 56-64.
- Tongraar, A., and Rode, B. M. (1999). Preferential solvation of Li^+ in 18.45% aqueous ammonia: A Born-Oppenheimer *ab initio* quantum mechanics/molecular mechanics MD simulation. **The Journal of Physical Chemistry A**. 103: 8524-8527.
- Tongraar, A., and Rode, B. M. (2001). A Born-Oppenheimer *ab initio* quantum mechanical/molecular mechanical molecular dynamics simulation on preferential solvation of Na^+ in aqueous ammonia solution. **The Journal of Physical Chemistry A**. 105: 506-510.
- Tongraar, A., and Rode, B. M. (2003). The hydration structures of F^- and Cl^- investigated by *ab initio* QM/MM molecular dynamics simulations. **Physical Chemistry Chemical Physics**. 5: 357-362.

- Tongraar, A., and Rode, B. M. (2004). Dynamical properties of water molecules in the hydration shells of Na^+ and K^+ : *Ab initio* QM/MM molecular dynamics simulations. **Chemical Physics Letters**. 385: 378-383.
- Tongraar, A., and Rode, B. M. (2005). *Ab initio* QM/MM dynamics of anion–water hydrogen bonds in aqueous solution. **Chemical Physics Letters**. 403: 314-319.
- Tongraar, A., Sagarik, K., and Rode, B. M. (2001). Effects of many-body interactions on the preferential solvation of Mg^{2+} in aqueous ammonia solution: A Born-Oppenheimer *ab initio* QM/MM dynamics study. **The Journal of Physical Chemistry B**. 105: 10559-10564.
- Tongraar, A., Sagarik, K., and Rode, B. M. (2002). Preferential solvation of Ca^{2+} in aqueous ammonia solution: Classical and combined *ab initio* quantum mechanical/molecular mechanical molecular dynamics simulations. **Physical Chemistry Chemical Physics**. 4: 628-634.
- Tomasi, J., and Persico, M. (1994). Molecular interactions in solution: An overview of methods based on continuous distributions of the solvent. **Chemical Reviews**. 94: 2027-2094.
- Triolo, R., and Narten, A. H. (1975). Diffraction pattern and structure of aqueous hydrochloric acid solutions at 20° C. **The Journal of Chemical Physics**. 63: 3624-3631.
- Tuckerman, M. E., Laasonen, K., Sprik, M., and Parrinello, M. (1995a). *Ab initio* molecular dynamics simulation of the solvation and transport of hydronium and hydroxyl ions in water. **The Journal of Chemical Physics**. 103: 150-161.

- Tuckerman, M. E., Laasonen, K., Sprik, M., and Parrinello, M. (1995b). *Ab initio* molecular dynamics simulation of the solvation and transport of H_3O^+ and OH^- ions in water. **The Journal of Physical Chemistry**. 99: 5749-5752.
- Tuckerman, M. E., Marx, D., Klein, M. L., and Parrinello, M. (1997). On the quantum nature of the shared proton in hydrogen bonds. **Science**. 275: 817-820.
- von Grothuss, C. J. D. (1806). **Annali di Chimica**. 54.
- Vuilleumier, R., and Borgis, D. (1997). Molecular dynamics of an excess proton in water using a non-additive valence bond force field. **Journal of Molecular Structure**. 436: 555-565.
- Vuilleumier, R., and Borgis, D. (1998a). An extended empirical valence bond model for describing proton transfer in $\text{H}^+(\text{H}_2\text{O})_n$ clusters and liquid water. **Chemical Physics Letters**. 284: 71-77.
- Vuilleumier, R., and Borgis, D. (1998b). Quantum dynamics of an excess proton in water using an extended empirical valence-bond hamiltonian. **The Journal of Physical Chemistry B**. 102: 4261-4264.
- Vuilleumier, R., and Borgis, D. (1999). Transport and spectroscopy of the hydrated proton: A molecular dynamics study. **The Journal of Chemical Physics**. 111: 4251-4266.
- Vuilleumier, R., and Borgis, D. (1999). **Israel Journal of Chemistry**. 39: 457.
- Wang, F., and Voth, G. A. (2005). A linear-scaling self-consistent generalization of the multistate empirical valence bond method for multiple excess protons in aqueous systems. **The Journal of Chemical Physics**. 122: 144105-1 - 144105-9.

- Wang, Y., Lu, M., and Draper, D. E. (1993). Specific ammonium ion requirement for functional ribosomal RNA tertiary structure. **Biochemistry** 32: 12279-12282.
- Warshel, A., and Levitt, M. (1976). Theoretical studies of enzymic reactions: Dielectric, electrostatic and steric stabilization of the carbonium ion in the reaction of lysozyme. **Journal of Molecular Biology**. 103: 227-249.
- Wei, D. Q., and Salahub, D. R. (1994). Hydrated proton clusters and solvent effects on the proton transfer barrier: A density functional study. **The Journal of Chemical Physics**. 101: 7633-7642.
- William, R. J. P. (1971). **Bio-inorganics Chemistry**. Washington, DC: American Chemical Society.
- Wishaw, B. F., and Stokes, R. H. (1954). The diffusion coefficients and conductances of some concentrated electrolyte solutions at 25°. **Journal of the American Chemical Society**. 76: 2065-2071.
- Woon, D. E., and Dunning, T. H., Jr. (1993). Gaussian basis sets for use in correlated molecular calculations. III. The atoms aluminum through argon. **The Journal of Chemical Physics**. 98: 1358-1371.
- Xenides, D., Randolph, B. R., and Rode, B. M. (2005). Structure and ultrafast dynamics of liquid water: A quantum mechanics/molecular mechanics molecular dynamics simulations study. **The Journal of Chemical Physics**. 122: 174506-1 – 174506-10.

APPENDICES

APPENDIX A

LISTS OF PRESENTATIONS

1. Patoomwadee Intaratap, Anan Tongraar, Kritsana Sagarik. (April 25-27, 2003). Investigation of hydration structure of ammonium ion using *ab initio* QM/MM molecular dynamics simulation. **RGJ-Ph.D. Congress IV**. Jomtien Palm Beach Hotel&Resort, Chonburi, Thailand.
2. Pathumwadee Intharathap, Anan Tongraar and Kritsana Sagarik. (July, 21-23 2004). Quantum-Mechanical based simulations of an ammonium ion in aqueous solution. **The 8th Annual National Symposium on Computational Science and Engineering (ANSCSE8)**. Suranaree University of Technology, Nakhon Ratchasima, Thailand.
3. Pathumwadee Intharathap, Anan Tongraar and Kritsana Sagarik. (October 19-21, 2004). Dynamical properties of NH_4^+ in water studied by *ab initio* QM/MM MD simulation. **30th Congress on Science and Technology of Thailand (STT30th)**. IMPACT Muang Thong Thani, Bangkok, Thailand.
4. Pathumwadee Intharathap, Anan Tongraar and Kritsana Sagarik (May 2-6, 2005). *Ab initio* QM/MM dynamics of H_3O^+ in water. **2nd Asian Pacific Conference on Theoretical & Computational Chemistry (APCTCC2)**. Chulalongkorn University, Bangkok, Thailand.
5. Pathumwadee Intharathap, Anan Tongraar and Kritsana Sagarik. (October 18-20, 2005). Effects of electron correlation on the structural properties of H_3O^+ in water: Combined *ab initio* QM/MM molecular dynamics simulations. **31st Congress on Science and Technology of Thailand (STT31st)**. Suranaree University of Technology, Nakhon Ratchasima, Thailand.

APPENDIX B

LISTS OF PUBLICATIONS

1. Intharathep, P., Tongraar, A., and Sagarik, K. (2005). Structure and dynamics of hydrated NH_4^+ : An *ab initio* QM/MM molecular dynamics simulation. **Journal of Computational Chemistry**. 26 : 1329-1338.
2. Intharathep, P., Tongraar, A., and Sagarik, K. (2006). *Ab initio* QM/MM dynamics of H_3O^+ in water. **Journal of Computational Chemistry**. accepted for publication.

Structure and Dynamics of Hydrated NH_4^+ : An *ab initio* QM/MM Molecular Dynamics Simulation

PATHUMWADEE INTHARATHEP, ANAN TONGRAAR, KRITSANA SAGARIK
School of Chemistry, Institute of Science, Suranaree University of Technology, Nakhon
Ratchasima 30000, Thailand

Received 7 February 2005; Accepted 21 April 2005

DOI 10.1002/jcc.20265

Published online in Wiley InterScience (www.interscience.wiley.com).

Abstract: A combined *ab initio* quantum mechanical/molecular mechanical (QM/MM) molecular dynamics simulation has been performed to investigate solvation structure and dynamics of NH_4^+ in water. The most interesting region, the sphere includes an ammonium ion and its first hydration shell, was treated at the Hartree–Fock level using DZV basis set, while the rest of the system was described by classical pair potentials. On the basis of detailed QM/MM simulation results, the solvation structure of NH_4^+ is rather flexible, in which many water molecules are cooperatively involved in the solvation shell of the ion. Of particular interest, the QM/MM results show fast translation and rotation of NH_4^+ in water. This phenomenon has resulted from multiple coordination, which drives the NH_4^+ to translate and rotate quite freely within its surrounding water molecules. In addition, a “structure-breaking” behavior of the NH_4^+ is well reflected by the detailed analysis on the water exchange process and the mean residence times of water molecules surrounding the ion.

© 2005 Wiley Periodicals, Inc. J Comput Chem 26: 1329–1338, 2005

Key words: NH_4^+ ; QM/MM; water exchange; mean residence time

Introduction

Solvation structure and dynamics of ions in water play an important role in many chemical and biological systems.^{1–4} Besides the simple alkaline and alkaline–earth metal cations, ammonium ion (NH_4^+) is an important chemical species that provides a simple model for solvated amides.^{5,6} In addition, in compactly folded RNAs, coordination or hydrogen bonding of this ion in specific sites is a crucial aspect for its ability to stabilize the RNA fragment structure.⁷ The detailed interpretation on the structure and dynamics of NH_4^+ in aqueous solution has been studied extensively.^{8–20} Of particular interest, recent NMR measurements^{6,8} have shown that NH_4^+ rotates quite fast in aqueous solution, despite the expected strong hydrogen bonding between the NH_4^+ and its surrounding water molecules. To explain such surprising phenomenon, several rotational mechanisms have been proposed based on either *ab initio* geometry optimizations^{11–13} as well as Monte Carlo (MC)¹⁴ and molecular dynamics (MD)^{10,15–20} simulations. Most of the previous studies have provided useful information on the dynamical properties of the hydrated NH_4^+ , such as its fast diffusive rotational motion. However, the agreement on the structure of the first solvation shell of NH_4^+ , which is a necessary prerequisite for understanding its rotational mechanism, is still far from satisfactory. On the structural viewpoint of NH_4^+ in aqueous

solution, the most representative picture of the coordination to emerge is of two groups of water molecules. There is a first group of four, which is strongly oriented so as to create nearly linear N—H···O interactions. This structural aspect is supported by experimental X-ray and neutron diffraction studies.^{9,10} The second group of water molecules is much less strongly oriented than the first, and its structure is a source of major disagreement between the theoretical observations, consisting of 1–8 water molecules.^{10,14–20} Thus, the comprehensive knowledge of how NH_4^+ interacts with water molecules remains incomplete.

Recently, MD simulation with polarizable models¹⁷ has been performed to provide a qualitative prediction on the rotational dynamics of NH_4^+ in water, which is in good agreement with the experimental observations. However, the contributions of the ion's polarizability are not directly obtainable because there is no direct measurement of this quantity in aqueous solution, and the available data are usually extrapolations from ionic crystal and salt solu-

Correspondence to: A. Tongraar; email: anan_tongraar@yahoo.com

Contract/grant sponsor: The Thailand Research Fund under the Royal Golden Jubilee Ph.D. Program; contract/grant number: PHD/0225/2543 (to P.I. and K.S.)

Contact/grant sponsor: The Thailand Research Fund under the TRF Basic Research Grant (to A.T.)

Table 1. Average Binding Energies (in kcal mol⁻¹) and Average N—H···O Distances (in Å) of the Optimized NH₄⁺-(H₂O)₄ Complex. Calculated at HF, DFT, and Higher Correlated Methods.

| Basis Set | DZV | | DZP | |
|-----------|--|------------------------------------|--|------------------------------------|
| | $E_{\text{bond}}^{\text{a}}$ (kcal mol ⁻¹) | $R_{\text{N-H}\cdots\text{O}}$ (Å) | $E_{\text{bond}}^{\text{a}}$ (kcal mol ⁻¹) | $R_{\text{N-H}\cdots\text{O}}$ (Å) |
| HF | -19.40 | 1.83 | -16.19 | 1.90 |
| BLYP | -21.61 | 1.74 | -18.26 | 1.78 |
| B3LYP | 21.89 | 1.74 | 18.44 | 1.78 |
| MP2 | -19.69 | 1.82 | -17.25 | 1.81 |
| MP4-DQ | -19.68 | 1.81 | -16.78 | 1.84 |
| CC-D | -19.70 | 1.82 | -16.73 | 1.84 |
| CI-D | -19.57 | 1.81 | -16.58 | 1.85 |

^aThe average values of energy per ligand.

tions.^{21–24} Another attempt to obtain a reliable picture of NH₄⁺ in water is based on first-principle simulation method introduced by Car and Parrinello (CP).¹⁸ This approach relies on the density functional theory (DFT) at the BLYP level, and has been applied on a relatively small system of one NH₄⁺ and 63 water molecules, which has been documented as a severe limitation of the CP-MD applicability for the treatment of electrolyte solutions.^{25,26} In addition, although both exemplary approaches can provide quite reasonable detailed information on the rotational dynamics of NH₄⁺ in water, the observed coordination numbers of 5.8¹⁷ and 5.3¹⁸ are considerably low when compared to the results from the X-ray measurement.¹⁰

Because both theoretical and experimental observations have provided a rather inhomogeneous picture of NH₄⁺ in water, the motivation of the present work was to obtain more reliable data for the structure and dynamics of this hydrate complex. An alternative approach to elucidate such detailed information is to apply the so-called combined *ab initio* quantum mechanical/molecular mechanical (QM/MM) MD technique.^{26–41} This technique has been proven to be a very reliable simulation scheme, which puts confidence in many new insights into composition, property, and reactivity of various solvated ions.^{26–41} In the present study, therefore, the structural and dynamical properties of NH₄⁺ in water will be investigated by means of *ab initio* QM/MM MD simulation.

Methods

By the QM/MM technique,^{26–30} the system is divided into two parts, namely the QM and MM regions. The total interaction energy of the system is defined as

$$E_{\text{total}} = \langle \Psi_{\text{QM}} | \hat{H} | \Psi_{\text{QM}} \rangle + E_{\text{MM}} + E_{\text{QM-MM}}, \quad (1)$$

where $\langle \Psi_{\text{QM}} | \hat{H} | \Psi_{\text{QM}} \rangle$ refers to the interactions within the QM region, while E_{MM} and $E_{\text{QM-MM}}$ represent the interactions within the MM and between the QM and MM regions, respectively. The QM region is considered to be the chemically most important region, which includes NH₄⁺ and its first hydration shell. It is

treated by Born–Oppenheimer *ab initio* Hartree–Fock (HF) quantum mechanics, while the rest of the system is described by classical pair potentials. Basically, the reliability of the QM/MM results—besides the requirement of adequate simulation time—depends crucially on the QM size and the basis sets employed for describing all interactions within the QM region. According to the N—O radial distribution function (RDF) obtained by a preliminary pair potential simulation (data not shown), the first minimum of the N—O peak is located approximately at 3.8 Å. Within this region, about 8–12 water molecules are involved in the first solvation shell of NH₄⁺. Thus, a QM diameter of 7.6 Å and a moderate basis set, like DZV,⁴² seems to be acceptable within the available computational feasibility, leading to 4–8 min to compute quantum mechanical forces in each QM/MM MD step (on a DEC Alpha XP1000 workstation).

In principle, the inclusion of electron correlation in the quantum mechanical calculations can improve the quality of the simulation results, but this is far too time-consuming, even at the simple MP2 correlated level. To estimate the effects of electron correlation, geometry optimizations of the NH₄⁺-(H₂O)₄ complex were conducted using *ab initio* calculations at different levels of theory. The average binding energies with basis set superposition error (BSSE) correction, and the average N—H···O distances calculated at HF, DFT, and highly correlated levels using DZV and DZP⁴² basis sets are summarized in Table 1. The QM calculations with the DZP basis set were carried out to provide a systematic comparison of the effects of electron correlation, as well as to critically evaluate the adequacy of the DZV basis set employed in the present QM/MM MD simulation. In comparison to the results of the highly correlated methods, the neglect of electron correlation in the HF calculations yields slightly weaker binding energies with slightly larger N—H···O distances. In the opposite direction, the DFT calculations, either with BLYP or B3LYP functional, yield stronger binding energies and significantly short N—H···O distances, most probably caused by an overestimation of the correlation energy. This could be one of the reasons why the previous CP MD study,¹⁸ using the BLYP functional, yielded a rather high rigidity of the ammonium hydrate complex. In general, the main advantage of the DFT, over the HF formalism, is that it uses the

Table 2. Optimized Parameters of the Analytical Pair Potential for the Interaction of Water with NH_4^+ (Interaction Energies in kcal mol^{-1} and Distances in \AA).

| Pair | A ($\text{kcal mol}^{-1} \text{\AA}^5$) | B ($\text{kcal mol}^{-1} \text{\AA}^7$) | C (kcal mol^{-1}) | D (\AA^{-1}) |
|-------------------------|---|---|------------------------------|-------------------------|
| N—O | 305.575926 | 3783.8268 | -1794.3299 | 2.14078153 |
| N—H(W) | -3508.815861 | 1388.9633379 | 10361.9735 | 2.50568598 |
| H(A ⁺)—O | -349.7620287 | 176.0625425 | -9493.42614 | 3.79455210 |
| H(A ⁺)—H(W) | 27.04923252 | 23.91613451 | -31.5685243 | 1.039927027 |

exchange-correlation operator instead of the exchange operator, so it partially includes electron correlation according to the $E_{xc}[\rho]$ functional. However, because the extent of electron correlation included in DFT calculations is not exactly known, lower coordination numbers and the overly rigid structures were often found when using this method, especially for the treatment of ionic solutions.^{26,35–38} From the data obtained in Table 1, it could be assumed, therefore, that the effects of electron correlation would have a minor influence on the ammonium–water interactions, and that the *ab initio* calculations at the HF level using DZV basis set are accurate enough to produce reliable structure and dynamics details of the hydrated NH_4^+ . On the other hand, a comparison of the HF calculations with the DFT results with their inherent tendency towards lower coordination numbers and a too rigid hydration shell also appeared helpful to estimate the methodical boundaries.

During the QM/MM simulation, exchange of water molecules between the QM and MM region can occur frequently. In this case, the forces acting on each particle in the system are switched according to which region the water molecule is entering or leaving, and can be defined as

$$F_i = S_m(r)F_{\text{QM}} + (1 - S_m(r))F_{\text{MM}}, \quad (2)$$

where F_{QM} and F_{MM} are quantum mechanical and molecular mechanical forces, respectively. $S_m(r)$ is a smoothing function,⁴³

$$\begin{aligned} S_m(r) &= 1, & \text{for } r \leq r_1, \\ S_m(r) &= \frac{(r_0^2 - r^2)^2(r_0^2 + 2r^2 - 3r_1^2)}{(r_0^2 - r_1^2)^3}, & \text{for } r_1 < r \leq r_0, \\ S_m(r) &= 0, & \text{for } r > r_0, \end{aligned} \quad (3)$$

where r_1 and r_0 are distances characterizing the start and the end of the QM region, applied within an interval of 0.2 \AA (i.e., between the N—O distance of 3.8–4.0 \AA) to ensure a continuous change of forces at the transition between the QM and MM regions.

For interactions within the MM and between the QM and MM regions, a flexible model,^{44,45} which describes inter- and intramolecular interactions, was employed for water. The use of flexible model is favored over any of the popular rigid water models, to ensure compatibility and a smooth transition, when water molecules move from the QM region with their full flexibility to the MM region. The pair potential function for describing NH_4^+ – H_2O interactions was newly constructed using the Aug-cc-PVTZ basis set.^{46–48} With respect to a symmetric tetrahedral geometry of the

ammonium ion, 878 HF interaction energy points for various NH_4^+ – H_2O configurations, obtained from Gaussian98⁴⁹ calculations, were fitted to an analytical form of

$$\Delta E_{\text{NH}_4^+ - \text{H}_2\text{O}} = \sum_{i=1}^5 \sum_{j=1}^3 \left[\frac{A_{ij}}{r_{ij}^5} + \frac{B_{ij}}{r_{ij}^7} + C_{ij} \exp(-D_{ij}r_{ij}) + \frac{q_i q_j}{r_{ij}} \right] \quad (4)$$

where A , B , C , and D are the fitting parameters (see Table 2), r_{ij} denotes the distances between the i -th atoms of ammonium ion and the j -th atoms of water molecule, and q are atomic net charges. The Mulliken charges on N and H of NH_4^+ , obtained from *ab initio* calculation using the Aug-cc-PVTZ basis set, and on O and H of the water molecule, which adopted from CF2 model,⁴⁴ were set to -0.5186, 0.3796, -0.6598, and 0.3299, respectively. It is known that, through ion–water interactions, these values change. However, the changes are partially compensated by the other terms in the potential during fitting to the *ab initio* energy surfaces.

The QM/MM MD simulation was performed in a canonical ensemble at 298 K. The temperature of the ensemble was kept constant using the Berendsen algorithm,⁵⁰ with a relaxation time of 0.1 ps. The cubic box, with a box length of 18.17 \AA , contains one NH_4^+ , and 199 water molecules with periodic boundary conditions. The Newtonian equations of motion were treated by a general predictor–corrector algorithm and the time step was set to 0.2 fs, which allowed for explicit movement of hydrogen atoms of NH_4^+ and water. The reaction-field method⁵¹ was employed for the treatment of long-range interactions. The system was initially equilibrated by performing a QM/MM MD simulation, in which only the NH_4^+ was treated quantum mechanically, for 200,000 time steps. Then, the QM/MM simulation with a QM diameter of 7.6 \AA , was started with the system's reequilibration for 30,000 time steps, followed by another 80,000 time steps to collect configurations every 10th step.

Because the characteristics of pure water represent a most important reference for the description of a hydrated ion, a comparison of the results with water data obtained at similar QM/MM level of accuracy was performed. Thus, the bulk properties discussed in this work refer to the properties of pure water obtained by a compatible simulation,⁴¹ namely a QM/MM simulation with a QM diameter of 7.6 \AA was carried out under the same conditions as reported in this work, simply replacing the ion by a water molecule.

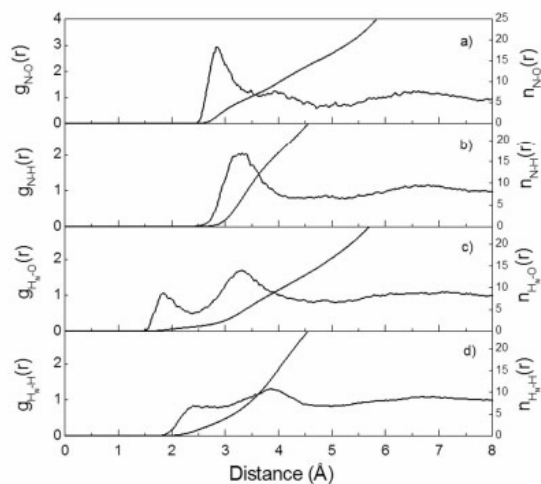


Figure 1. (a) N—O, (b) N—H, (c) H_N—O, and (d) H_N—H radial distribution functions and their corresponding integration numbers.

Results and Discussion

Structural Properties

The hydration structure of NH₄⁺ is characterized by means of N—O, N—H, H_N—O, and H_N—H RDFs and their corresponding integration numbers, as shown in Figure 1. The QM/MM simulation reveals a broad unsymmetrical first N—O peak at 2.84 Å, together with considerable tailing up to around 4.7 Å. In comparison to the O—O RDF of bulk water, as depicted in Figure 2, the shape of N—O RDF indicates a high flexibility of the NH₄⁺–water complex, as well as a high mobility of first-shell water molecules. In addition, the first minimum of the N—O peak is not well separated from the bulk, suggesting that water molecules surrounding the NH₄⁺ are quite labile, and are loosely held by the ion. The observed hydration structure of NH₄⁺ is significantly different to those obtained by the most recent MD simulations,^{17,18} which reported rather well defined the first and even the second solvation shells of the ammonium ion. In the present QM/MM simulation, the minimum position of the N—O RDF may be roughly estimated to be 3.5 Å, where an integration up to this N—O range gives coordination number of 6.5 ± 0.2. Figure 3 shows the probability distributions of the number of surrounding water molecules, calculated within the N—O distances of 3.0, 3.5, and 4.0 Å, respectively. With respect to the N—O distance of 3.5 Å, a preferred coordination number of 6 is observed, followed by 7, 5, and 8 in smaller amounts. Apparently, numerous possible species of hydrated NH₄⁺ exist, varying from 4- to 10-fold coordinated complexes. In fact, a small shift of N—O minimum will have significant impact on the coordination number. For example, at a slight larger N—O distance of 4.0 Å, the most frequent observed number of water molecules increases rapidly from 6 to 10. The QM/MM results demonstrate that numerous water molecules can mutually play a role in the hydrogen bond formation of NH₄⁺ in water.

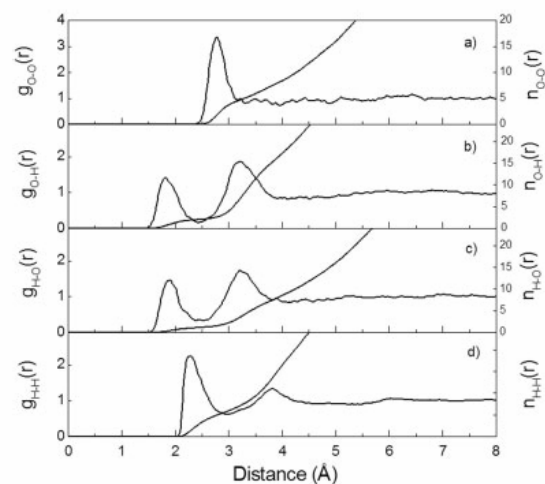


Figure 2. (a) O—O, (b) O—H, (c) H—O, and (d) H—H radial distribution functions and their corresponding integration numbers. The first atom of each pair refers to the atoms of the water molecule, whose oxygen position was defined as center of the QM region during the QM/MM simulation.

Compared to the experimentally observed coordination number of 8,¹⁰ good agreement can then be achieved. In fact, comparison between experiments and theories is not always straightforward because most of the experimental methods for structural analysis have to be performed with solutions of relatively high concentrations, while the theoretical approaches mostly refer to very dilute

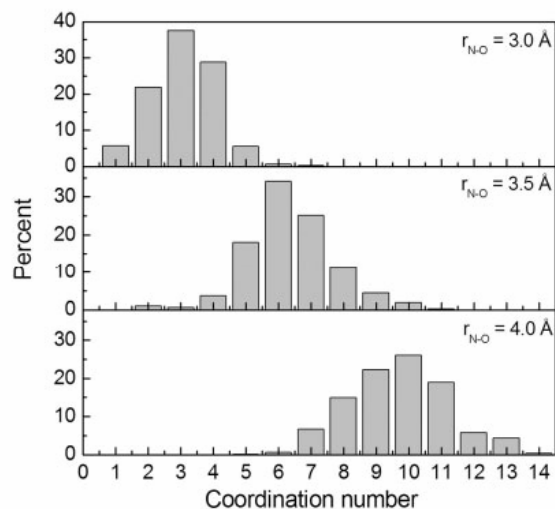


Figure 3. Coordination number distributions, calculated up to the N—O distances of 3.0, 3.5, and 4.0 Å, respectively.

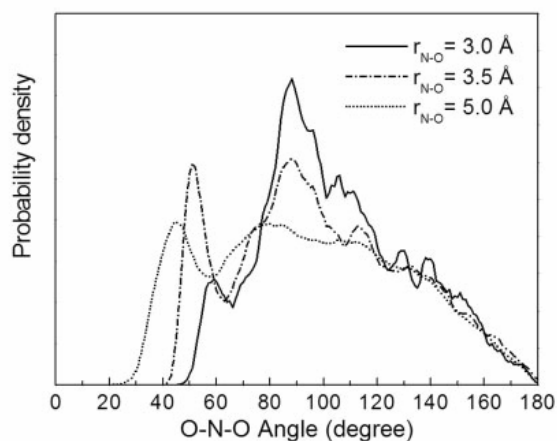


Figure 4. O-N-O angular distributions, calculated up to the N-O distances of 3.0, 3.5, and 5.0 Å, respectively.

solutions. As a consequence, a coordination number determined experimentally for high concentration solutions can be affected by coexisting counterions. Rapid ligand exchange poses another problem for the interpretation of experimental data, as it often leads to the simultaneous coexistence of several solvate species with different geometry and coordination number. When trying to fit a single (averaged) model to the spectroscopic data of such a system, errors will necessarily be introduced.

The hydrogen bonding between NH_4^+ and water can be interpreted via the $\text{H}_\text{N}-\text{O}$ and $\text{H}_\text{N}-\text{H}$ RDFs, as depicted in Figure 1c and d, respectively. The first $\text{H}_\text{N}-\text{O}$ peak is centered at 1.84 Å, which is an indicative of hydrogen bonds between the ammonium hydrogens and their nearest-neighbor water molecules. Integrating up to the first $\text{H}_\text{N}-\text{O}$ minimum yields about 1.1 waters, indicating that each of ammonium hydrogens coordinates to single water molecule. Compared to the O-H and H-O RDFs of pure water (Fig. 2b and c), the first $\text{H}_\text{N}-\text{O}$ peak is not well separated from the second one, pointing at a more frequent and easy exchange of water molecules between the first shell and the outer region. Together with a rather broad N-H RDF, the QM/MM results clearly show that the hydrogen bonds between NH_4^+ and water is not extremely strong, in contrast to the recent MD simulations^{17,18} which suggested that the first four water molecules formed a tight first solvation shell around the NH_4^+ . From the QM/MM simulation, the hydration enthalpy of the NH_4^+ can be approximated by calculation of the energy difference between the ion-water and the water-water interactions of the solution and the water-water interaction energy of the pure water, under the identical conditions. In this work, the hydration enthalpy of NH_4^+ is estimated to be $-85.7 \text{ kcal mol}^{-1}$, which is in good agreement with the experimental values of between -84 and $-89 \text{ kcal mol}^{-1}$.⁵²⁻⁵⁴

Figure 4 displays the O-N-O angular distributions, calculated up to the N-O distances of 3.0, 3.5, and 5.0 Å, respectively. At short N-O distances, a tetrahedral cage structure of the hydrated NH_4^+ is recognizable by a pronounced large peak between 80–120°. The slight distortion from the ideally tetrahedral arrange-

ment can be understood due to the interference between the first four water molecules that are directly hydrogen bonded to NH_4^+ , with the other nearest-neighbor water molecules. It is obvious that some other nearest-neighbor water molecules can also position closely to the ion, even at a short N-O distance of 3.0 Å, as can be seen from a slight pronounced peak around 60°. This phenomenon is understandable because water molecules are quite small, in which many of them can form cluster around the ammonium ion. As a consequence, water molecules can involve in the hydrogen bond formation with the ion, and thus, providing the flexible structure of the NH_4^+ -water complex.

Figure 5 illustrates the characteristics of the hydrogen bonds between NH_4^+ and water by means of the distributions of N-H...O angle, calculated within the $\text{H}_\text{N}-\text{O}$ distances of 1.8, 2.0, and 2.5 Å, respectively. At the short $\text{H}_\text{N}-\text{O}$ distances of 1.8 and 2.0 Å, the N-H...O hydrogen bonds are nearly linear, with peak maxima around 160–170°. Considering at the $\text{H}_\text{N}-\text{O}$ distance of 2.5 Å, which corresponds to the first $\text{H}_\text{N}-\text{O}$ RDF minimum, the probability of finding linear hydrogen bonds apparently decreases, while the pronounced peak between 90–140° becomes more significant. The latter peak implies the presence of multiple, nonlinear hydrogen bonds within the first solvation shell of each of ammonium hydrogens. The observed multiple coordination can be analyzed by plotting the H-N...O angular distributions, calculated within the N-O distance of 3.5 Å, as depicted in Figure 6. The two pronounced peaks around 0–30 and 90–120° correspond to the distributions of the four nearest-neighbor water molecules that form nearly linear hydrogen bonds to each of ammonium hydrogens. Apart from the water molecules that are directly hydrogen-bonded to the NH_4^+ , it seems that other nearest-neighbor water molecules prefer to form bifurcated complex between two ammonium hydrogens. The preferred bifurcated structure of the nonhydrogen bonding waters, over the trifurcated one, can be recognizable from a more pronounced shoulder peak around 50–80°, compared to that of around 150–180°. The QM/MM results are in

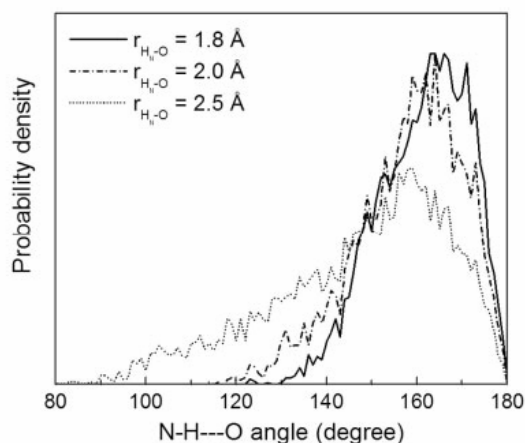


Figure 5. N-H...O angular distributions, calculated up to the $\text{H}_\text{N}-\text{O}$ distances of 1.8, 2.0, and 2.5 Å, respectively.

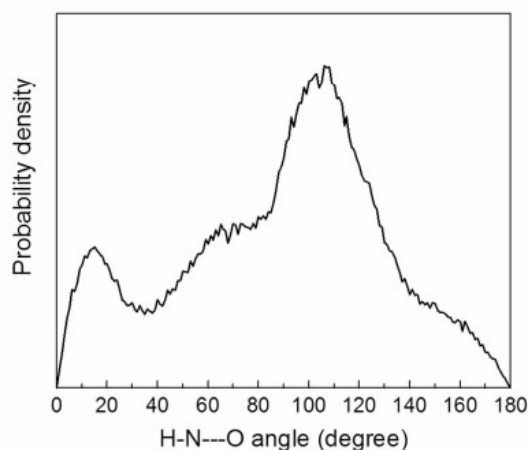


Figure 6. H—N...O angular distributions, calculated within the N—O distance of 3.5 Å.

contrast to that reported in the CP-MD simulation,¹⁸ in which only one nondirectional hydrogen bonding water molecule was observed within the defined first solvation shell and this water molecule was found to occupy a position near the center of a triangular face of the tetrahedron.

To provide additional insights into the hydrogen bonds between NH_4^+ and water, the water orientations within the $\text{H}_\text{N}\cdots\text{O}$ distance of 2.5 Å is plotted, as shown in Figure 7. The orientation of water molecules is described in terms of the distribution of angle θ , as defined by the $\text{H}_\text{N}\cdots\text{O}$ axis and the dipole vector of the water molecule. The QM/MM simulation indicates clear dipole-oriented arrangements of the hydrogen bonding waters towards the NH_4^+ , by a pronounced

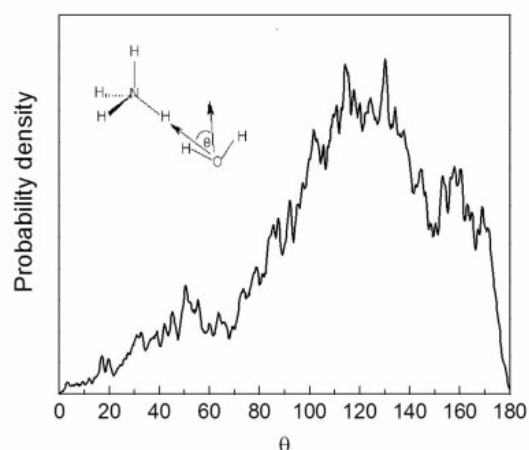


Figure 7. Distributions of θ , calculated within the N—O distance of 3.5 Å.

Table 3. Self-Diffusion Constants for NH_4^+ and Water.

| Species | Self-diffusion constants ($10^{-5} \text{ cm}^2 \text{ s}^{-1}$) | Method/ref. |
|---|---|------------------------|
| NH_4^+ in water | 3.46 | QM/MM-MD (this work) |
| | 0.82 | MD ¹⁵ |
| | ~2.7 | MD ¹⁷ |
| H_2O around NH_4^+ ($r_{\text{N-O}} = 3.5 \text{ \AA}$) | 1–2 | Expt. ⁵⁶ |
| | 3.23 | QM/MM-MD (this work) |
| Pure H_2O | 3.31 ^a | QM/MM-MD ⁴¹ |
| | 2.30 | Expt. ^{57,58} |

^aThis value is calculated from the center-of-mass VACFs of water molecules obtained by the QM/MM simulation of pure water.⁴¹

peak around 100–170°. A slight pronounced peak around 30–70° could be attributed to the dipole-oriented arrangements of the nearest-neighbor nonhydrogen bonding water molecules that are less induced by the ammonium ion. Instead, they are rather arranged by the influences of other surrounding water molecules that located within and/or beyond the $\text{H}_\text{N}\cdots\text{O}$ distance of 2.5 Å.

Because the QM/MM approach allows the charge distributions on NH_4^+ and its surrounding water molecules to vary dynamically during the simulation process, the polarizability of water molecules surrounding the ion, as well as the effects of charge-transfer in the ion–water complex, which affect the structure of the hydrated NH_4^+ , are automatically included. In the QM/MM simulation, the average Mulliken charge on NH_4^+ is +0.893, and those on O and H of water molecules surrounding the ion are −0.921 and +0.465, respectively. Although the use of polarizable models can provide qualitative predictions for such circumstance,¹⁷ the present QM/MM results suggest that it could never reach the quality of the QM/MM approach, where all charges are corrected dynamically according to the structural changes of the hydrated NH_4^+ .

Dynamical Properties

Translational Motions

Due to a relatively short time of the QM/MM simulation, the dynamical properties of hydrated NH_4^+ reported in this work are discussed with care and will not be overinterpreted. The self-diffusion coefficients (D) for NH_4^+ as well as for water molecules surrounding the ion and those in the bulk⁴¹ were calculated from the center-of-mass velocity autocorrelation functions (VACFs) using the Green-Kubo relation,⁵⁵

$$D = \frac{1}{3} \lim_{t \rightarrow \infty} \int_0^t C_v(t) dt. \quad (5)$$

All of the calculated D values are summarized in Table 3. Based on our QM/MM simulation, the self-diffusion coefficient for NH_4^+ in water is estimated to be $3.46 \times 10^{-5} \text{ cm}^2 \text{ s}^{-1}$, which is about two to three times larger than the experimental values.⁵⁶ It should be noted that discrepancy between experiment and theory is

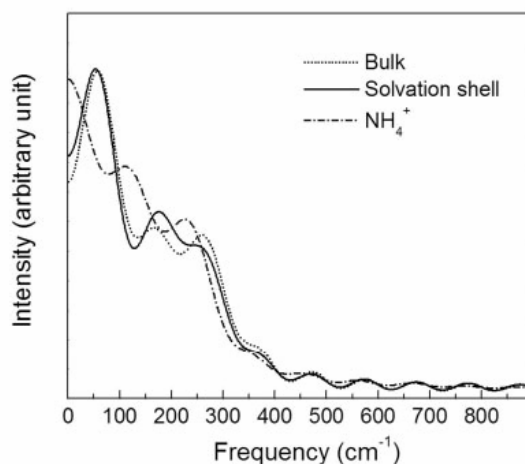


Figure 8. Power spectra of the translational motions of NH_4^+ and of water molecules in the bulk and in the hydration shell of the ion, calculated from the center-of-mass VACFs of the ion and water.

often found because the experimentally observed dynamics parameters are usually determined for high concentration solutions, in which the counterion effects can influence the results, while the values obtained in this work correspond to a very dilute solution. In comparison to bulk water,⁴¹ the QM/MM results indicate that NH_4^+ diffuses quite fast, while water molecules in the solvation shell of the ion diffuse on a time scale comparable to that of the bulk. The observed fast diffusive translation of NH_4^+ can be described due to the flexible NH_4^+ solvation, thus allowing the NH_4^+ to translate more freely without carrying any of nearest-neighbor waters with it.

Spectral densities, corresponding to the hindered translations of NH_4^+ and of water molecules, were analyzed by Fourier transformations of the center-of-mass VACFs, as shown in Figure 8. For bulk water,⁴¹ a pronounced peak with maximum at about 60 cm^{-1} and a broad band around $150\text{--}300\text{ cm}^{-1}$ are identified as hindered translational motions of the center-of-mass parallel and perpendicular to the dipole vector of water molecules, which have been attributed to the hydrogen bond bending and the $\text{O}\cdots\text{O}$ stretching motions, respectively.⁵⁹ In comparison to bulk water, the power spectra of water molecules in the hydration sphere of NH_4^+ are not significantly different to that of the pure water, indicating a small influence of this ion on the translational motions of its surrounding water molecules. For the translational motion of NH_4^+ itself, the Fourier transforms show a maximum at zero frequency, which correspond to the high probability of translation of this ion in the environment of water molecules.

Librational Motions

Based on the normal-coordinate analyses,⁶⁰ the power spectra of the librational motions of water molecules, calculated within the $\text{H}_\text{N}\cdots\text{O}$ distance of 2.5 \AA , and of NH_4^+ (only for a rotation around C_{3V} axis) are displayed in Figure 9. In comparison to the frequen-

cies of pure water,⁴¹ the librational frequencies, of the order of $R_z < R_x < R_y$, of water molecules surrounding the ammonium hydrogens are all blue-shifted. The shift to higher frequencies can be attributed to the steric hindrance in the NH_4^+ -water complex, in which water molecules form cluster with the ion. For the rotation of NH_4^+ in water, the rotational frequency of this ion around its C_{3V} axis is red-shifted, compared to the C_{2V} rotation of water molecules. The shift to lower frequency implies that NH_4^+ can rotate rather freely in an environment of water molecules. The rotational motion of NH_4^+ in water can be characterized by its rotational diffusion constant, D_R . Because NH_4^+ has an approximately symmetric tetrahedral environment, all three principal moments of inertia are equivalent. Consequently, the rotational diffusion constant can then be obtained from the mean-square angle displacements,

$$\langle \theta(t)^2 \rangle = 4D_R t, \quad (6)$$

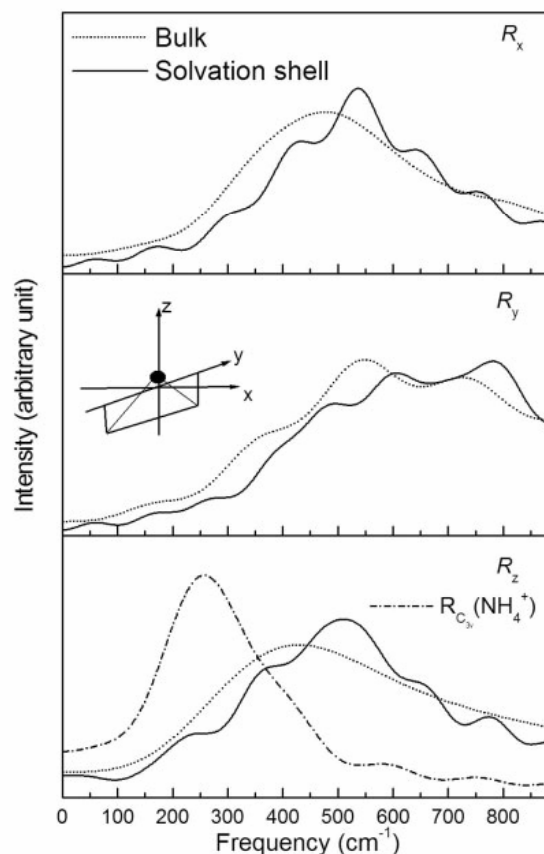


Figure 9. Power spectra of the librational motions of NH_4^+ and of water molecules in the bulk and in the hydration shell of the ion, as obtained by the QM/MM simulations.

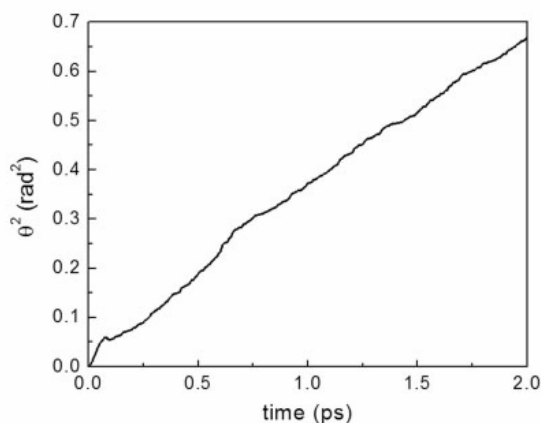


Figure 10. Mean-square angular displacements of NH_4^+ in water as a function of time.

where $\theta(t)$ denotes the angle formed by a vector in the body-fixed frame at with its initial direction ($\theta = 0$ at $t = 0$). The computed mean-square angle $\langle \theta(t)^2 \rangle$ as a function of time is displayed in Figure 10, and the rotational diffusion constant estimated from the slope was $0.088 \times 10^{12} \text{ rad}^2 \text{ s}^{-1}$, which is in good agreement with the experimental value of about $0.075 \times 10^{12} \text{ rad}^2 \text{ s}^{-1}$ obtained by the NMR measurements.^{6,8}

The ease of NH_4^+ rotation can be ascribed due to the presence of numerous water molecules around the ion that facilitate the rotation. Based on the QM/MM results, the most probable rotational dynamics of the NH_4^+ in water can be considered as follow. Because the hydrogen bond between NH_4^+ and water is not extremely strong, its strength maybe somewhat comparable to that of between water and water. Hence, when a number of water molecules interact with the ion, the first four nearest-neighbor waters are temporarily immobilized at each edge of the tetrahedral NH_4^+ –water cage structure, while the others are more labile and are placed in bifurcated configurations between two ammonium hydrogens. Thus, it is obvious that because of the bifurcated waters that significantly enhance the ease for each of ammonium hydrogens to break its original hydrogen bond (with its original water molecule) and then to form a new hydrogen bond with another (bifurcated) water molecule. With sufficient amount of bifurcated waters, possibly up to six water molecules (according to the rough estimated first hydration shell, see Fig. 3), all possible reestablished N–H...O hydrogen bonds can easily occur along any rotational pathway of the NH_4^+ . The QM/MM results support well a proposed multiple hydrogen bonding rotational mechanism,⁶ and are in good agreement with the NMR experiments,⁶ as well as being consistent with the reported rather low activation energy, E_a , for the reorientation of NH_4^+ in aqueous solution.^{6,13,61}

Water Exchange in the Hydration Shell of NH_4^+

Within the total simulation time of 16 ps, several water exchange processes occurring at each of ammonium hydrogens are observed.

To focus more distinctly on the water exchange processes, the plot of $\text{H}_\text{N}\cdots\text{O}$ distance is zoomed within the $\text{H}_\text{N}\cdots\text{O}$ distance of 4.0 Å and for only the first 8 ps of the QM/MM simulation trajectory, as depicted in Figure 11. It is obvious that water molecules surrounding the ammonium hydrogens can exchange by any of the proposed “classical” types, namely associative (A) and dissociative (D) as well as associative (I_a) and dissociative (I_d) interchange mechanisms.⁶² These data confirm the structural lability of the NH_4^+ in aqueous solution, corresponding to the appearance of various possible species of the hydrate complex formed in the solution.

The rate of water exchange processes at each of ammonium hydrogens was evaluated by means of mean residence time (MRT) of the water molecules. In this work, the MRT values were calculated using a “direct” method,⁶³ being the product of the average number of nearest-neighbor water molecules located within the $\text{H}_\text{N}\cdots\text{O}$ distance of 2.5 Å with the duration of the QM/MM simulation, divided by the number of exchange events. Based on the direct accounting and setting various time parameter t^* , the MRT values are listed in Table 4. The time parameter t^* has been defined as a minimum duration of the ligand’s displacement from its original coordination shell. For such weakly hydrated NH_4^+ , the $t^* = 0.5$ ps was proposed to be the best choice⁶³ as it corresponds to the mean lifetime of hydrogen bonds. With respect to this criterion, only the data obtained with $t^* = 0.0$ ps make sense for the estimation of H-bond lifetimes, while the MRT data obtained with $t^* = 0.5$ ps can be considered as a good measure for ligand exchange processes. In accordance with the $t^* = 0.5$ ps, an order of $\tau_{\text{H}_2\text{O}}(\text{H}_\text{N}) < \tau_{\text{H}_2\text{O}}(\text{H}_2\text{O})$ is observed. The QM/MM results clearly show that water molecules binding to each of ammonium hydrogens are quite labile, and that the hydrogen bond between NH_4^+ and water is not very strong, allowing numerous water

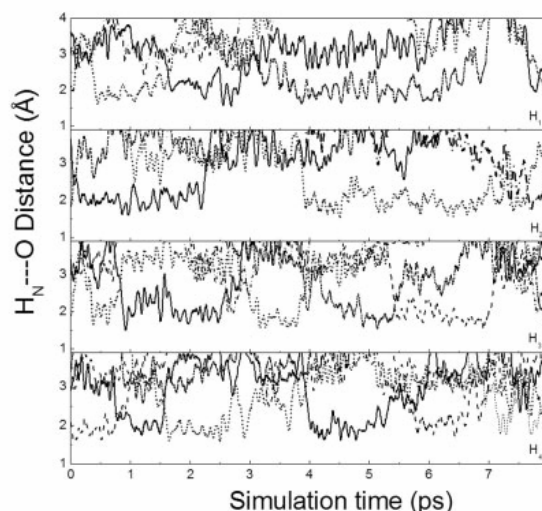


Figure 11. Water exchange in the first solvation shell of each of ammonium hydrogens, emphasizing for only the first 8 ps of the QM/MM simulation.

Table 4. Mean Residence Times of Water Molecules in Bulk and in the First Solvation Shell of Each of Ammonium Hydrogens, Calculated within the $\text{H}_\text{N}\cdots\text{O}$ Distance of 2.5 Å.

| Solute/ion | CN | t_{sim} | $t^* = 0$ ps | | $t^* = 0.5$ ps | |
|---------------------------------------|------|------------------|-------------------|-------------------------------|-----------------------|-----------------------------------|
| | | | N_{ex}^0 | $\tau_{\text{H}_2\text{O}}^0$ | $N_{\text{ex}}^{0.5}$ | $\tau_{\text{H}_2\text{O}}^{0.5}$ |
| H ₁ | 1.05 | 16.0 | 204 | 0.08 | 13 | 1.29 |
| H ₂ | 1.14 | 16.0 | 231 | 0.08 | 12 | 1.52 |
| H ₃ | 1.13 | 16.0 | 267 | 0.07 | 14 | 1.29 |
| H ₄ | 1.08 | 16.0 | 227 | 0.07 | 13 | 1.33 |
| Pure $\text{H}_2\text{O}^{\text{d1}}$ | 4.6 | 12.0 | 292 | 0.19 | 31 | 1.78 |

N_{ex} is the number of accounted exchange events, t_{sim} the simulation time in ps, and CN the average coordination number of the first hydration shell of water and of each of ammonium hydrogens.

exchange processes within the hydration sphere of the NH_4^+ to frequently occur. In addition, the MRT data also reveal the “structure-breaking” ability of the NH_4^+ in aqueous solution. The “structure-breaking” effect of the NH_4^+ can be recognized from its flexible hydration structure, as well as from the MRT values of water molecules surrounding the ion, which are smaller than that of the bulk. The QM/MM results suggest that the NH_4^+ cannot form a well-defined ion–water complex, and its influence can be concerned mainly to disrupt the solvent’s hydrogen-bonded structure.

The detailed information on the solvation structure and dynamics of NH_4^+ in water is very crucial to fundamentally understand the reactivity of this ion in chemical and biological systems. For example, in the specific ion stabilization of the RNA structure, the potential of NH_4^+ to donate four hydrogen bonds in a tetrahedral geometry has been considered to responsible for its ability to stabilize the RNA fragment structure more effectively than the alkali metal cations.⁷ Furthermore, because the RNA fragment selectivity for NH_4^+ is the result of a match between a tetrahedral array of hydrogen bond acceptors in the RNA and NH_4^+ , the correct coordination or hydrogen bonding of NH_4^+ in specific sites is of particular importance to promote the correct conformation of the RNA.

Conclusion

The combined *ab initio* QM/MM molecular dynamics simulation has provided more detailed descriptions on the structure and dynamics of NH_4^+ in water. The QM/MM simulation has revealed a flexible and more labile hydration structure of NH_4^+ , in which numerous species of hydrated NH_4^+ appear, varying possibly from 4- to 10-fold coordinated complexes. Consequently, the observed fast translation and rotation of NH_4^+ in water can be understood due to its flexible hydration as well as the cooperative involvement of the multiple coordination that drives the ammonium ion to translate and rotate rather freely around its surrounding water molecules. In addition, the QM/MM simulation has demonstrated the behavior related to the “structure-breaking” ability of this ion in aqueous solution. We believe that the QM/MM results presented

here are accurate, and that the QM/MM technique can be seen as a very promising tool to investigate the structural and dynamical properties of such highly labile NH_4^+ hydrate.

References

- Frank, H. S. *Chemical Physics of Ionic Solutions*; John Wiley & Sons: New York, 1956, p. 60.
- Robinson, R. A.; Stokes, R. H. *Electrolyte Solutions*; Butterworth: London, 1959, 2nd ed.
- William, R. J. P. *Bio-inorganics Chemistry*; Gould, R. F., Ed.; American Chemical Society: Washington, DC, 1971.
- Hille, B. *Ionic Channels of Excitable Membranes*; Sinauer: Sunderland, MA, 1992, 2nd ed.
- Perrin, C. L.; Gipe, R. K. *J Am Chem Soc* 1984, 96, 5631.
- Perrin, C. L.; Gipe, R. K. *J Am Chem Soc* 1986, 108, 1088.
- Wang, Y.; Lu, M.; Draper, D. E. *Biochemistry* 1993, 32, 12279.
- Perrin, C. L.; Gipe, R. K. *Science* 1987, 238, 1393.
- Hewish, N. A.; Neilson, G. W. *Chem Phys Lett* 1981, 84, 425.
- Pálinkás, G.; Radnai, T.; Szász, G. I.; Heinzinger, K. *J Chem Phys* 1981, 74, 3522.
- Jiang, J. C.; Chang, H.; Lee, Y. T.; Lin, S. H. *J Phys Chem A* 1999, 103, 3123.
- Brugé, F.; Bernasconi, M.; Parrinello, M. *J Chem Phys* 1999, 110, 4734.
- Kassab, E.; Evleth, E. M.; Hamou–Tahra, Z. D. *J Am Chem Soc* 1990, 112, 103.
- Jorgensen, W. L.; Gao, J. *J Phys Chem* 1986, 90, 2174.
- Karim, O. A.; Haymet, A. D. J. *J Chem Phys* 1990, 93, 5961.
- Dang, L. X. *Chem Phys Lett* 1993, 213, 541.
- Chang, T.; Dang, L. X. *J Chem Phys* 2003, 118, 8813.
- Brugé, F.; Bernasconi, M.; Parrinello, M. *J Am Chem Soc* 1999, 121, 10883.
- Szász, G. I.; Heinzinger, K. *Z Naturforsch* 1979, 34a, 840.
- Bohm, H.; McDonald, I. R. *Mol Phys* 1984, 80, 887.
- Jungwirth, P.; Tobias, D. J. *J Phys Chem A* 2002, 106, 379.
- Tobias, D. J.; Jungwirth, P.; Parrinello, M. *J Chem Phys* 2001, 114, 7036.
- Coker, H. *J Phys Chem* 1976, 80, 2078.
- Pyper, N. C.; Pike, C. G.; Edwards, P. P. *Mol Phys* 1992, 76, 353.
- Schwenk, C. F.; Loeffler, H. H.; Rode, B. M. *Chem Phys* 2001, 115, 10808.
- Rode, B. M.; Schwenk, C. F.; Tongraar, A. *J Mol Liq* 2004, 110, 105.
- Kerdcharoen, T.; Liedl, K. R.; Rode, B. M. *Chem Phys* 1996, 211, 313.
- Tongraar, A.; Liedl, K. R.; Rode, B. M. *J Phys Chem A* 1997, 101, 6299.
- Tongraar, A.; Liedl, K. R.; Rode, B. M. *J Phys Chem A* 1998, 102, 10340.
- Marini, G. W.; Liedl, K. R.; Rode, B. M. *J Phys Chem A* 1999, 103, 11387.
- Tongraar, A.; Rode, B. M. *J Phys Chem A* 2001, 105, 506.
- Tongraar, A.; Sagarik, K.; Rode, B. M. *J Phys Chem B* 2001, 105, 10559.
- Tongraar, A.; Sagarik, K.; Rode, B. M. *Phys Chem Chem Phys* 2002, 4, 628.
- Tongraar, A.; Rode, B. M. *Phys Chem Chem Phys* 2003, 5, 357.
- Hofer, T. S.; Rode, B. M. *J Phys Chem A* 2004, 108, 1509.
- Schwenk, C. F.; Rode, B. M. *J Chem Phys* 2003, 119, 9523.
- Hofer, T. S.; Rode, B. M. *J Chem Phys* 2004, 121, 6406.
- Schwenk, C. F.; Loeffler, H. H.; Rode, B. M. *J Chem Phys* 2001, 115, 10808.

39. Schwenk, C. F.; Loeffler, H. H.; Rode, B. M. *J Am Chem Soc* 2003, 125, 1618.
40. Tongraar, A.; Rode, B. M. *Phys Chem Chem Phys* 2004, 6, 411.
41. Tongraar, A.; Rode, B. M. *Chem Phys Lett* 2004, 385, 378.
42. Dunning, T. H., Jr.; Hay, P. J. *Modern Theoretical Chemistry*; Schaefer, H. F., Ed.; Plenum: New York, 1976.
43. Brooks, B. R.; Bruccoleri, R. E.; Olafson, B. D.; States, D. J.; Swaminathan, S.; Karplus, M. *J Comput Chem* 1983, 4, 187.
44. Bopp, P.; Jancsó, G.; Heinzinger, K. *Chem Phys Lett* 1983, 98, 129.
45. Stillinger, F. H.; Rahman, A. *J Chem Phys* 1978, 68, 666.
46. Dunning, T. H., Jr. *J Chem Phys* 1989, 90, 1007.
47. Kendall, R. A.; Dunning, T. H., Jr.; Harrison, R. J. *J Chem Phys* 1992, 96, 6769.
48. Woon, D. E.; Dunning, T. H., Jr. *J Chem Phys* 1993, 98, 1358.
49. Frisch, M. J.; Trucks, G. W.; Schlegel, H. B.; Scuseria, G. E.; Robb, M. A.; Cheeseman, J. R.; Zakrewski, V. G.; Montgomery, J. A.; Stratmann, R. E.; Burant, J. C.; Dapprich, S.; Millam, J. M.; Daniels, A. D.; Kudin, K. N.; Strain, M. C.; Farkas, O.; Tomasi, J.; Barone, V.; Cossi, M.; Cammi, R.; Mennucci, B.; Pomelli, C.; Adamo, C.; Clifford, S.; Ochterski, J.; Peterson, G. A.; Ayala, P. Y.; Cui, Q.; Morokuma, K.; Malick, D. K.; Rabuck, A. D.; Raghavachari, K.; Foresman, J. B.; Cioslowski, J.; Ortiz, J. V.; Stefanov, B. B.; Liu, G.; Liashenko, A.; Piskorz, P.; Komaromi, I.; Gomperts, R.; Martin, R. L.; Fox, D. J.; Keith, T.; Al-Laham, M. A.; Peng, C. Y.; Nanayakkara, A.; Gonzalez, C.; Challacombe, M.; Gill, P. M. W.; Johnson, B. G.; Chen, W.; Wong, M. W.; Andres, J. L.; Head-Gordon, M.; Replogle, E. S.; Pople, J. A. *GAUSSIAN 98*; Gaussian, Inc.: Pittsburgh, PA, 1998.
50. Berendsen, H. J. C.; Postma, J. P. M.; van Gunsteren, W. F.; DiNola, A.; Haak, J. R. *J Phys Chem* 1984, 81, 3684.
51. Adams, D. J.; Adams, E. H.; Hills, G. J. *Mol Phys* 1979, 38, 387.
52. Arnett, E. M.; Jones, F. M.; Taagepera, M.; Henderson, W. G.; Beauchamp, J. L.; Holta, D.; Taft, R. W. *J Am Chem Soc* 1972, 94, 4724.
53. Aue, D. H.; Webb, H. M.; Bowers, M. T. *J Am Chem Soc* 1976, 98, 318.
54. Klots, C. E. *J Phys Chem* 1981, 85, 3585.
55. McQuarrie, D. A. *Statistical Mechanics*; Harper & Row: New York, 1976.
56. Wishaw, B. F.; Stokes, R. H. *J Am Chem Soc* 1954, 76, 2065.
57. Gillen, K. T.; Douglass, D. C.; Hoch, M. J. R. *J Chem Phys* 1972, 57, 5117.
58. Woolf, L. A. *J Chem Soc Faraday Trans 1* 1975, 71, 784.
59. Sceats, M. G.; Rice, S. A. *J Chem Phys* 1980, 72, 3236.
60. Bopp, P. *Chem Phys* 1986, 106, 205.
61. Brown, R. J. C. *J Mol Struct* 1995, 345, 77.
62. Langford, C. H.; Gray, H. B. *Ligand Substitution Processes*; Benjamin, W. A. Inc. Press, New York, 1966.
63. Hofer, T. S.; Tran, H. T.; Schwenk, C. F.; Rode, B. M. *J Comput Chem* 2004, 25, 211.

CURRICULUM VITAE

MS. PATHUMWADEE INTHARATHEP

Birth: February 17, 1979 in Nakhon Si Thammarat, Thailand

Father's name: Jumlong Intharathep

Mother's name: Jaree Intharathep

Education:

1997-2000 B.Sc. (Chemistry), Ramkhamhaeng University, Bangkok, Thailand

2001-2006 Ph.D. (Chemistry), Suranaree University of Technology, Nakhon
Ratchasima, Thailand

Experience:

May-December, 2001 Teaching Assistant, School of Chemistry, Institute of
Science, Suranaree University of Technology, Nakhon
Ratchasima, Thailand

January-April, 2005 Scholar Visitor, the Institute for Materials and Processes
in Energy System (IWV-3), Forschungszentrum Jülich,
Jülich, Germany

October, 2005-March, 2006 Scholar Visitor, University of Minnesota, Minneapolis,
Minnesota, United State

Scholarship:

2001-2006 The Royal Golden Jubilee (RGJ) Ph.D. scholarship from Thailand
Research Fund (TRF)